

Editorial Team

CHAIRMAN

Attaallah Heidari

Deputy of Research and Technology,
Kurdistan University of Medical
Sciences, Sanandaj, Iran

EDITOR-IN-CHIEF

Afshin Maleki

Professor, Editor-in-Chief Journal of
Advances in Environmental Health
Research, Iran

ASSOCIATE EDITOR

Behzad Shahmoradi

Associate Editor, Journal of Advances
in Environmental Health Research
(JAEHR), Iran

EDITORIAL ASSISTANT

Hassan Amini, Lecturer, Kurdistan Environmental Health
Research Center, Kurdistan University of Medical
Sciences, Sanandaj, Iran

Alireza Gharib, Lecturer, Deputy of Research and
Technology, Kurdistan University of Medical Sciences,
Sanandaj, Iran

Hiua Daraei, Lecturer, Kurdistan Environmental Health
Research Center, Kurdistan University of Medical
Sciences, Sanandaj, Iran

Pari Teymouri, Lecturer, Kurdistan Environmental Health
Research Center, Kurdistan University of Medical
Sciences, Sanandaj, Iran

Esmail Ghahramani, Lecturer, Kurdistan Environmental
Health Research Center, Kurdistan University of Medical
Sciences, Sanandaj, Iran

EDITORIAL BOARD

Nadali Alavi, Assistant Professor, Department of
Environmental Health Engineering, Ahvaz Jondishapour
University of Medical Sciences, Ahvaz, Iran

Enayatollah Kalantar, Associate Professor, Alborz
University of Medical Sciences, Karaj, Iran

Mahmood Alimohammadi, Associate Professor, School
of Public Health and Institute of Public Health Research,
Tehran University of Medical Sciences, Tehran, Iran

Puttaswamy Madhusudhan, Assistant Professor, Post
Doctoral Research Fellow, State Key Laboratory of Advanced
Technology for Material Synthesis and Processing, School of
Chemical Engineering, Wuhan University of Technology,
Hubei, China

Behrooz Davari, Associate Professor, Hamedan University
of Medical Sciences, Hamedan, Iran

Amir Hossein Mahvi, Assistant Professor, School of
Public Health and Institute of Public Health Research, Tehran
University of Medical Sciences, Tehran, Iran

Saeed Dehestani Athar, Assistant Professor, Kurdistan
Environmental Health Research Center, Kurdistan University
of Medical Sciences, Sanandaj, Iran

Reza Rezaee, Lecturer, Kurdistan Environmental Health
Research Center, Kurdistan University of Medical Sciences,
Sanandaj, Iran

Mehdi Farzad Kia, Associate Professor, Environmental
Health Engineering Department, Tehran University of Medical
Sciences, Tehran, Iran

Mahdi Safari, Assistant Professor, Kurdistan
Environmental Health Research Center, Kurdistan University
of Medical Sciences, Sanandaj, Iran

Omid Giahi, Assistant Professor, Kurdistan Environmental
Health Research Center, Kurdistan University of Medical
Sciences, Sanandaj, Iran

H.P. Shivaraju, Assistant Professor, Department of
Environmental Science, School of Life Science, J.S.S.
University, Shivarathreshwara Nagara, Mysore-570015,
India

Akbar Islami, Assistant Professor, Department of
Environmental Health Engineering, Shahid Beheshti
University, Tehran, Iran

Kamyar Yagmoeian, Associate Professor, School of
Public Health and Institute of Public Health Research, Tehran
University of Medical Sciences, Tehran, Iran

Ali Jafari, Professor assistant, Lorestan University of
Medical Sciences, Khorramabad, Iran.

Ahmad Joneidi Jafari, Associate Professor, School of
Public Health and Institute of Public Health Research, Tehran
University of Medical Sciences, Tehran, Iran

Mohammad Ali Zazouli, Associate Professor, Department
of Environmental Health Engineering, Mazandaran University
of Medical Sciences, Sari, Iran

EXECUTIVE MANAGER

Pari Teymouri, Lecturer, Kurdistan Environmental Health Research Center,
Kurdistan University of Medical Sciences, Sanandaj, Iran

Information for Authors

AIM AND SCOPE

Journal of Advances in Environmental Health Research (JAEHR) is a quarterly peer-reviewed scientific journal published by Kurdistan University of Medical Sciences. The manuscripts on the topic of environmental science and engineering will be published in this journal. This contains all aspects of solid waste management, air pollution, water and wastewater, environmental monitoring and modeling, innovative technologies and studies related to the environmental science.

Instruction to Authors

MANUSCRIPTS

Manuscripts containing original material are accepted for consideration if neither the article nor any part of its essential substance, tables, or figures has been or will be published or submitted elsewhere before appearing in the *Journal of Advances in Environmental Health Research*. This restriction does not apply to abstracts or press reports published in connection with scientific meetings. Copies of any closely related manuscripts must be submitted along with the manuscript that is to be considered by the *Journal of Advances in Environmental Health Research*. Authors of all types of articles should follow the general instructions given below.

HUMAN AND ANIMAL RIGHTS

The research involves human beings or animals must adhere to the principles of the Declaration of Helsinki (<http://www.wma.net/e/ethicsunit/helsinki.htm>).

Types of Articles

- *Original article* which reports the results of an original scientific research should be less than 4000 words.
- *Review article* which represents the researches and works on a particular topic.
- *Brief communication* is a short research article and should be limited to 1500 words. This article contains all sections of an original article.

- *Case report* is a detailed report of an individual patient that may represent a previously non-described condition and contains new information about different aspects of a disease. It should be less than 2000 words.
- *Letter to the Editor* must be less than 400 words in all cases.
- *Book Review* must be less than 1000 words on any book topics related to the scope of *Journal of Advances in Environmental Health Research*.

SUBMISSION

- Only online submission is acceptable. Please submit online at: <http://www.jaehr.muk.ac.ir>
- This manuscripts should be divided into the following sections: (1) Title page, (2) Abstract and Keywords, (3) Introduction, (4) Materials and Methods, (5) Results and Discussion, (6) Acknowledgements, (7) Author contribution, (8) References, (9) Figure legends, (10) Tables and (11) Figures (figures should be submitted in separate files if the file size exceeds 2 Mb).
- Please supply a word count in title page.
- Use normal page margins (2.5 cm), and double-space throughout the manuscript.
- Use Times New Roman (12) font throughout the manuscript.
- Prepare your manuscript text using a Word processing package (save in .doc or .rtf format). Submissions of text in the form of PDF files are not permitted.

COVER LETTER

A covering letter signed by all authors should identify the corresponding author (include the address, telephone number, fax number, and e-mail address). Please make clear that the final manuscript has been seen and approved by all authors, and that the authors accept full responsibility for the design and conduct of the study, had access to the data, and controlled the decision to publish.

Authors are also asked to provide the names and contact information for three potential reviewers in their cover letter. However, the journal is not obliged to use the suggested reviewers. Final selection of reviewers will be determined by the editors.

AUTHORSHIP

As stated in the Uniform Requirements for Manuscripts Submitted to Biomedical Journals (<http://www.icmje.org/icmje-recommendations.pdf>), credit for authorship requires substantial contributions to: 1. Substantial contributions to the conception or design of the work; or the acquisition, analysis, or interpretation of data for the work; AND 2. Drafting the work or revising it critically for important intellectual content; AND 3. Final approval of the version to be published; AND 4. Agreement to be accountable for all aspects of the work in ensuring that questions related to the accuracy or integrity of any part of the work are appropriately investigated and resolved. Each author must sign authorship form attesting that he or she fulfills the authorship criteria. There should be a statement in manuscript explaining contribution of each author to the work. Acknowledgments will be limited to one page of *Journal of Advances in Environmental Health Research*, and those acknowledged will be listed only once.

Any change in authorship after submission must be approved in writing by all authors.

ASSURANCES

In appropriate places in the manuscript please provide the following items:

- If applicable, a statement that the research protocol was approved by the relevant institutional review boards or ethics committees and that all human participants gave written informed consent
- The source of funding for the study
- The identity of those who analyzed the data
- Financial disclosure, or a statement that none is necessary

TITLE PAGE

With the manuscript, provide a page giving the title of the paper; titles should be concise and descriptive (not declarative). Title page should include an abbreviated running title of 40 characters, the names of the authors, including the complete first names, the name of the department and institution in which the work was done, the institutional affiliation of each author. The name, post address, telephone number, fax number, and e-mail address of the corresponding author should be separately addressed. Any grant support that requires acknowledgment should be mentioned on this page. Word count of abstract and main text as well as number of tables and figures and references should be mentioned on title page. If the work was derived from a project or dissertation, its code should also be stated.

Affiliation model: Department, Institute, City, Country.

Example: Department of Environmental Health Engineering, School of Health, Kurdistan University of Medical Sciences, Sanandaj, Iran.

ABSTRACT

Provide on a separate page an abstract of not more than 250 words. This abstract should consist of ONE paragraph (Non-structured Abstract). It should briefly describe the problem being addressed in the study, how the study was performed, the salient results, and what the authors conclude from the results respectively. Three to seven keywords may be included. Keywords are preferred to be in accordance with MeSH (<http://www.ncbi.nlm.nih.gov/mesh>) terms.

CONFLICT OF INTEREST

Authors of research articles should disclose at the time of submission any financial arrangement they may have with a company whose product is pertinent to the submitted manuscript or with a company making a competing product. Such information will be held in confidence while the paper is under review and will not influence the editorial decision, but if the article is accepted for publication, a disclosure will appear with the article.

Because the essence of reviews and editorials is selection and interpretation of the literature, the *Journal of Advances in Environmental Health Research* expects that authors of such articles will not have any significant financial interest in a company (or its competitor) that makes a product discussed in the article.

REVIEW AND ACTION

Submitted papers will be examined for the evidence of plagiarism using some automated plagiarism detection service. Manuscripts are examined by members of the editorial staff, and two thirds are sent to external reviewers. Communications about manuscripts will be sent after the review and editorial decision-making process is complete within **3-6 weeks** after receiving the manuscript. After acceptance, editorial system makes a final language and scientific edition. No substantial change is permitted by authors after acceptance. It is the responsibility of corresponding author to answer probable questions and approve final version.

COPYRIGHT

Journal of Advances in Environmental Health Research is the owner of all copyright to any original work published by the

JAEHR. Authors agree to execute copyright transfer forms as requested with respect to their *Journal of Advances in Environmental Health Research* has the right to use, reproduce, transmit, derive works from, publish, and distribute the contribution, in the *Journal* or otherwise, in any form or medium. Authors will not use or authorize the use of the contribution without the Journal Office' written consent

JOURNAL STYLE

Tables

Double-space tables and provide a title for each.

Figures

Figures should be no larger than 125 (height) x 180 (width) mm (5 x 7 inches) and should be submitted in a separate file from that of the manuscript. The name of images or figures files should be the same as the order that was used in manuscript (fig1, fig2, etc.). Only JPEG, tif, gif and eps image formats are acceptable with CMYK model for colored image at a resolution of at least 300 dpi. Graphs must have the minimum quality: clear text, proportionate, not 3 dimensional and without disharmonic language. Electron photomicrographs should have internal scale markers. If photographs of patients are used, either the subjects should not be identifiable or the photographs should be accompanied by written permission to use them. Permission forms are available from the Editorial Office.

Scientific illustrations will be created or recreated in-house. If an outside illustrator creates the figure, the *Journal of Advances in Environmental Health Research* reserves the right to modify or redraw it to meet our specifications for publication. The author must explicitly acquire all rights to the illustration from the artist in order for us to publish the illustration. Legends for figures should be an editable text as caption and should not appear on the figures.

References

The Vancouver style of referencing should be used. References must be double-spaced and numbered as **superscripts** consecutively as they are cited. References first cited in a table or figure legend should be numbered so that they will be in sequence with references cited in the text at the point where the table or figure is first mentioned. List all authors when there are six or fewer; when there are seven or more, list the first six, then "et al." The following are sample references:

1. Maleki A, Shahmoradi B, Daraei H, Kalantar E. Assessment of ultrasound irradiation on inactivation of gram negative and positive bacteria isolated from hospital in aqueous solution. *J Adv Environ Health Res* 2013; 1(1): 9-14.
2. Buckwalter JA, Marsh JL, Brown T, Amendola A, Martin JA. Articular cartilage injury. In: Robert L, Robert L, Joseph V, editors. *Principles of Tissue Engineering*. 3rd ed. Burlington, MA: Academic Press; 2007. p. 897-907.
3. Kuczumski RJ, Ogden CL, Grammer-Strawn LM, Flegal KM, Guo SS, Wei R, et al. CDC growth charts: United States. Advance data from vital and health statistics. No. 314. Hyattsville, Md: National Center for Health Statistics, 2000. (DHHS publication no. (PHS) 2000-1250 0-0431)
4. World Health organization. Strategic directions for strengthening nursing and midwifery services [online]. Available from:
URL:<http://www.wpro.who.int/themes/focuses/theme3/focus2/nursingmidwifery.pdf>2002

Units of Measurement

Authors should express all measurements in conventional units, with Système International (SI) units given in parentheses throughout the text. Figures and tables should use conventional units, with conversion factors given in legends or footnotes. In accordance with the Uniform Requirements, however, manuscripts containing only SI units will not be returned for that reason.

Abbreviations

Except for units of measurement, abbreviations are discouraged. Consult *Scientific Style and Format: The CBE Manual for Authors, Editors, and Publishers* (Sixth edition. New York: Cambridge University Press, 1994) for lists of standard abbreviations. Except for units of measurement, the first time an abbreviation appears, it should be preceded by the words for which it stands.

Chemical Structure

Structures should be produced with a chemical drawing program, preferably ChemDraw 4.5 or higher, and submitted in TIFF format to allow use of electronic files in production. Structures should also be submitted in native file formats, e.g., RDX.

For any more detail about the writing style for your manuscripts refer to:

<http://www.jaehr.muk.ac.ir>

Authorship Form

Title of the manuscript:

.....
.....

We, the undersigned, certify that we take responsibility for the conduct of this study and for the analysis and interpretation of the data. We wrote this manuscript and are responsible for the decisions about it. Each of us meets the definition of an author as stated by the International Committee of Medical Journal Editors (see <http://www.icmje.org/icmje-recommendations.pdf>). We have seen and approved the final manuscript. Neither the article nor any essential part of it, including tables and figures, will be published or submitted elsewhere before appearing in the *Journal of Advances in Environmental Health Research* [All authors must sign this form or an equivalent letter.]

Name of Author

Contribution

Signature

_____	_____	_____
_____	_____	_____
_____	_____	_____
_____	_____	_____
_____	_____	_____
_____	_____	_____
_____	_____	_____
_____	_____	_____
_____	_____	_____
_____	_____	_____

Please scan this form and upload it as a supplementary file in “Step 4” of submitting articles.

Table of Contents

Original Article(s)

- Kinetic modeling of methylene blue adsorption onto acid-activated spent tea: A comparison between linear and non-linear regression analysis**
Ali Akbar Babaei, Zahra Alaei, Elham Ahmadpour, Amirhosein Ramazanpour-Esfahani197-208
- Effects of different temperatures and durations of heating on the reduction of Ochratoxin A in bread samples**
Masoud Hashemi-Karoui, Issa Gholampour-Azizi, Samaneh Rouhi, Mahdi Tashayyo209-214
- Radiological dose assessment of naturally occurring radioactive materials generated by the petroleum industry in wildlife: A case study of chinkaras of Lavan Island, Iran**
Siavash Sedighian, Mohammad Ali Abdoli, Mohammad Hossein Niksokhan, Min Jun Kim, Seung-Yeon Cho215-222
- Ecological Potential assessment of soil in agricultural lands in Hamedan Province, Iran, using geographic information system**
Karim Naderi-Mahdei, Abdolali Bahrami223-233
- Removal of hexavalent chromium from aqueous solution using canola biomass: Isotherms and kinetics studies**
Davoud Balarak, Yousef Mahdavi, Fardin Gharibi, Shahram Sadeghi234-241
- Assessment of health impacts attributed to PM10 exposure during 2011 in Kermanshah City, Iran**
Elahe Zallaghi, Mohammad Shirmardi, Zahra Soleimani, Gholamreza Goudarzi, Mohammad Heidari-Farsani, Ghassem Al-Khamis, Ali Sameri.....242-250
- Reduction of chromium toxicity by applying various soil amendments in artificially contaminated soil**
Mahboub Saffari, Najafali Karimian, Abdolmajid Ronaghi, Jafar Yasrebi, Reza Ghasemi-Fasaei251-262
- Estimation of target hazard quotients for metals by consumption of fish in the North Coast of the Persian Gulf, Iran**
Reza Khoshnood, Nemat Jaafarzadeh, Zahra Khoshnood, Mehdi Ahmadi, Pari Teymouri263-271



Kinetic modeling of methylene blue adsorption onto acid-activated spent tea: A comparison between linear and non-linear regression analysis

Ali Akbar Babaei¹, Zahra Alae², Elham Ahmadpour³, Amirhosein Ramazanpour-Esfahani⁴

1 Environmental Technologies Research Center AND Department of Environmental Health Engineering, School of Public Health, Ahvaz Jundishapur University of Medical Sciences, Ahvaz, Iran

2 Student Research Committee, Ahvaz Jundishapur University of Medical Sciences, Ahvaz, Iran

3 Department of Environmental and Occupational Health, Deputy of Health, Ahvaz Jundishapur University of Medical Sciences, Ahvaz, Iran

4 Department of Soil Science, School of Agriculture, Shahid Chamran University, Ahvaz, Iran

Original Article

Abstract

The kinetic study of methylene blue (MB) adsorption using acid-activated spent tea (AASST) as an adsorbent from aqueous solution with the aim of comparing linear and non-linear regression analysis methods was performed at varying initial MB concentrations (10-100 mg/l). Hence, spent tea leaves, which were activated using concentrated sulfuric acid, were prepared. The physicochemical characteristics of the prepared adsorbent were also measured. In addition, a scanning electron microscope (SEM) and Fourier transform infrared spectroscopy (FTIR) instruments were employed to determine the size, morphology, and functional groups of AASST. Furthermore, the influence of different particle sizes of adsorbent on the adsorptive removal efficiency of MB was evaluated. The obtained data on MB adsorption were fitted using 4 kinetic models, namely pseudo first-order, pseudo second-order, Elovich, and intraparticle diffusion (I-D). The results of kinetic investigations showed that pseudo second-order kinetic model compared to the other applied models, with significant coefficient of determination ($r^2 > 0.98$), could best fit the experimental data of MB adsorption. In addition, among all linear forms of the pseudo second-order model, form 1 could better fit the MB adsorption data. Additionally, by comparing the performance of both linear and non-linear forms of the pseudo second-order kinetic model, it can be postulated that non-linear regression analysis could be more appropriate than the linear approach for kinetic study of MB adsorption onto the AASST adsorbent. Ultimately, based on the results of particle size experiments, the smaller the size of the adsorbent particles, the higher the adsorption efficiency of MB will be.

KEYWORDS: Adsorption, Kinetic, Linear and Non-Linear Models, Methylene Blue, Spent Tea

Date of submission: 16 May 2014, **Date of acceptance:** 19 Jul 2014

Citation: Babaei AA, Alae Z, Ahmadpour E, Ramazanpour-Esfahani A. **Kinetic modeling of methylene blue adsorption onto acid-activated spent tea: A Comparison between linear and non-linear regression analysis.** J Adv Environ Health Res 2014; 2(4): 197-208.

Introduction

Removal of toxic compounds from soil and water resources has always been one of the most paramount concerns of environmentalists. Dyes

are colored substances and are found in the wastewater of several industries, such as textile, leather, paper, and plastic.¹ The discharge of such wastewater into the water resources will cause a wide range of problems, like harmful influence on photosynthesis and enhancement of the chemical oxygen demand (COD).²

Until now, numerous conventional

Corresponding Author:

Amirhosein Ramazanpour Esfahani

Email: a-ramazanpour@mscstu.scu.ac.ir

techniques, such as oxidation or ozonation,^{3,4} coagulation and flocculation,⁵ reduction,⁶ and membrane separation,⁷ have been employed to treat water polluted with MB or other colored compounds. These processes are apparently costly and have several operational difficulties, due to which they are not able to effectively eliminate large concentrations of MB from industrial and agricultural effluents. Therefore, the application of a cost-effective and highly efficient remediation technique is prescribed.

Among all treatment techniques, adsorption is recommended as a well-known and popular approach for removal of dyes due, in essence, to its operational simplicity, economic benefits, and insensitive nature toward poisonous substances. Based on existing literature, some agricultural waste products, such as wheat husk,^{8,9} rice husk,^{10,11} pomelo (*Citrus grandis*) peel,¹² and *Posidonia oceanica* (L.) fibres,¹³ as well as some cheap materials, like sawdust,¹⁴ perlite and clay,^{15,16} fly ash,¹⁷ and natural zeolite,¹⁸ were extensively investigated as alternative adsorbents for MB removal.

Tea plantation farms are widely visible in Northern Iran. Dried and smashed leaves of tea bushes have largely been consumed as one of the most popular beverages among Iranians. The remaining spent tea materials of tea production process are not practical and are either stored or disposed as waste. Hence, the management and utilization of these enormous wastes in the environmental context is a critical necessity. Until today, spent tea leaves have been used for remediation of a large number of environmental pollutants. Amarasinghe and Williams reported that the application of spent tea materials in the removal of copper and lead showed fruitful results.¹⁹ In another research, Wasewar et al. stated that tea factory waste materials, during batch experiment studies, could easily remove high concentrations of zinc from aqueous solution.²⁰ In the present study, spent tea materials were treated with concentrated sulfuric acid in order to increase their capacity to

adsorb MB from aqueous media.

To design a batch sorption system, the determination of kinetics reaction is a crucial point because through kinetic data, information on the rate of adsorbate uptake onto the adsorbent surfaces and factors influencing reaction rate are obtained.²¹ Generally, the most commonly used kinetic models to express the processes between liquid and solid surfaces are pseudo first-order and pseudo second-order models. Although some studies have revealed that pseudo first-order model can best fit the experimental data of contaminants adsorption,²² a research has confirmed the lack of ability of the corresponding model to predict the theoretical adsorption capacity of adsorbents.²³ In recent years, pseudo second-order model has been commonly used as it best expresses the kinetic reaction of some pollutants in a series of batch experiments. However, the linear form of the pseudo second-order model proposed by Blanchard et al. results in lackluster performance in the prediction of the adsorption capacity of pollutants.²³ Therefore, an analysis of the performance and ability of both linear and non-linear forms of kinetic models in predicting kinetic parameters is vital.

Even though MB adsorption using spent tea has been performed previously, to the best of our knowledge, no comparative study of non-linear and linear kinetic approaches of MB adsorption onto acid-activated spent tea (AAST) has been performed. Therefore, the objectives of the present paper are synthesis and characterization of AAST, and comparison of kinetic model efficiency and obtained kinetic parameters of MB adsorption onto AAST using both non-linear and linear methods.

Materials and Methods

MB ($C_{16}H_{18}ClN_3S \cdot 3H_2O$) (Figure 1), concentrated hydrochloric acid, sulfuric acid, and sodium hydroxide were purchased from Merck & Co. (Kenilworth, NJ, USA). All reagents were

analytical grades. The stock solution of MB was prepared by dissolving a segment of MB into 1000 mL of distilled water, then, diluting to reach MB solutions with desirable concentrations. Furthermore, the solutions were kept in a dry environment at 4 °C.

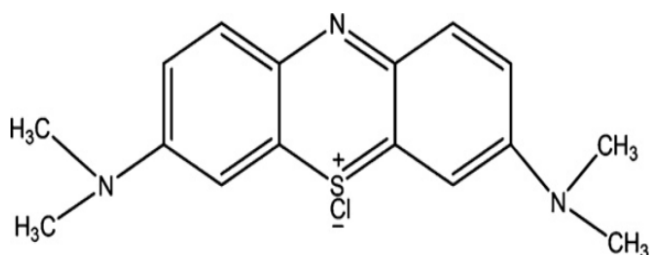


Figure 1. The structure of methylene blue

To prepare the adsorbent, spent tea material of household tea waste were employed. Initially, tea leaves were washed completely with distilled water to remove all chemical or physical impurities. Then, spent tea was decolorized through boiling in distilled water at 100 °C, and, subsequently, kept and dried in an electric oven at 65 °C. Then, the resulted spent tea was activated through immersion in a strong sulfuric acid solution followed by a few minutes of vigorous shaking. Then, they were washed with distilled water to reach a pH of 7. The principal objective of acid washing of adsorbent was the activation of the adsorbent surfaces through the creation of numerous pores on the internal and external surfaces in order to increase the ability of adsorbent to remove MB. In the next step, obtained AAST materials were oven dried at 105 °C, and then, passed through a range of steel sieves. In accordance with the ASTM Method, only particles between 100 and 250 µm in diameter mesh size were used throughout the study, apart from studying the effect of adsorbent particle size. Finally, AAST was dried at 80-85 °C for about 2 hours, and then, kept in plastic bags in a dry environment until the beginning of the batch experiments.

Initially, the moisture and ash content, chemical composition, water soluble and insoluble substances, and the volatile fraction of

the adsorbent were determined. To find the morphological features of AAST, a scanning electron microscope (SEM) (Philips Co., Netherlands) was applied. Furthermore, Fourier transform infrared spectroscopy (FTIR) was used to find the surface functional groups of the AAST. The specific surface area of adsorbent was measured using adsorption/desorption technique using the Brunauer-Emmett-Teller (BET) method. Moreover, pH of zero point charge (pH_{ZPC}) of AAST was measured at varying pH values according to the Yargic et al. method.²⁴ In addition, the sieve and Gay-Lussac pycnometer methods were also applied to determine the size and bulk density of AAST, respectively.

In this research, kinetic study of MB adsorption onto AAST was carried out in a series of batch experiments at room temperature (25 ± 2 °C). Regarding batch experiments, 0.5 g of adsorbent was added to amber glass bottles containing various initial MB concentrations (10, 25, 50, and 100 mg/l) with optimum pH of 7.0. The optimum pH value of 7.0 of the batch experiments was obtained from similar previous experiments. In addition, both 0.1 M HCl and 0.1 M NaOH solutions were used to adjust the pH of MB solution. Then, the bottles were placed in a shaker and rotated vigorously with the intensity of 300 rpm for 1 to 300 minute time intervals. Subsequently, to separate the adsorbents from MB solutions, samples were centrifuged at 5000 rpm for around 5 minutes. The residual concentration of MB in solutions was measured using a UV-visible spectrophotometer (SPEKOL 2000, Analytik Jena, Germany) at its maximum MD absorbance wavelength of 665 nm. Finally, the adsorption capacity (q_t) of MB onto the AAST was calculated using the following equation:

$$q_t = \frac{V(C_0 - C_e)}{m} \quad (1)$$

Where C_0 and C_e are the initial and final concentrations of MB (mg/l) in the solution, V is the solution volume (L), and m is the weight of adsorbent (g).

Finally, the effect of the size of AAST particles was also studied in two different size ranges of 210-250 μm and 53-63 μm for varying dosages of AAST adsorbent (0.5 and 5.0 g/l).

The kinetic investigation of MB adsorption onto the AAST surfaces was performed via four widely used models, namely Lagergren's pseudo first-order, Ho's pseudo second-order, Elovich, and Weber and Morris's intraparticle diffusion. The non-linear forms of pseudo first-order, pseudo second-order, Elovich, and intraparticle diffusion kinetic models are expressed in equations 2, 3, 4, and 5, respectively, as follows:²⁵⁻²⁸

$$q_t = q_e(1 - \exp(-k_1 t)) \quad (2)$$

$$q_t = \frac{k_2 q_e^2 t}{1 + k_2 q_e t} \quad (3)$$

$$q_t = \left(\frac{1}{\beta}\right) \ln(1 + \alpha\beta t) \quad (4)$$

$$q_t = k_{id} \sqrt{t} + C_i \quad (5)$$

Where q_e and q_t (mg/g) are the adsorbed amount of MB at equilibrium state and at any time (t) (min). Furthermore, k_1 (1/min) and k_2 (mg/g.min) are the rate of sorption for pseudo first and pseudo second-order models, respectively. α (mg/g.min) and β (g/mg) are the constants of the Elovich kinetic model. Moreover, k_{id} (mg/g.min) and C_i are the intraparticle diffusion constant and constant depicting the boundary layer effect, respectively.

The complete linear forms of pseudo second-order kinetic model are demonstrated in table 1. Furthermore, to examine the reliability of all

applied models and their fitness to the experimental data of MB adsorption, r^2 as a valid and authenticated index was used as follows:²⁹

$$r^2 = \frac{\sum(q_m - q)^2}{\sum(q_m - q)^2 + \sum(q_m - q_t)^2} \quad (6)$$

Where q_m and q_t are the quantity of adsorbed pollutant onto the adsorbent at equilibrium contact time and any time (t) (mg/g), respectively. Moreover, q is the average of q_t .

Additionally, to obtain the kinetic parameters of MB adsorption onto the AAST using non-linear and linear approaches, MATLAB® version 7.11.0 (R2010b, The Mathworks Inc. Natick, MA, USA) and Microsoft Excel (Microsoft, Redmond, WA, USA) were used, respectively.

Results and Discussion

Characterization

Several selected physicochemical features of AAST are presented in table 2. Accordingly, pH_{zpc} of AAST was obtained (5.0 ± 0.2). Since, pH value of solution is lower than 5, surface charges of AAST will be positive. However, at pH values higher than 5, negative charges will occupy the surfaces of AAST and this plays a critical role in cationic dye adsorption. In this study, all experiments were performed at a pH value of 7.0, based on 2 degrees deviation from pH_{zpc} , and desirable conditions were provided for MB adsorption. Moreover, specific surface area of AAST was obtained to be 285.5 m^2/g that will be considered as an undeniable proof of the ability of AAST in MB adsorption.

Table 1. Linear forms of pseudo second-order kinetic model

Model type	Equation	Plot	Parameters
1	$\frac{t}{q} = \frac{1}{k_2 q_e^2} + \frac{1}{q_e} t$	t/q vs. t	$q_e = 1/\text{slope}$, $k_2 = \text{slope}^2/\text{intercept}$
2	$\frac{1}{q} = \left(\frac{1}{k_2 q_e^2}\right) \frac{1}{t} + \frac{1}{q_e}$	1/q vs. 1/t	$q_e = 1/\text{intercept}$, $k_2 = \text{intercept}^2/\text{slope}$
3	$q = q_e - \left(\frac{1}{k_2 q_e}\right) \frac{q_t}{t}$	q vs. q/t	$q_e = \text{intercept}$, $k_2 = -1/(\text{intercept} \times \text{slope})$
4	$\frac{q}{t} = k_2 q_e^2 - k_2 q_e q$	q/t vs. q	$q_e = -\text{intercept}/\text{slope}$, $k_2 = \text{slope}^2/\text{intercept}$

q_e : 1/slope; k_2 : slope²/intercept; t: Time

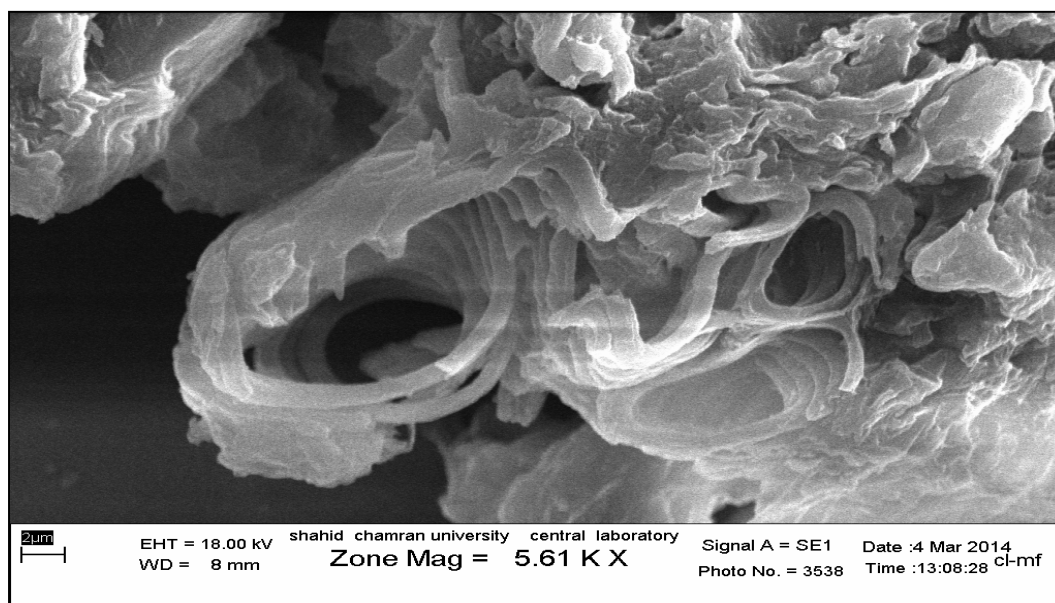
Table 2. Several physicochemical characteristics of acid-activated spent tea (AAST)

Parameters	Values
Moisture content (%)	3.72 ± 0.4
Water soluble compounds (%)	1.20 ± 0.3
Insoluble compounds (%)	95.10 ± 0.4
Volatile fraction (%)	64.30 ± 2.9
Ash content (%)	30.90 ± 2.7
Elemental analysis (%)	
C	57.50 ± 1.1
H	7.30 ± 0.5
N	0.4
O	30.30 ± 0.9
S	4.50 ± 0.3
pH _{pzc}	5.00 ± 0.2
Bulk density (kg/m ³)	258
Particle size (μm)	100-250
BET surface area (m ² /g)	285.5

BET: Brunauer–Emmett–Teller

Figure 2 illustrates the SEM image of AAST. Based on figure 2, the porous and rough structure of AAST is evident which is attributed to the effect of treatment with strong sulfuric acid. The created porosity on the AAST surfaces is a great tool to increase the capacity of the adsorbent in adsorbing the adsorbate. The FTIR spectra of AAST before and after adsorption of MB are presented in figure 3. As shown in figure 3 and table 3, the spectra display a number of

absorption peaks, indicating the complex nature of the AAST. As it is clear from figure 3, the presence of OH-phenolic functional group is proved by a broad band peak at 3396 cm⁻¹.³⁰ The aliphatic C-H stretch in cellulose and hemicelluloses are assigned at wave numbers of 2924 cm⁻¹, 2853 cm⁻¹, and 1457 cm⁻¹.³¹⁻³³ In addition, the carbonyl stretch of carboxyl and C=O stretching mode conjugated with the NH₂ are illustrated in 1719 cm⁻¹ and in the range of 1640–1660 cm⁻¹, respectively.³¹ The two peaks at wave numbers of 1519 cm⁻¹ and 1319 cm⁻¹ are attributed to the secondary amine group and symmetric bending of CH₃, respectively.³³ Table 3 illustrates the absorption peak of all functional groups of AAST surfaces before and after adsorption of MB. It can be seen that among all mentioned functional groups, bonded -OH groups, secondary amine group, C=O stretching of ether group, aliphatic C-H group, C-N stretch of aliphatic amines, and symmetric bending of CH₃ have important roles in the process of adsorption of MB from aqueous solution.³⁴ Several adsorption bands participating in the biosorbent indicated that AAST is an excellent sorbent for the removal of MB.

**Figure 2.** Scanning electron microscope (SEM) image of acid-activated spent tea (AAST)

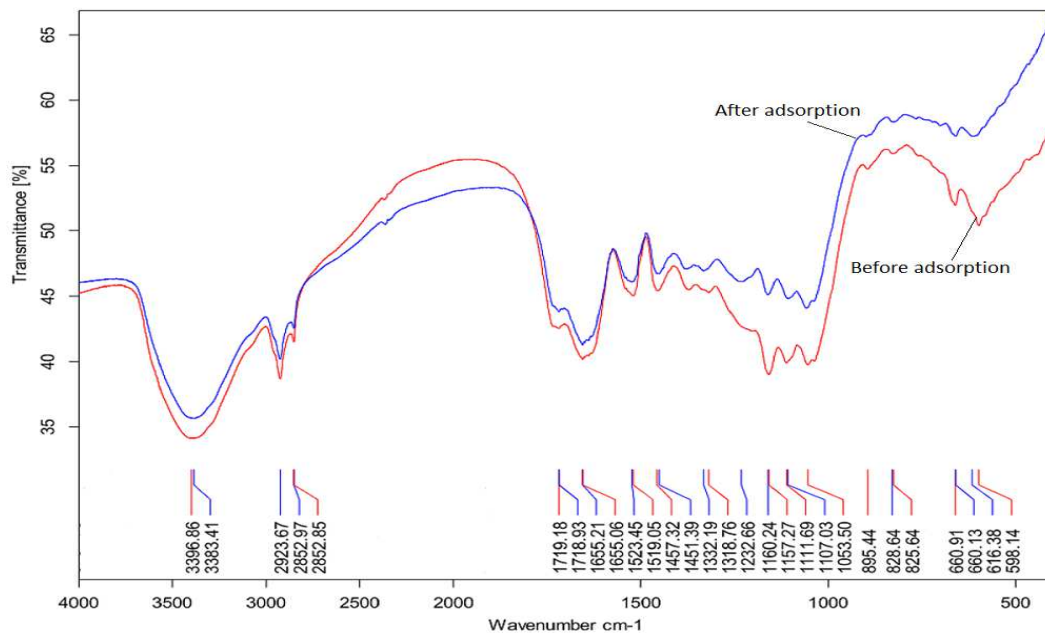


Figure 3. Fourier transform infrared spectroscopy (FTIR) spectra of acid-activated spent tea (AAST) before and after adsorption of methylene blue (MB)

Table 3. Fourier transform infrared spectroscopy (FTIR) spectra of acid-activated spent tea (AAST) before and after adsorption of methylene blue (MB)

FTIR peaks	Frequencies (cm ⁻¹)			Assignment
	Before adsorption	After adsorption	Differences	
1	3397	3383	+14	Bonded-OH groups
2	2924	2924	0	aliphatic C-H stretch
3	2853	2853	0	aliphatic C-H stretch
6	1719	1719	0	carbonyl stretch of carboxyl
7	1655	1655	0	C=O stretching
8	1519	1523	-4	secondary amine group
9	1457	1451	+6	aliphatic C-H stretch
10	1319	1332	-13	symmetric bending of CH ₃
11	1157	1160	-3	C=O stretching of ether groups
12	1112	1107	+5	C-N stretch of aliphatic amines
13	1054	Disappeared	Unknown	C=O stretching
14	895	Disappeared	Unknown	aromatic C-H stretching
15	826	829	-3	aromatic C-H stretching
16	661	660	+1	C-Br stretch of alkyl halides
17	598	616	-18	C-Br stretch of alkyl halides

FTIR: Fourier transform infrared spectroscopy

Kinetic studies

Kinetic studies of MB adsorption onto AAST surfaces were accurately carried out using four widely used non-linear kinetic models together with four linear types of the pseudo second-order model. The non-linear graphs of pseudo first-order, pseudo second-order, Elovich, and

intraparticle diffusion models were depicted based on the adsorption time (t) against the adsorption capacity of MB (q_t) (Figure 4). As is clear from figure 4, the kinetic of reaction between adsorbent and adsorbate was apparently high in the first 30 minutes of the experiments; over 90% of the initial MB concentration was adsorbed onto the AAST

surfaces. However, with the passing of time, reaction decreases and reaches equilibrium state. The most probable reason for this observation is rooted mainly in the vacancy of surface area of adsorbents and their extreme tendency toward adsorbate sorption which will drop significantly with the passing of reaction time and filling of the surface area. The results of non-linear kinetic studies have been reported in table 4. Accordingly, the obtained q_t of pseudo first-order and pseudo second-order models has a significant correlation with the experimental q_t . Furthermore, the pseudo second-order model, in

comparison with other models, has the highest r^2 with the experimental data in all initial MB concentrations (except 10 mg/l). The findings of the study by Yao et al. showed that the data on MB adsorption onto the carbon nanotube had the most significant correlation with the pseudo second-order kinetic model.³⁵

Moreover, the linear graphs of the pseudo second-order model are illustrated in figure 5. In order to obtain kinetic parameters using linear approach, the graphs 5 (a-d) were drawn based on t vs. t/q , $1/t$ vs. $1/q$, q vs. q/t , and q/t vs. q , respectively.

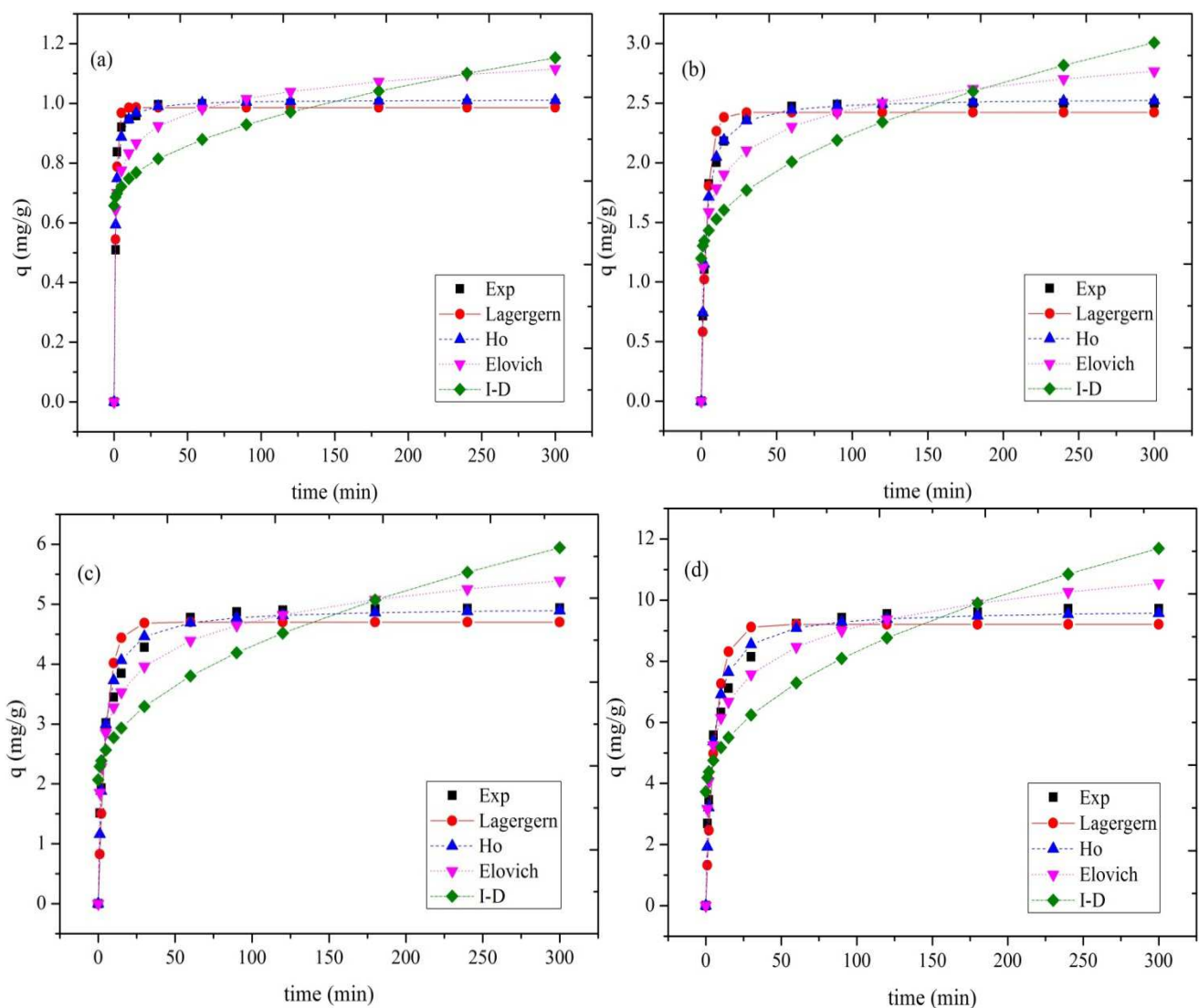


Figure 4. Non-linear kinetic plot of MB adsorption onto AAST surfaces at different initial MB concentrations (a: 10, b: 25, c: 50, and d: 100 mg/l⁻¹)

Table 4. Kinetic parameters of methylene blue (MB) adsorption onto acid-activated spent tea (AAST) surfaces using non-linear regression approach

Model	Parameter	Initial MB concentrations (mg/l)			
		10	25	50	100
Pseudo first-order	q_e (mg/g)	0.986	2.422	4.700	9.207
	k_1 (1/min)	0.803	0.274	0.193	0.156
	r^2	0.991	0.979	0.944	0.940
Pseudo second-order	q_e (mg/g)	1.013	2.543	4.946	9.702
	k_2 (g/mg.min)	1.398	0.163	0.062	0.026
	r^2	0.984	0.998	0.990	0.987
Elovich	α (mg/g.min)	197.10	14.15	12.26	14.93
	β (g/mg)	12.09	3.47	1.61	0.77
	r^2	0.889	0.922	0.966	0.973
Intraparticle diffusion	k_{id} (mg/g.min)	0.029	0.104	0.224	0.460
	C_i	0.658	1.199	2.068	3.727
	r^2	0.326	0.552	0.660	0.702

q_e : 1/slope; k_2 : slope²/intercept; k_{id} : intraparticle diffusion constant; C_i : constant depicting the boundary layer effect

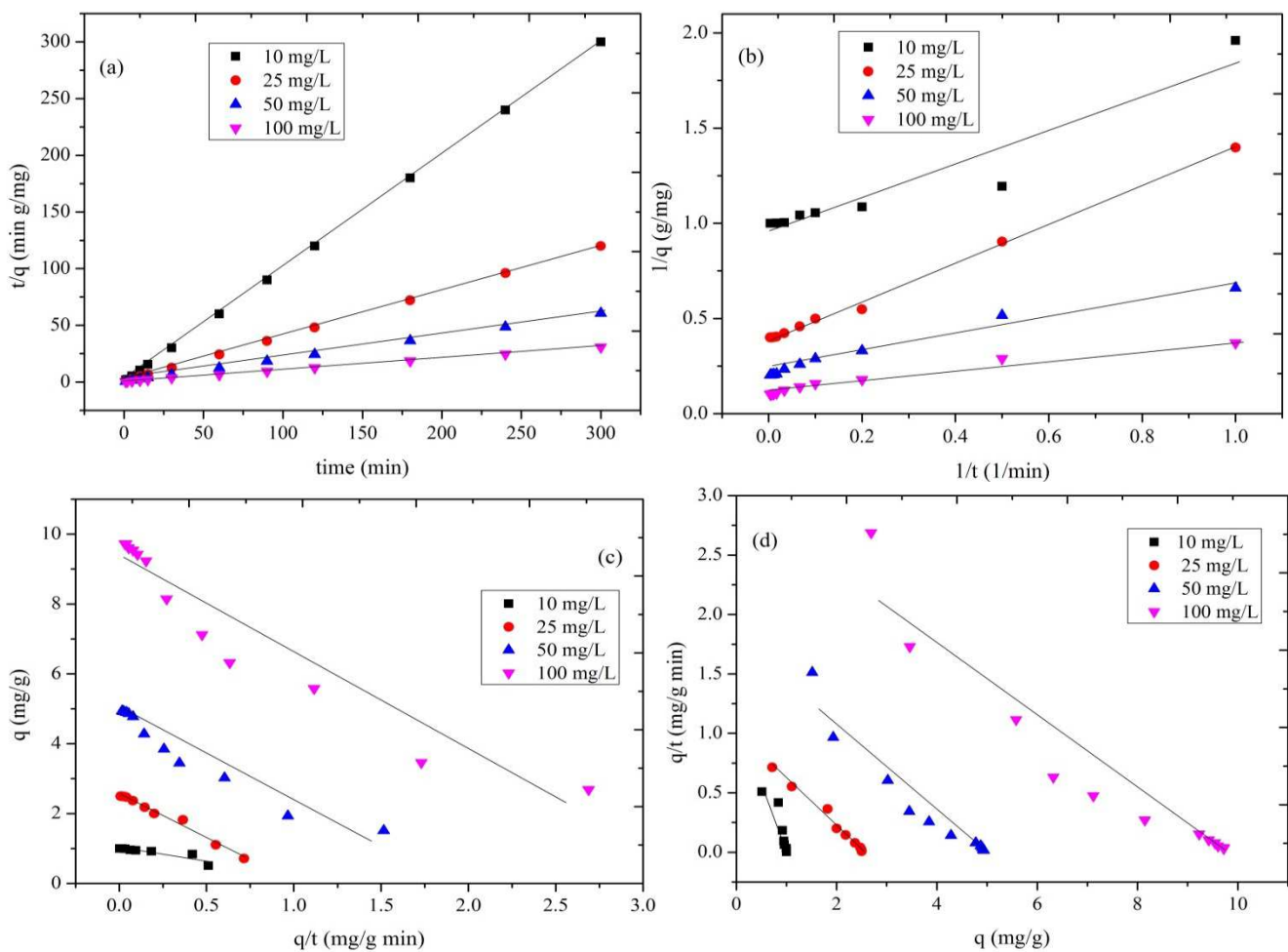
**Figure 5.** Linear plot of pseudo second-order kinetic model of methylene blue (MB) onto acid-activated spent tea (AAST) surfaces (a: form 1, b: form 2, c: form 3, and d: form 4)

Table 5 shows the kinetic parameters of four linear forms of the pseudo second-order model at various initial MB concentrations. Increasing initial MB concentrations from 10 to 100 mg/l caused considerable enhancement in the adsorption capacity of MB. Kumar and Tamilarasan, in a similar study, stated that an increasing trend was observed in MB adsorption capacities onto the *Acacia fumosa* seed shell activated carbon as a result of increasing the initial MB concentrations.³⁶ According to table 5, the linear form 1 of pseudo second-order had the maximum r^2 value that confirm its correlation with experimental data of MB adsorption, while forms 3 and 4 showed lower correlation. The differences between obtained parameters of linear models were mainly derived from the complexity in calculating the kinetic parameters. Such contradiction revealed that changing the non-linear to linear methods triggered significant transformation in obtained results and reduction of their validity. The various outcome parameters, in addition, of varying linear types of pseudo second-order are principally due to the changing error function that is differentiated by the linearization process of non-linear models. Of course, such error function, depending on the linearization method, may lead to either better or worse outcome parameters. The linear regression

concept is based on the belief that the distribution of points in adjacency of the line follows the Gaussian distribution in which the standard deviation is relatively similar at each X value. Such assumptions are not correct after the alteration of the experimental data that will entirely change the relationship between X and Y . In this regard, form 1 of the pseudo second-order model, compared to forms 3 and 4, can better fit the experimental data of MB adsorption with relatively high r^2 . Consequently, it can be said that changing the non-linear to linear approach led to improvement of the efficiency of form 1, while in the case of forms 3 and 4, lower performance efficiency was observed. Additionally, different outputs of the four linear types of pseudo second-order can be ascribed to the various axial conditions that change the findings of linear regression method and impact the determination procedure.³⁷ linear method only indicates the slope and intercept that are useful for predicting Y for corresponding X values. Therefore, the appropriateness of fitting experimental data to various linear forms which originate from different axial settings would be adjustable. In the linear regression approach, it is not considered whether the kinetic reaction trend is linear or not, but it is supposed that the experimental data are intrinsically linear.

Table 5. kinetic parameters of methylene blue (MB) adsorption onto acid-activated spent tea (AAST) surfaces using linear regression approach

Pseudo second-order kinetic model	Parameter	Initial MB concentrations (mg/l)			
		10	25	50	100
Form 1	q_e (mg/g)	1.002	2.522	5.005	9.881
	k_2 (g/mg.min)	2.166	0.196	0.058	0.022
	r^2	1.000	1.000	1.000	1.000
Form 2	q_e (mg/g)	1.044	2.568	4.710	9.093
	k_2 (g/mg.min)	0.965	0.150	0.090	0.041
	r^2	0.920	0.998	0.968	0.965
Form 3	q_e (mg/g)	1.031	2.566	4.653	8.961
	k_2 (g/mg.min)	1.076	0.151	0.096	0.044
	r^2	0.920	0.998	0.968	0.965
Form 4	q_e (mg/g)	.031	2.490	4.774	9.278
	k_2 (g/mg.min)	1.089	0.115	0.029	0.007
	r^2	0.836	0.989	0.927	0.774

q_e : 1/slope; k_2 : slope²/intercept; MB: Methylene blue

In addition, different outputs of the linearization process apparently proved that in the case of linear method, X value is absolutely clear while Y is uncertain. Moreover, according to tables 4 and 5, the reaction rate coefficient (k_2), an important parameter in the adsorption process design, estimated by linear models differs from that estimated by non-linear models. Therefore, the use of a linear model is a questionable and controversial approach to determining kinetic parameters. This evidence supports the likelihood of abnormality assumption for linear regression approach. Therefore, since in non-linear regression method, error structure does not change and all the kinetic parameter are fixed in a similar axis, it would be advantageous to predict the parameters related to kinetic study of experimental data of MB adsorption.

Effect of particles size

In the adsorption process, particle size and surface area of the adsorbent are the most important factors affecting the adsorption capacity. Therefore, the effect of particle size on the removal of MB was studied with two different size ranges of 210-250 μm and 53-63 μm . As shown in figure 6, decreasing the particle size of AAST adsorbent from the range of 210-250 μm to 53-63 μm has increased the removal efficiency of the initial concentration of 50 mg/l MB dye from 31.8 to 42.5% and from 87.0 to 97.5% using 0.5 g/L and 5.0 g/l AAST adsorbents, respectively. The extent of the adsorption process increases with increased specific surface areas. The specific surface available for adsorption will be greater for smaller particles, and hence, the adsorption efficiency of MB increases as particle size decreases. For larger particles, the diffusion resistance to mass transport is higher, and most of the internal surface of the particle may not be utilized for adsorption. Consequently, lower amounts of MB are adsorbed. These results demonstrate that smaller particles provide more surface area, and thus, increase the adsorption capacity.

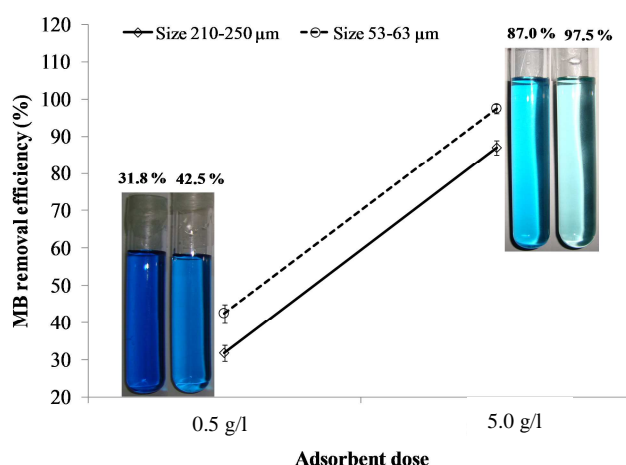


Figure 6. Particle size effect of acid-activated spent tea (AAST) on methylene blue (MB) adsorption efficiency ($\text{pH} = 7.0 \pm 0.1$; time = 120 min, $C_0 = 50 \text{ mg/l}$)

Conclusion

In the present study, a kinetic survey of MB adsorption was performed using the four most common kinetic models. Furthermore, the linear and non-linear forms of pseudo second-order kinetic model were fitted to the experimental data of MB adsorption onto AAST surfaces. The findings of batch experiments revealed that MB adsorption is a merely concentration-dependent process and entirely depends on the initial MB concentration. Among all kinetic models, the pseudo second-order model, due, principally, to its high r^2 , best fit the obtained data. Moreover, investigation of the linear forms of pseudo second-order model demonstrated that, in all initial MB concentrations, form 1 best fit the MB adsorption data. Additionally, comparison of linear and non-linear kinetic methods revealed that non-linear approach, due to the lack of disorder on error construction, is the best method to undertake a kinetic study. Therefore, based on the findings of this research, the use of the non-linear approach of kinetic models is confidently advised in the study of contaminant removal. Furthermore, results of particle size experiments indicated that higher MB adsorption was apparently achieved in lower size adsorbents. This study shows that AAST is a promising biosorbent for the removal of dye

from colored aqueous solutions.

Conflict of Interests

Authors have no conflict of interests.

Acknowledgements

The authors would like to thank the Student Research Committee and the Research and Technology Deputy of Ahvaz Jundishapur University of Medical Sciences for providing financial support (grant No: 92.S.12) for this study.

References

- Ravikumar K, Deebika B, Balu K. Decolourization of aqueous dye solutions by a novel adsorbent: application of statistical designs and surface plots for the optimization and regression analysis. *J Hazard Mater* 2005; 122(1-2): 75-83.
- Bulut Y, Aydin H. A kinetics and thermodynamics study of methylene blue adsorption on wheat shells. *Desalination* 2006; 194(1-3): 259-67.
- Malik PK, Saha SK. Oxidation of direct dyes with hydrogen peroxide using ferrous ion as catalyst. *Separation and Purification Technology* 2003; 31(3): 241-50.
- Koch M, Yediler A, Lienert D, Insel G, Kettrup A. Ozonation of hydrolyzed azo dye reactive yellow 84 (CI). *Chemosphere* 2002; 46(1): 109-13.
- Panswad T, Wongchaisuwan S. Mechanisms of Dye Wastewater Colour Removal by Magnesium Carbonate-Hydrated Basic. *Water Science & Technology* 1986; 18(3): 139-44.
- Arabi S, Sohrabi MR. Removal of methylene blue, a basic dye, from aqueous solutions using nano-zerovalent iron. *Water Sci Technol* 2014; 70(1): 24-31.
- Al-Bastaki N, Banat F. Combining ultrafiltration and adsorption on bentonite in a one-step process for the treatment of colored waters. *Resources, Conservation and Recycling* 2004; 41: 103-13.
- Gupta VK, Jain R, Varshney S. Removal of Reactofix golden yellow 3 RFN from aqueous solution using wheat husk-an agricultural waste. *J Hazard Mater* 2007; 142(2): 443-8.
- Gupta VK, Jain R, Varshney S, Saini VK. Removal of Reactofix Navy Blue 2 GFN from aqueous solutions using adsorption techniques. *J Colloid Interface Sci* 2007; 307(2): 326-32.
- Han R, Wang Y, Yu W, Zou W, Shi J, Liu H. Biosorption of methylene blue from aqueous solution by rice husk in a fixed-bed column. *J Hazard Mater* 2007; 141(3): 713-8.
- Vadivelan V, Kumar KV. Equilibrium, kinetics, mechanism, and process design for the sorption of methylene blue onto rice husk. *J Colloid Interface Sci* 2005; 286(1): 90-100.
- Hameed BH, Mahmoud DK, Ahmad AL. Sorption of basic dye from aqueous solution by pomelo (*Citrus grandis*) peel in a batch system. *Colloids and Surfaces A: Physicochemical and Engineering Aspects* 2008; 316(1-3): 78-84.
- Ncibi MC, Mahjoub B, Seffen M. Kinetic and equilibrium studies of methylene blue biosorption by *Posidonia oceanica* (L.) fibres. *J Hazard Mater* 2007; 139(2): 280-5.
- Garg VK, Amita M, Kumar R, Gupta R. Basic dye (methylene blue) removal from simulated wastewater by adsorption using Indian Rosewood sawdust: a timber industry waste. *Dyes and Pigments* 2004; 63(3): 243-50.
- Gurses A, Dogar C, Yalcin M, Acikyildiz M, Bayrak R, Karaca S. The adsorption kinetics of the cationic dye, methylene blue, onto clay. *J Hazard Mater* 2006; 131(1-3): 217-28.
- Dogan M, Alkan M, Turkyilmaz A, Ozdemir Y. Kinetics and mechanism of removal of methylene blue by adsorption onto perlite. *J Hazard Mater* 2004; 109(1-3): 141-8.
- Kumar KV, Ramamurthi V, Sivanesan S. Modeling the mechanism involved during the sorption of methylene blue onto fly ash. *J Colloid Interface Sci* 2005; 284(1): 14-21.
- Han R, Wang Y, Zou W, Wang Y, Shi J. Comparison of linear and nonlinear analysis in estimating the Thomas model parameters for methylene blue adsorption onto natural zeolite in fixed-bed column. *J Hazard Mater* 2007; 145(1-2): 331-5.
- Amarasinghe BMWP, Williams RA. Tea waste as a low cost adsorbent for the removal of Cu and Pb from wastewater. *Chemical Engineering Journal* 2007; 132(1-3): 299-309.
- Wasewar KL, Atif M, Prasad B, Mishra IM. Batch adsorption of zinc on tea factory waste. *Desalination* 2009; 244(1-3): 66-71.
- Ho YS, McKay G. Pseudo-second order model for sorption processes. *Process Biochemistry* 1999; 34(5): 451-65.
- Allen SJ, Gan Q, Matthews R, Johnson PA. Kinetic modeling of the adsorption of basic dyes by kudzu. *J Colloid Interface Sci* 2005; 286(1): 101-9.
- Blanchard G, Maunaye M, Martin G. Removal of heavy metals from waters by means for natural zeolites. *Water Res* 1984; 18(2): 1501-7.
- Yargic A, Yarbay Sahin RZ, Ozbay N, Onal E. Assessment of toxic copper(II) biosorption from aqueous solution by chemically-treated tomato waste. *Journal of Cleaner Production* 2015; 88(0): 152-9.

25. Lagergren S. About the theory of so-called adsorption of soluble substances, *Kungliga Sven. Vetensk Handl* 1898; 24: 1-39.
26. Ho YS, McKay G. The kinetics of sorption of basic dyes from aqueous solution by sphagnum moss peat. *The Canadian Journal of Chemical Engineering* 1998; 76(4): 822-7.
27. Ho YS, McKay G. Application of Kinetic Models to the Sorption of Copper(II) on to Peat. *Adsorption Science & Technology* 2002; 20(8): 797-815.
28. Weber WJ, Morris JC. Kinetics of Adsorption on Carbon from Solution. *Journal of the Sanitary Engineering Division* 1963; 89(2): 31-60.
29. Ng JCY, Cheung WH, McKay G. Equilibrium Studies of the Sorption of Cu(II) Ions onto Chitosan. *Journal of Colloid and Interface Science* 2002; 255(1): 64-74.
30. Lin-Vien D, Colthup NB, Fateley WG, Grasselli JG. *The Handbook of Infrared and Raman Characteristic Frequencies of Organic Molecules*. Philadelphia, PA: Elsevier; 1991.
31. Kapoor A, Viraraghavan T. Heavy metal biosorption sites in *aspergillus niger*. *Bioresource Technology* 1997; 61(3): 221-7.
32. Yun YS, Park D, Park JM, Volesky B. Biosorption of trivalent chromium on the brown seaweed biomass. *Environ Sci Technol* 2001; 35(21): 4353-8.
33. Malkoc E, Nuhoglu Y. Removal of Ni(II) ions from aqueous solutions using waste of tea factory: adsorption on a fixed-bed column. *J Hazard Mater* 2006; 135(1-3): 328-36.
34. Baran A, Bicak E, Baysal SH, Onal S. Comparative studies on the adsorption of Cr(VI) ions on to various sorbents. *Bioresour Technol* 2007; 98(3): 661-5.
35. Yao Y, Xu F, Chen M, Xu Z, Zhu Z. Adsorption behavior of methylene blue on carbon nanotubes. *Bioresour Technol* 2010; 101(9): 3040-6.
36. Kumar M, Tamilarasan R. Modeling studies for the removal of methylene blue from aqueous solution using *Acacia fumosa* seed shell activated carbon. *Journal of Environmental Chemical Engineering* 2013; 1(4): 1108-16.
37. Ho YS. Selection of optimum sorption isotherm. *Carbon* 2004; 42: 2113-30.



Effects of different temperatures and durations of heating on the reduction of Ochratoxin A in bread samples

Masoud Hashemi-Karouei¹, Issa Gholampour-Azizi², Samaneh Rouhi², Mahdi Tashayyo¹

¹ Department of Microbiology, Islamic Azad University, Tonekabon Branch, Tonekabon, Iran

² Department of Microbiology, Islamic Azad University, Babol Branch, Babol, Iran

Original Article

Abstract

Ochratoxin A (OTA) is a mycotoxin produced in corn, rice, and flour. It is a major concern for animal and human health. The purpose of this study was the evaluation of OTA contamination in bread samples gathered from bakeries, in different temperatures and durations of heating. In this study, 32 samples (4 samples of flour and 28 samples of bread) were randomly collected from different bakeries in Babol city, Mazandaran province, Iran, in fall 2013. The OTA content of the samples was measured in different temperatures and durations of heating using competitive direct enzyme-linked immunosorbent assay (CD-ELISA) method. Nonparametric Kruskal-Wallis was applied for data analysis. Results proved that reduction in the amount of OTA in samples during the heating process was significant and longer duration of heating was more effective, than raising the temperature, on OTA reduction. The highest percentage of OTA reduction occurred in constant temperature and when 2 minutes were added to the original time of heating. The lowest reduction rate of this toxin was observed in constant temperature and when 4 minutes was deducted from the original time in each bakery. Our study showed that bread and flour samples do in fact contain OTA, but this toxin is being reduced through heating. Since bread is the most consumed food in the world and also Iran, determination, management, and reduction of OTA in bread should be considered seriously.

KEYWORDS: Bread, Ochratoxin A Reduction, Temperatures, Heating

Date of submission: 16 May 2014, **Date of acceptance:** 19 Jul 2014

Citation: Hashemi Karouei M, Gholampour-Azizi I, Rouhi S, Tashayyo M. **Effects of different temperatures and durations of heating on the reduction of Ochratoxin A in bread samples.** *J Adv Environ Health Res* 2014; 2(4): 209-14.

Introduction

Mycotoxins are secondary metabolites that are produced by fungi. Aflatoxins, trichothecenes, zearalenone, fumonisins, and ochratoxins are important mycotoxins found in cereals.¹ Ochratoxin has three types of A, B, and C which have some chemical differences. This toxin has a colorless and crystallized compound. Ochratoxin A (OTA) is a common type of Ochratoxin.² The chemical structure of OTA is 7-L- β -phenylalanylcarbonyl-5-chloro-8-hydroxy-3, 4-

dihydro-3-R-methyl-isocoumarin.³ OTA is produced by *Aspergillus ochraceus*, *Aspergillus carbonarius*, and *Aspergillus niger* in tropical regions, and by *Penicillium verrucosum* in temperate regions.⁴ This toxin has been found in different foods such as corn, rice, soybean, coffee, cocoa, bean, and pea and also corn derivatives such as flour, bread, and pasta.⁵ OTA has nephrotoxic, immunotoxic, carcinogenic, teratogenic, and genotoxic effects and it has been associated with human and animal kidney diseases.⁶ The International Agency for Research on Cancer (IARC) has given a group 2B classification to OTA.³ The Iranian maximum tolerated level for OTA is 5 ng/g in human

Corresponding Author:

Mahdi Tashayyo

Email: microbiol_sci@yahoo.com

food.⁷ European Commission (EC) has determined the maximum tolerated OTA level to be 5 ng/g for cereals and 3 ng/g for their derived products. According to EC, the tolerable weekly intake (TWI) of OTA is 120 ng/kg bw/week for humans.⁶ Several studies have shown the production of mycotoxins in food products, and the reduction and change in concentration of different mycotoxins based on heating in human food. Meca et al., in Canada, detected *Fusarium* mycotoxin (Beauvericin (BEA) (5 mg/kg)) decomposition in barley and wheat flour during beer and bread making. During the bread making process, BEA reduction ranged from 75% to 95%.⁸ van der Stegen et al., in the Netherlands, studied green coffee contaminated by OTA and showed that during the roasting time which lasted from 2.5 to 10 minutes, OTA was reduced 69%.⁹ Kristensen et al., in Denmark, using 64 °C for 10.5 minutes, reduced 99% of the yeast and 98% of the filamentous fungi in rye bread and confirmed that drum drying did not destroy OTA.¹⁰ In another study in Iran, Gholampour Azizi reported that from 100 grape juice and raisin samples, 32 grape juice and 4 raisin samples had contamination rates higher than that of the EC limit (10 µg/kg).¹¹ The climatic conditions of Mazandaran province (northern Iran) provide a good environment for fungi growth and mycotoxins occurrence such as OTA (because in northern regions of Iran, the weather is humid and mild). Bread is the most consumed food in the world and Iran. Therefore, the purpose of this study was to evaluate OTA in several bread samples, based on different temperatures and durations of heating, using the competitive direct enzyme-linked immunosorbent assay (CD-ELISA) method in Babol city (Mazandaran province, Northern Iran).

Materials and Methods

In this study, 32 samples from 4 bakeries (8 samples per bakery: 1 sample of flour and 7

samples of bread) in Babol were randomly collected. The constant temperature and time of heating in each bakery, which prepared normal bread, were bakery A: 320 °C and 6 minutes, B: 185 °C and 8:45 minutes, C: 280 °C and 6:30 minutes, and D: 200 °C and 8:30 minutes. Samples from each bakery included: 1 sample of wheat flour (the flour with which bread was baked and was the basis for other samples and it was not heated), 1 sample of normal bread baked for the original time and with constant temperature of heating in the bakeries, 1 sample baked for the original time and constant temperature increased by 20 °C from the original temperature of heating in the bakeries, 1 sample baked for the original time and constant temperature deducted by 20 °C, 1 sample baked for the original time and constant temperature deducted by 40 °C, 1 sample baked constantly with the original temperature and time of heating increased by 2 minutes, 1 sample baked constantly with the original temperature and time of heating deducted by 2 minutes, 1 sample baked constantly with the original temperature and time of heating deducted by 4 minutes.

In this procedure all samples were dried and ground to powder. Subsequently, 20 g of each sample was mixed with 100 cc of 70% methanol in a blender, and then, the mixture was shaken in an Erlenmeyer flask continuously for 3 minutes. After settling, the extract was filtered with Whatman filter paper No.1 (Kamyab Tabib Tajhiz, Iran).¹²

The OTA content of the samples was measured using the AgraQuant OTA assay kit (Romer Lab, Singapore) which was based on the CD-ELISA format. Then, 200 ml of conjugated enzyme was added to uncoated-antibody wells, and then, 100 ml of both standard solution and sample extract were added to it. Subsequently, 100 µl of these solutions were transferred to coated-antibody microplate wells and were incubated at room temperature (20-25 °C) for 10 minutes. OTA in samples and standards competitively bind to solid phase antibody specific to this toxin. Tetramethylbenzidine/

hydrogen peroxide was used as a substrate for color development. After the washing phase, 100 µl of enzyme substrate was added to wells and incubated at room temperature for 5 minutes. After this step, a blue color was observed in the wells. Finally, 100 µl of stopping solution was added to stop the reactions, as a result, the blue color changed to yellow. The color intensity was inversely proportional to the OTA concentration and was measured with the ELISA reader in the wavelength of 450-630 nm (according to the manufacturer's instructions).

Data were calculated by a nonparametric Kruskal-Wallis test (to check normality of data) using SPSS software (version 18, SPSS Inc., Chicago, IL, USA) ($P < 0.05$).

Results and Discussion

Results of OTA reduction in bakeries

In bakery A, the highest reduction percentage of OTA (16.53%) was observed when the bread sample was baked in a constant temperature (320 °C) and time was increased by 2 minutes (8

minutes) from the original time (6 minutes). The lowest reduction (9.09%) was observed with a constant temperature (320 °C) and the deduction of time by 4 minutes (2 minutes) in the same bakery (Table 1).

In bakery B, the highest percentage of OTA reduction (88.93%) was observed in bread samples baked in constant temperature (185 °C) in the same bakery and time increased by 2 minutes (10:45 minutes) from the original time (8:45 minutes). The lowest reduction (80.33 %) of this toxin in bakery B was observed in samples baked in constant temperature (185 °C) and time deducted by 4 minutes (4:45 minutes) (Table 2).

In bakery C, the highest percentage of OTA reduction (87.32%) was observed in bread sample baked in a constant temperature (280 °C) in the same bakery and time increased by 2 minutes (8:30 minutes) from the original time (6:30 minutes). The lowest reduction (74.85%) of this toxin in this bakery was observed in a constant temperature (280 °C) and when time was deducted by 4 minutes (2:30 minutes) (Table 3).

Table 1. Distribution and reduction of Ochratoxin A (OTA) contamination in bread samples of bakery A

Bakery	Time (min)	Temperature (°C)	OTA contamination (ppb)	OTA reduction (%)
Wheat flour	-	-	48.4	Basis
Normal bread	6	320	41.2	14.88
Bread sample	6	340	41.4	14.46
Bread sample	6	300	42.1	13.02
Bread sample	6	280	43.5	10.12
Bread sample	8	320	40.4	16.53
Bread sample	4	320	43.5	10.12
Bread sample	2	320	44.0	9.09

* Normal bread: Bread prepared in constant temperature and duration of heating in any bakery without a change in those factors; Basis: flour not affected by different temperatures and durations of heating for reduction of OTA and chosen as the basis for comparison with the bread samples; OTA: Ochratoxin A

Table 2. Distribution and reduction of Ochratoxin A (OTA) contamination in bread samples of bakery B

Bakery	Time (min)	Temperature (°C)	OTA contamination (ppb)	OTA reduction (%)
Wheat flour	-	-	48.8	Basis
Normal bread	8:45	185	7.1	85.45
Bread sample	8:45	205	6.1	87.50
Bread sample	8:45	165	7.5	84.63
Bread sample	8:45	145	7.4	84.84
Bread sample	10:45	185	5.4	88.93
Bread sample	6:45	185	9.1	81.35
Bread sample	4:45	185	9.6	80.33

* Normal bread: Bread prepared in constant temperature and duration of heating in any bakery without a change in those factors; Basis: flour not affected by different temperatures and durations of heating for reduction of OTA and chosen as the basis for comparison with the bread samples; OTA: Ochratoxin A

Table 3. Distribution and reduction of Ochratoxin A (OTA) contamination in bread samples of bakery C

Bakery	Time (min)	Temperature (°C)	OTA contamination (ppb)	OTA reduction (%)
Wheat flour	-	-	48.9	Basis
Normal bread	6:30	280	7.2	85.28
Bread sample	6:30	300	10.1	79.35
Bread sample	6:30	260	7.6	84.46
Bread sample	6:30	240	7.8	84.05
Bread sample	8:30	280	6.2	87.32
Bread sample	4:30	280	11.0	77.51
Bread sample	2:30	280	12.3	74.85

* Normal bread: Bread prepared in constant temperature and time in bakery without change in the temperature and time of heating; Basis: flour not affected by different temperatures and durations of heating for reduction of OTA and chosen as the basis for comparison with the bread samples; OTA: Ochratoxin A

Table 4. Distribution and reduction of Ochratoxin A (OTA) contamination in bread samples of bakery D

Bakery	Time (min)	Temperature (°C)	OTA contamination (ppb)	OTA reduction (%)
Wheat flour	-	-	48.8	Basis
Normal bread	8:30	200	8.4	82.79
Bread sample	8:30	220	7.7	84.22
Bread sample	8:30	180	8.4	82.79
Bread sample	8:30	160	9.6	80.33
Bread sample	10:30	200	7.6	84.43
Bread sample	6:30	200	8.9	81.76
Bread sample	4:30	200	9.8	79.92

* Normal bread: Bread prepared in constant temperature and time in bakery without change in the temperature and time of heating; Basis: flour not affected by different temperatures and durations of heating for reduction of OTA and chosen as the basis for comparison with the bread samples; OTA: Ochratoxin A

In bakery D, the highest percentage of reduction in this toxin (84.43%) was observed in constant temperature of 200 °C and when time was increased by 2 minutes (10:30 minutes) from the original time (8:30 minutes). The lowest reduction of OTA (79.92%) was observed in the constant temperature of 200 °C and when the time was deducted by 4 minutes (4:30 minutes) from the original time (8:30 minutes) (Table 4). In all bakeries, it was specified that temperature and time of heating are prominent factors for reduction of OTA in bread samples. All bread samples showed less OTA contamination than raw flour.

Results of statistical analysis

The results indicate that in all bakeries, OTA level is higher than recommended standard values. Depending on the OTA amount in wheat flour, different temperatures and times of heating caused significant reductions in OTA level in bread ($P < 0.05$), which ranged from 9.09-16.53%,

80.33-88.93%, 77.51-87.32%, and 79.92-84.43% in bakeries A, B, C, and D, respectively.

More information about this toxin and comparison with other studies

OTA is a type of mycotoxin that occurs frequently in cereals and can be found in starch-rich foods such as grains, cereal, and bread.^{13,14} Valle-Algarra et al., in Spain, showed that OTA reduced by 32.9% during the baking process. Our study showed that the highest reduction of OTA was 88.93% (10:45 minute, 185 °C) in bakery B when bread samples were baked in a constant temperature in the same bakery and time of heating was increased by 2 minutes. A higher rate of OTA reduction was achieved in our study compared to that in the study by Valle-Algarra et al. Different baking conditions, such as dough fermentation or yeasts selected in industrial fermentations, are effective on the levels and reduction of mycotoxins in flour that are used to bake bread.¹³ Scudamore et al., in Britain, showed

that OTA decreased only a small amount during the bread making process.¹⁵ We showed that the highest rates of reduction in bakeries A, B, C, and D were 16.53% (8 minutes, 320 °C), 88.93% (10:45 minutes, 185 °C), 87.32% (8:30 minutes, 280 °C), and 84.43% (10:30 minutes, 200 °C), respectively. Different researches reported that food processing (cleaning, milling, baking, and fractionating), hygienic conditions, and workers' health in the bakeries can be effective on the levels of mycotoxin contamination of flour and bread.¹⁴⁻¹⁶ Pacin et al., in Argentina, after studying several wheat flour samples, reported that French bread and Vienna bread were contaminated with deoxynivalenol (DON) (35.5 µg/kg and 22 µg/kg, respectively). OTA was not detected in the flour in their study. A 33% and 58.5% reduction in DON after the bread making process was observed in French bread and Vienna bread, respectively.¹⁷ In our study, 32 samples were contaminated by this toxin. Common processes in manufacturing and physical treatment of grain, such as scouring and cleaning the grain prior to milling, can reduce the initial contamination by mycotoxins in the raw material used for bakery and bread making.^{17,18} Osborne et al. showed that when OTA was added to flour samples which were subsequently baked into bread, it was recovered after the baking processes without becoming decomposed.¹⁹ Furthermore, in our study, toxins, in some cases, were destroyed in the samples. For example, in bakery A samples, the level of OTA was higher than the other samples. This toxin has a moderately stable molecule and is able to survive most food processes; thus, it is only partly destroyed during cooking and bread making processes. Baking and roasting bread can reduce the existing OTA content up to 20%.^{20,21} Castells et al., in Spain, reported that the cooking temperature of 160 °C applied for 70 seconds reduces OTA up to 86% in barley bread.²² In our research, the highest reduction (88.93%) of OTA was observed when the bread sample was baked in a constant temperature (185 °C) and 2 minutes was added to the original time (10:45) (bakery B). Different

factors that influence the OTA content and quantity in food products are: different ecological niches of the ochratoxigenic mycobiota, such as *Aspergillus* spp. and *Penicillium verrucosum*, and accurate agricultural practices, such as better harvest procedures and storage conditions, the type of grains, nature and extent of technological advancements in agricultural equipments.^{12,23} Since most wheat flour is processed into various foods such as bread and consumption of a food that is contaminated by OTA causes different diseases in humans, greater attention should be paid to OTA in wheat and wheat products. Results of our study are effective in the management, detection, and reduction of fungi growth and OTA production in food.

Conclusion

In this study, OTA concentration in several samples was measured after employing different temperatures and durations of heating using ELISA. Therefore, we can conclude that there was a significant relationship between OTA reduction in the samples, and temperature and durations of heating ($P < 0.05$). The highest rate of reduction in OTA was observed when a constant temperature was maintained in each bakery and when the time of heating was increased by 2 minutes from the original time.

Conflict of Interests

Authors have no conflict of interests.

Acknowledgements

The Faculty of Microbiology, Research Branch, Islamic Azad University, Babol, and the Islamic Azad University, Tonekabon Branch, Iran, supported this study.

References

1. Kumar V, Basu MS, Rajendran TP. Mycotoxin research and mycoflora in some commercially important agricultural commodities. *Crop Protection* 2008; 27(6): 891-905.

2. Pohland AE, Nesheim S, Friedman L. Ochratoxin A: A review. *Pure and Applied Chemistry* 1992; 64(7): 1029-46.
3. Tam J, Pantazopoulos P, Scott PM, Moisey J, Dabeka RW, Richard ID. Application of isotope dilution mass spectrometry: determination of ochratoxin A in the Canadian Total Diet Study. *Food Addit Contam Part A Chem Anal Control Expo Risk Assess* 2011; 28(6): 754-61.
4. Rosa CA, Keller KM, Keller LA, Gonzalez Pereyra ML, Pereyra CM, Dalcero AM, et al. Mycological survey and ochratoxin A natural contamination of swine feedstuffs in Rio de Janeiro State, Brazil. *Toxicon* 2009; 53(2): 283-8.
5. Gholampour Azizi I, Rahimi K, Shateri S. Ochratoxin: Contamination and Toxicity (A Review). *Global Vet* 2012; 8(5): 519-24.
6. Bento JMV, Pena A, Lino CM, Pereira JA. Determination of ochratoxin a content in wheat bread samples collected from the Algarve and Bragança regions, Portugal: Winter 2007. *Microchemical Journal* 2009; 91(2): 165-9.
7. Institute of Standards & Industrial Research of Iran. Food and feed- mycotoxins: maximum tolerated level. 1st ed. Tehran, Iran: Institute of standards and industrial research of Iran (ISIRI) .p. 3-20; 2002.
8. Meca G, Zhou T, Li XZ, Ma+les J. Beauvericin degradation during bread and beer making. *Food Control* 2013; 34(1): 1-8.
9. van der Stegen GH, Essens PJ, van der Lijn J. Effect of roasting conditions on reduction of ochratoxin a in coffee. *J Agric Food Chem* 2001; 49(10): 4713-5.
10. Kristensen EF, Elmholt S, Thrane U. High-temperature Treatment for Efficient Drying of Bread Rye and Reduction of Fungal Contaminants. *Biosystems Engineering* 2005; 92(2): 183-95.
11. Gholampour Azizi E. Evaluation of the presence of Ochratoxin in grape juices and raisins. *J Food Technol Nutr* 2012; 9(1): 95-100.
12. Gholampour Azizi I, Rouhi S. The Comparison of Total Fumonisin and Total Aflatoxin Levels in Biscuit and Cookie Samples in Babol City, Northern Iran. *Iranian Journal of Public Health* 2013; 42(4): 422-7.
13. Valle-Algarra FM, Mateo EM, Medina A, Mateo F, Gimeno-Adelantado JV, Jimenez M. Changes in ochratoxin A and type B trichothecenes contained in wheat flour during dough fermentation and bread-baking. *Food Addit Contam Part A Chem Anal Control Expo Risk Assess* 2009; 26(6): 896-906.
14. Lasram S, Belli N, Chebil S, Nahla Z, Ahmed M, Sanchis V, et al. Occurrence of ochratoxigenic fungi and ochratoxin A in grapes from a Tunisian vineyard. *Int J Food Microbiol* 2007; 114(3): 376-9.
15. Scudamore KA, Banks J, MacDonald SJ. Fate of ochratoxin A in the processing of whole wheat grains during milling and bread production. *Food Addit Contam* 2003; 20(12): 1153-63.
16. Roohi S, Gholampour Azizi I, Hashemi M. Fumonisin contamination based on flour quality used in bakeries and confectioneries in Qaemshahr (city of the Northern Iran). *African Journal of Microbiology Research* 2012; 6(8): 1815-8.
17. Pacin A, Ciancio Bovier E, Cano G, Taglieri D, Hernandez Pezzani C. Effect of the bread making process on wheat flour contaminated by deoxynivalenol and exposure estimate. *Food Control* 2010; 21(4): 492-5.
18. Food and Agriculture Organization of the United Nations. Joint fao/who food standards programme. Codex committee on food additives and contaminants [Online]. [cited 1998]; Available from: URL: <http://www.iss.it/binary/cnra/cont/position%20paper%20ochratoxin%20A.1121359601.pdf>
19. Osborne BG, Ibe F, Brown GL, Petagine F, Scudamore KA, Banks JN, et al. The effects of milling and processing on wheat contaminated with ochratoxin A. *Food Addit Contam* 1996; 13(2): 141-53.
20. Centre for Food Safety. Risk Assessment Studies Report No. 19 [Online]. [cited 2013]; Available from: URL: http://www.cfs.gov.hk/english/programme/programme_rafs/programme_rafs_ft_01_02_mcf.html
21. Kolossova A, Stroka J, Breidbach A, Kroeger K, Bouten K, Ulberth F. Evaluation of the effect of mycotoxin binders in animal feed on the analytical performance of standardised methods for the determination of mycotoxins in feed follow-up study. Geel, Belgium: European Commission Joint Research Centre Institute for Reference Materials and Measurements; 2011.
22. Castells M, Pardo E, Ramos AJ, Sanchis V, Marin S. Reduction of ochratoxin A in extruded barley meal. *J Food Prot* 2006; 69(5): 1139-43.
23. Duarte SC, Pena A, Lino CM. A review on ochratoxin a occurrence and effects of processing of cereal and cereal derived food products. *Food Microbiol* 2010; 27(2): 187-98.



Radiological dose assessment of naturally occurring radioactive materials generated by the petroleum industry in wildlife: A case study of chinkaras of Lavan Island, Iran

Siavash Sedighian¹, Mohammad Ali Abdoli², Mohammad Hossein Niksokhan³, Min Jun Kim¹, Seung-Yeon Cho¹

¹ Department of Environmental Engineering, School of Health Sciences, Yonsei University, Wonju, South Korea

² Department of Solid Waste Engineering, Graduate School of Environment, University of Tehran, Tehran, Iran

³ Department of Coastal Engineering, Graduate School of Environment, University of Tehran, Tehran, Iran

Original Article

Abstract

Human activities such as oil and gas production can enhance the natural level of naturally occurring radioactive materials (NORM) in by-product and waste streams. Iran has been among the top five oil producing countries since 2005. This high production rate emphasizes the importance of NORM management to ensure the safety of humans and wildlife. Petroleum storage and transport facilities are located at Lavan Island, Iran. Presence of animals including dolphins, sea turtles, and chinkaras make this island one of the most unique wildlife refuges in Iran. This paper combines waste disposal methods relevant to the petroleum offshore industries, NORM waste characteristics, and geographical, geological, and climate conditions of Lavan Island in order to develop enveloping exposure scenarios. Sludge burning is determined as the most concerning scenario by assuming chinkaras as the endpoint. Ecological and radiological assessment procedure is modeled with MATLAB-Simulink as a dynamic system. Clearance level for radiation protection of chinkaras is calculated as 41 Bq/kg. This value may be insufficient for radiation protection of workers, because exposure pathways are not derived based on human behavior. According to environmental pathways and condition of chinkaras, this value sufficiently covers all aspects of radiation protection.

KEYWORDS: Radioactive Wastes, Radiological Health, Radioactive Soil Pollutants, Radioactive Food Contamination, Radiation Protections

Date of submission: 5 May 2014, **Date of acceptance:** 9 Jul 2014

Citation: Sedighian S, Abdoli MA, Niksokhan MH, Kim MJ, Cho SY. **Radiological dose assessment of naturally occurring radioactive materials generated by the petroleum industry in wildlife: A case study of chinkaras of Lavan Island, Iran.** J Adv Environ Health Res 2014; 2(4): 215-22.

Introduction

The majority of radionuclides in naturally occurring radioactive materials (NORM) are essential constituents of the earth's crust.¹ Primordial radionuclides ²³⁸U, ²³²Th, and ²³⁵U, are the parent radionuclides for the three naturally occurring decay chains commonly called the uranium, thorium, and actinium

series, respectively.²

There are many industries and human activities that can enhance the level of NORM in their waste streams and by-products. It should be noted that NORM is typically associated with non-nuclear industries.³ Regardless of the activity from which NORM originates, there are six types of materials which could contain the elevated levels of radiation; waste rock, sand slag ash, sludge, and scale. Oil and gas production and processing is one of the most

Corresponding Author:

Siavash Sedighian

Email: siavashsedighian@gmail.com

notable industries that produces NORM, mainly in the form of sludge and scale.⁴

Uranium and thorium series exist in various concentrations in unground formations. Both ²³⁸U and ²³²Th are relatively insoluble and remain in place in subsurface formations; however, some of their decay products [²²⁶Ra (from uranium series) and ²²⁸Ra (from thorium decay series)] are slightly soluble and can become mobilized in liquid phase of the formation.⁵

During drilling and production operations, produced water is extracted from underground formations and brought to the surface. Discharge of the produced water into the marine environment is a typical disposal method in Brazil⁶, European commission,⁷ and many other countries. If the produced water is disposed in surface pits, the liquid content would evaporate, and thus, the concentration of NORM in the pits could be considerably enhanced.

Many studies have investigated the radiological hazards of NORM in the petroleum industry⁸⁻¹⁰ and a limited number of researches have been conducted on NORM originated in the Iranian petroleum industry^{11,12} which prove the existence of NORM in scales and sludges.

Gas oil separation plants (GOSP), storage tanks, and pipelines are possible locations for accumulation of sludge and scale. In Iran, scales are generally discharged into the sea, surface ponds, or landfills along with other kinds of wastes. Other methods, like encapsulation, which are widely used around the world⁵, are not common in Iran. On Lavan Island, extracted scales are contained and stored in drums. Scales which are extracted offshore are usually discharged into the water. None of the wastes are landfilled on the island, so related exposure pathways are excluded from radiological assessment.

Incineration, land spreading, and landfilling are common practices applied for sludge management in Iran. These methods could harm both human and environmental health, if done without any appropriate system and monitoring. Sometimes, on Lavan Island, most of the sludges

are directly or accidentally burnt in the outdoor environment without any suitable isolation.

The main waste generators on Lavan Island are the Iranian Offshore Oil Company (IOOC), Lavan Oil Refining Company, Lez village, military facilities, and other sources including domestics.

On the island, there are facilities to contain and transport crude oil which produce significant amounts of sludge. In case of leakage, sludge can be burnt or contained in metallic drums. These drums are transported back to the onshore facilities and will not be included in the Lavan Island radiological assessment. Sludge burning is the only significant disposal scenario concerning chinkaras on the island. It should be noted that sludge burning is not a standard waste disposal activity, but sometimes it is unavoidable.

There are approximately 400 chinkaras on the Island. Due to absence of natural predators, lack of food, and limited pastures, most of them are attracted to residences and waste storage facilities. These facilities contain NORM; hence, radioactive exposure is inevitable. Sludge burning, and thus, ash settlement on the pastures is an important exposure pathway, which has been investigated thoroughly in this paper.

Materials and Methods

This research has been conducted by following "the principles of radiological ecological risk assessment"¹³. This study attempts to develop real and pervasive scenarios according to personal visits and the International Atomic Energy Agency (IAEA) context¹⁴, in order to predict the annual dose of NORM received by chinkaras. Each model consists of three major parts; source term, environmental pathway, and exposure pathway. Source term demonstrates the radioactive decay and growth inside the waste package. Environmental pathway investigates the transport of radionuclides from waste to a defined endpoint. In this paper, chinkaras are chosen as the endpoint. Exposure pathway encompasses possible ways through

which radionuclides may come into contact with the endpoint.

Incineration without any protection and equipment is not a favorable option. Open burning produces plume. If the plume moves toward inland, the following exposure pathways would be possible regarding chinkaras as the endpoint.

- Submersion in plume: Being submersed in the plume could expose the creature to NORM. The main pathways would be external irradiation and inhalation of NORM particles.

- External irradiation from soil: After deposition of plume on the surface of soil, external exposure from NORM particles could be a significant pathway. Due to lack of surface water and even fresh water ponds on the island, external irradiation from water is negligible.

Ingestion of pasture vegetation, soil, and water: Chinkaras graze in the limited meadows of the island every day. If NORM particles are deposited on the surface of pasture, soil, or water, chinkaras will ingest them without

noticing the contamination. The conceptual model of the sludge burning scenario is illustrated in figure 1.

This paper assigns the local data of Lavan Island into the ecological and radiological dose assessment models. Most mathematical relations and equations are taken from the Improvement of Safety Assessment Methodologies for Near Surface Disposal Facilities (ISAM) project.¹⁵ Generic models have been applied in this study. Generic models are the best tools to derive standard limits due to their reasonable degree of conservatism and reliable results. These results can be used as the basic standards for protection of chinkaras against NORM incineration accidents.

Source Term Modeling

The following differential equation has been used to model NORM decay chains in this paper¹⁶:

$$\frac{dN_i(t)}{dt} = \lambda_{i-1}N_{i-1}(t) - \lambda_i N_i(t)$$

where N_i and λ_i are the quantity and decay constants of i^{th} nuclide, respectively.

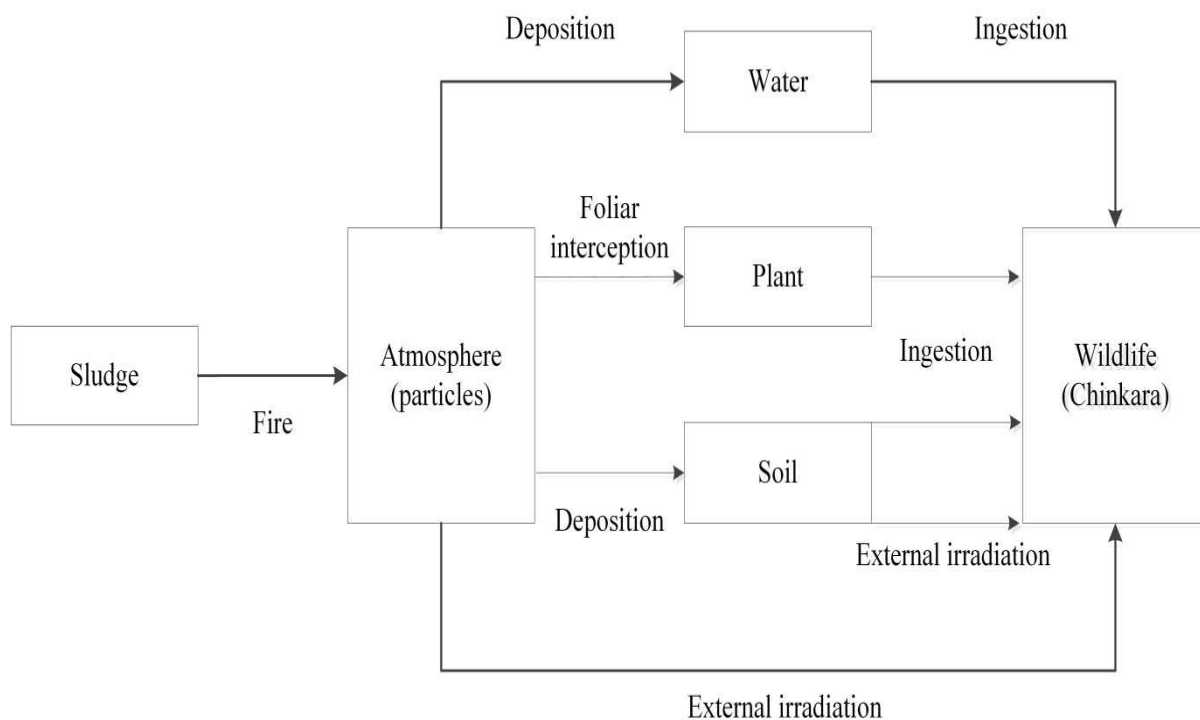


Figure 1. Conceptual assessment model of sludge burning scenario

Environmental Pathway Modeling

The release rate of a radionuclide from the fire, R_{fire} (Bq/h), is obtained through the following equation:

$$R_{\text{fire}} = f_{\text{rel,fire}} A_m V_{\text{fire}} \rho_{\text{bd}} / t_{\text{fire}}$$

where $f_{\text{rel,fire}}$ is the release fraction for radionuclide I (unitless), A_m is the specific activity of the radionuclide in the sludge (Bq/kg), V_{fire} is the volume of the waste consumed in the fire (m^3), ρ_{bd} is the bulk density of the waste (kg/m^3), and t_{fire} is the duration of the fire (h).

It is cautiously assumed that the associated plume is neutrally buoyant. Air concentration of a radionuclide at ground level, $C_{\text{air,fire}}$, is obtained by:

$$C_{\text{air,fire}} = R_{\text{fire}} C_{\text{integ,fire}}$$

where $C_{\text{integ,fire}}$ is the time-integrated air concentration at ground level [(Bq/ m^3) per (Bq/h)]. The above equation cautiously assumes that the plume is non-depleting during passage towards the endpoint (each individual chinkara).

The surface concentration of a radionuclide, $C_{\text{surf,fire}}$, resulting from deposition is:

$$C_{\text{surf,fire}} =$$

$$C_{\text{air,fire}} t_{\text{dep,fire}} (V_{\text{g,fire}} + W_{\text{out,fire}} h_{\text{fire}})$$

where $t_{\text{dep,fire}}$ is the time over which deposition occurs (s), $V_{\text{g,fire}}$ is the dry deposition velocity (m/s), $W_{\text{out,fire}}$ is the washout coefficient ($1/\text{s}$), and h_{fire} is the plume height (m).

Exposure Pathway Modeling

The total dose to an individual chinkara living on the island can be expressed as:

$$\text{Dose}_{\text{total}} = \text{Dose}_{\text{sub}} + \text{Dose}_{\text{ext}} + \text{Dose}_{\text{ing}}$$

where Dose_{sub} is the dose due to the external irradiation from submersion in the plume (Sv/y), Dose_{inh} is the dose from inhalation of NORM particles (Sv/y), Dose_{ext} is the dose from external irradiation of deposited NORM on the ground (Sv/y), and Dose_{ing} is the dose from the ingestion of NORM deposited on the pasture (Sv/y).

Dose of external irradiation from submersion in the plume can be obtained by:

$$\text{Dose}_{\text{sub}} = C_{\text{air,fire}} t_{\text{e,out}} \text{DF}_{\text{sub}} \text{Occ}_{\text{fire}}$$

where $t_{\text{out,fire}}$ is the exposure time to one

occurrence of fire (h), DF_{sub} is the dose factor for external irradiation from submersion in the plume [(Sv/h) per (Bq/ m^3)], and Occ_{fire} is the number of fires per year ($1/\text{y}$).

External dose by direct irradiation from soil can be expressed as:

$$\text{Dose}_{\text{ext,soil}} = C_{\text{surf,fire}} t_{\text{e,out}} \text{DF}_{\text{ext,soil}}$$

where $\text{DF}_{\text{ext,soil}}$ is the dose coefficient for contaminated soil ((Sv/h) per (Bq/ m^2)).

Chinkaras may receive internal radiation doses after ingesting contaminated pasture vegetation, soil, or water. Internal dose according to ingestion of contaminated material can be expressed as:

$$\text{Dose}_{\text{ing}} = \sum_{i=\text{pasture,soil,water}} \text{CN}_{\text{surf,fire}} Q_i \text{Occ}_{\text{fire}} t_{\text{pst}} \left[\frac{(1 - e^{-\lambda_{\text{pst}} t_{\text{pst}}})}{\lambda_{\text{pst}}} \right] \text{DF}_{\text{ing}}$$

where $\text{CN}_{\text{surf,fire}}$ is the activity concentration of radionuclides on the unit surface of the edible materials (food) ((Bq/kg) per (Bq/ m^2)), Q_{pst} , Q_{soil} , and Q_{water} are the pasture vegetation, soil, and water consumption rate (kg/d), respectively, λ_{pst} is the effective rate constant for removal of activity from the pasture ($1/\text{d}$), t_{pst} is the time following the release over which the pasture vegetation are consumed (d), and DF_{ing} is the dose conversion factor for ingestion (Sv/Bq). It should be mentioned that sludge burning has been considered as an accidental phenomena.

Parameters regarding to waste characteristics and chinkaras' habitat and diet are gathered from local people and organizations. Parameters for radionuclide transfer coefficients and other radiological and biological factors are adapted from relevant studies.¹⁷⁻²¹

The dose criterion of 1 mSv/yr is considered to fulfill radiation protection of the public and workers. In this paper, the same limit is assigned as annual dose limit for total exposures of chinkaras to NORM sources.

Mathematical relations which were used in this paper are modeled with MATLAB-Simulink (The MathWorks Inc., Natick, MA, USA). The MathWorks MATLAB software and its associated graphical extension Simulink have the ability to

simulate dynamic systems with ease and flexibility.²² Simulink is very effective in the analysis of the time variable signals and systems. In this research, fate and transport (contaminant migration through the environment) of NORM are considered as a dynamic system which varies with time; therefore, it has been modeled with Simulink. In addition to providing a user friendly environment, any modification and upgrade to the initial model can be easily performed using Simulink features.

Results and Discussion

NORM residue properties are based on previously conducted researches in Iran.^{11,12} Moreover, meteorological data were taken from local agencies. Table 1 indicates source term characteristics.

Exposure pathway parameters were broadly taken from personal observations, local agencies, and general assumptions for near surface disposal facilities.¹⁴ There is no documented or official record about the chinkaras' diet and habitat. In order to gain the most reliable results, these data were gathered from local veterinarians and the Health, Safety, and Environment (HSE) offices. Exposure related parameters are illustrated in table 2. Exposure dose coefficients, which include the ingestion, inhalation, and external irradiation pathways, are broadly consistent with the database of radionuclide transfer parameters for freshwater wildlife.²⁴

Occurrence of fire is assumed as an accident and is not very probable due to the safety protocols and equipment installed at the field.

This paper takes into account the worst case scenario which investigates an accident that may occur once a year. Due to the large volume of sludge, each accident is expected to last for a maximum duration of 12 hours. The HSE and fire department of petroleum facilities are capable of extinguishing the fire in a few hours, but in this case, the most conservative and realistic values are considered. Local interviews and surveys play the key role in gathering of these data.

Chinkaras' diet usually consists of natural vegetation of the island and the food provided by private contractors. They might also search for food in garbage bins, but this would not be considered as their common food source. In addition to the pasture vegetation and water, they consume a small proportion of soil with vegetation. This soil might be ingested via attachment to the roots or deposition of dust on the vegetation. Although the quantity of consumed food depends on many factors, like the gender and age of the animals, a typical fully grown male is taken into account in this research. Chinkaras' diet, behavior, and habitat pattern are also determined by local surveys and information from the local authorities. λ_{pst} , which indicates the removal of activity from the pasture, is directly adopted from IAEA documents.¹⁴

These parameters are considered to be the most conservative data in order to fulfill the maximum protection goals. Calculations are carried out mainly for ²²⁶Ra and its daughters due to their presence in sludge. By applying the data from tables 1 and 2 to the exposure model, figure 2 was achieved.

Table 1. Source term characteristics

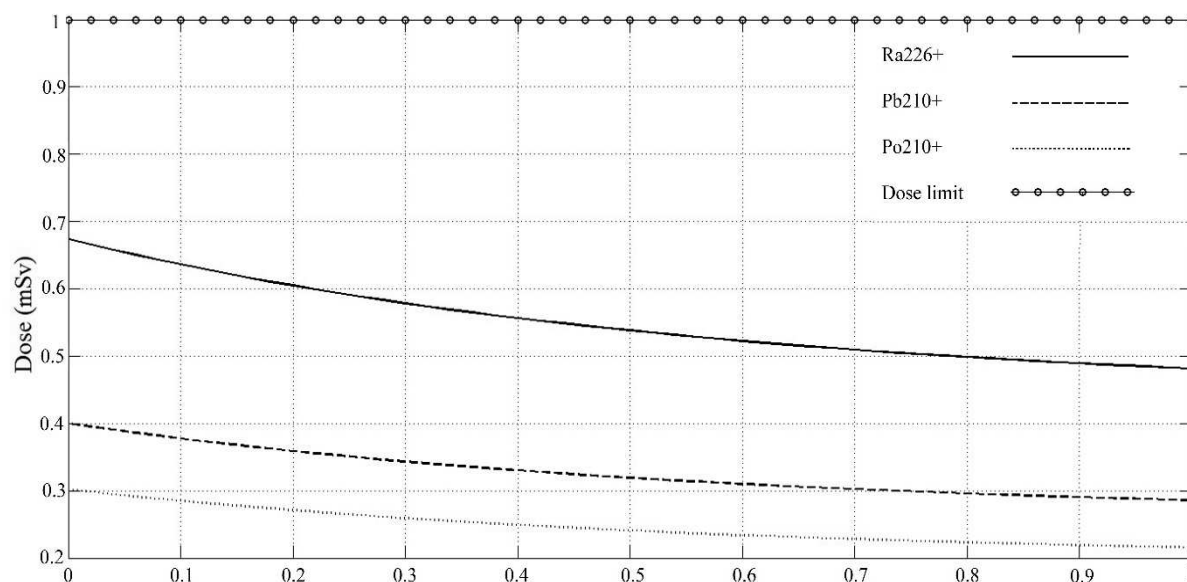
$f_{rel,fire}$ (-)	A_m^* (Bq/kg)	m (T)	V_{fire} (m^3)	ρ_{bd} (kg/m^3)	t_{fire} (h)	$C_{inteq,fire}^{**}$ (Bq/m ³) per (Bq/h)	$t_{dep,fire}$ (s)	$V_{g,fire}$ (m/s)	$W_{out,fire}$ (1/s)	h_{fire} (m)
0.001	Ra: 25.7 Pb: 25.7 Po: 25.7	1	1.8 E+7	1800	6	3.24	3600	0.02	0.003	12

*Radium and its progenies have been considered to be in secular equilibrium due to long retention time in storage tanks before disposal.

** Time-integrated air concentration at ground level is based on dominant atmospheric conditions of Lavan Island.²³

Table 2. Exposure term characteristics for an individual chinkara

$t_{\text{out,fire}}$ (h)	Occ_{fire} (1/y)	Q_{pst} (kg/d)	Q_{soil} (kg/d)	Q_{water} (kg/d)	λ_{pst} (1/d)	t_{pst} (d)
12	1	2.1	0.1	0.3	0.02	0.5

**Figure 2.** Dose assessment results for the chinkaras

It can be concluded that the wastes sampled at Lavan Island are cleared from any radiological hazards due to their lower dose responses compared with the standard limit. Figure 2 indicates an exponential trend of data. This is due to the decay of radium and its progenies in the environment. The longer it takes for the chinkaras to consume the pasture vegetation, the lower the dose they will, probably, receive. It is not easily possible to prevent the chinkaras from grazing in contaminated areas. If a chinkara preservation program is designed, their pasture should be carefully isolated in case of NORM contamination or completely replaced by non-contaminated food.

In order to calculate the accurate cleared values, iteration approach and reverse analysis should be applied to initial activity concentration and the results continuously compared with dose limit. The model has been executed 70 times until the initial activity concentration satisfied the dose criteria. The results were continuously examined and

modified to converge to a singular value. By following the aforementioned procedure, clearance levels for each radionuclide have been calculated and illustrated in table 3.

Table 3. Proposed clearance levels for sludge burning scenario

Radionuclide	Activity concentration (Bq/kg)
$^{226}\text{Ra}^*$	41
$^{210}\text{Pb}^*$	70
$^{210}\text{Po}^*$	92

* Also includes daughters

Each of these values illustrates the maximum concentration for each radionuclide that causes no harm to chinkaras after an accidental fire. In other words, the minimum activity concentration of $^{226}\text{Ra}^+$, $^{210}\text{Pb}^+$, and $^{210}\text{Po}^+$ should be 41, 70, and 92 (Bq/kg), respectively, in order to initiate the chinkara food preservation program. Considering the importance of radiation protection and conservative assumptions, the minimum value of clearance levels is usually declared as the general clearance level. In the present study, 41 Bq/kg (activity concentration of $^{226}\text{Ra}^+$) was chosen as the activity limit for sludge burning scenario.

This implies that if the activity concentration of sludge is higher than 41 (Bq/kg) and chinkaras are exposed to fire, their food and habitat should be isolated or decontaminated based on domestic policies. These efforts will ensure the protection of chinkaras from radiation hazards of NORM.

This value is not suitable for radiation protection of workers, because exposure pathways are not defined due to human behavior. According to environmental pathways and condition of chinkaras, this value sufficiently covers all aspects of ecological radiation protection. If humans are considered as the endpoint, new sets of scenarios must be developed.

This scenario covers accidental fire situations, but it could be applied to open burning of sludge. Although open incineration is not a recommended and safe disposal method, it should be considered that, in the case of open incineration, the activity of NORM should not exceed the clearance level.

In addition to sludge, hard scales from pipelines should also be investigated thoroughly. Activity concentration of scales has been recorded as the highest among other NORM wastes generated in the petroleum industry. Due to the discharge of scales into the Persian Gulf and their absence on the Island, their radiological assessment falls outside the scope of this study.

Conclusion

Typical measurements around the world indicate the average activity of sludge to be between 50 and 800000 Bq/kg. The only official document regarding NORM activity in the Iranian petroleum industry indicates the activity range of 10.6 to 1480 Bq/kg for ^{226}Ra . This research recommends the maximum activity limit of 41 Bq/kg for sludge wastes in Lavan Island which satisfies the radiological protection criteria for the chinkaras. Any waste with lower activity is simply cleared from further protection policies, but in case of higher activity, appropriate disposal and protection are required.

Conflict of Interests

Authors have no conflict of interests.

Acknowledgements

Authors would like to express their gratitude to Mr. Farzad Nejad Bahadori from the HSE Department of the Ministry of Petroleum for his generous supports in providing data, and Mr. Iman Soelimanpour from the DANA Energy Group, and Dr. Seon-Hong Kim from Yonsei University for their cooperation and kind efforts during the preparation of this paper.

References

1. Gazineu MH, Hazin CA. Radium and potassium-40 in solid wastes from the oil industry. *Appl Radiat Isot* 2008; 66(1): 90-4.
2. Ojovan M, Lee WE. Naturally occurring radionuclides. In: Ojovan M, Lee WE, Editors. *An introduction to nuclear waste immobilization*. Oxford, UK: Elsevier Ltd; 2005. p. 43-52.
3. Landa ER. Naturally occurring radionuclides from industrial sources: characteristics and fate in the environment. In: Shaw G, Editor. *Radioactivity in the terrestrial environment*. Oxford, UK: Elsevier; 2007. p. 211-37.
4. International Atomic Energy Agency. *Assessing the need for radiation protection measures in work involving minerals and raw materials*. Vienna, Austria: International Atomic Energy Agency; 2006. p. 11-26.
5. Smith K, Argonne national lab il environmental assessment and information sciences div. *Radiological Dose Assessment Related to Management of Naturally Occurring Radioactive Materials Generated by the Petroleum Industry*. Chicago, IL: Argonne national lab il environmental assessment and information Sciences Division, 1996. p. 10-6.
6. Jerez Vegueria SF, Godoy JM, Miekeley N. Environmental impact studies of barium and radium discharges by produced waters from the "Bacia de Campos" oil-field offshore platforms, Brazil. *J Environ Radioact* 2002; 62(1): 29-38.
7. Betti M, Aldave de las HL, Janssens A, Henrich E, Hunter G, Gerchikov M, et al. Results of the European Commission Marina II study: part II--effects of discharges of naturally occurring radioactive material. *J Environ Radioact* 2004; 74(1-3): 255-77.
8. Abo-Elmagd M, Soliman HA, Salman K, El-Masry NM. Radiological hazards of TENORM in the wasted petroleum pipes. *J Environ Radioact* 2010; 101(1): 51-4.

9. Hrichi H, Baccouche S, Belgaied JE. Evaluation of radiological impacts of tenorm in the Tunisian petroleum industry. *J Environ Radioact* 2013; 115: 107-13.
10. Gäfvert T, Færevik I, Rudjord AL. Assessment of the discharge of NORM to the North Sea from produced water by the Norwegian oil and gas industry. In: Povinec PP, Sanchez-Cabeza JA, Editors. *International conference on isotopes and environmental studies*. Oxford, UK: Elsevier; 2006. p. 193-205.
11. Khodashenas A, Roayaei E, Abtahi SM, Ardalani E. Evaluation of naturally occurring radioactive materials (NORM) in the South Western oil wells of Iran. *J Environ Radioact* 2012; 109: 71-5.
12. Moatar F, Shadizadeh S, Karbassi A, Ardalani E, Akbari Derakhshi R, Asadi M. Determination of naturally occurring radioactive materials (NORM) in formation water during oil exploration. *Journal of Radioanalytical and Nuclear Chemistry* 2010; 283(1): 3-7.
13. Till JE, Grogan HA. *Radiological risk assessment and environmental analysis*. 1st ed. Oxford, UK: Oxford University Press; 2008. p. 1-28.
14. International Atomic Energy Agency. *Derivation of activity limits for the disposal of radioactive waste in near surface disposal facilities*. Vienna, Austria: International Atomic Energy Agency; 2004. p. 73-138.
15. International Atomic Energy Agency. *Safety assessment methodologies for near surface disposal facilities*. Vienna, Austria: International Atomic Energy Agency; 2004. p. 90-138.
16. Amaku M, Pascholati PR, Vanin VR. Decay chain differential equations: Solution through matrix algebra. *Computer Physics Communications* 2010; 181(1): 21-3.
17. Johansen MP, Barnett CL, Beresford NA, Brown JE, Cerne M, Howard BJ, et al. Assessing doses to terrestrial wildlife at a radioactive waste disposal site: inter-comparison of modelling approaches. *Sci Total Environ* 2012; 427-428: 238-46.
18. Copplestone D, Beresford NA, Brown JE, Yankovich T. An international database of radionuclide concentration ratios for wildlife: development and uses. *J Environ Radioact* 2013; 126: 288-98.
19. International Atomic Energy Agency. *Quantification of radionuclide transfer in terrestrial and freshwater environments for radiological assessments*. Vienna, Austria: International Atomic Energy Agency; 2009. p. 476-94.
20. Amiro BD. Radiological dose conversion factors for generic non-human biota used for screening potential ecological impacts. *Journal of Environmental Radioactivity* 1997; 35(1): 37-51.
21. Howard BJ, Beresford NA, Copplestone D, Telleria D, Proehl G, Fesenko S, et al. *The IAEA handbook on radionuclide transfer to wildlife*. *J Environ Radioact* 2013; 121: 55-74.
22. Chermitti A, Boukli-Hacene O, Meghebbar A, Bibitriki N, Kherous A. Design of a library of components for autonomous photovoltaic system under Matlab/Simulink. *Physics Procedia* 2014; 55: 199-206.
23. International Atomic Energy Agency. *Generic models for use in assessing the impact of discharges of radioactive substances to the environment*. Vienna, Austria: International Atomic Energy Agency; 2001. p. 12-28.
24. Yankovich T, Beresford NA, Fesenko S, Fesenko J, Phaneuf M, Dagher E, et al. Establishing a database of radionuclide transfer parameters for freshwater wildlife. *J Environ Radioact* 2013; 126: 299-313.



Ecological Potential assessment of soil in agricultural lands in Hamedan Province, Iran, using geographic information system

Karim Naderi Mahdei¹, Abdolali Bahrami²

¹ Department of Agriculture Extension and Education, Bu-Ali Sina University, Hamedan, Iran

² School of Agricultural Development, Bu Ali Sina University, Hamadan, Iran

Original Article

Abstract

The main purpose of the present study was to assess the ecological potential of agricultural soils using geographic information system (GIS). This research was conducted during 2014 in Hamedan Province, Iran. A cross-sectional study was conducted mapping the 10 factors of soil characteristics (texture, depth, erosion, and aggregation, percentage of slope, direction of slope, height, soil salinity, pH, and fertility) that affect ecological potential. The maps were overlaid in ArcGIS software. The weighting of factors was performed using the analytical hierarchy process (AHP) technique in Expert Choice Software. Preference for the options (layers) was specified and an ecological potential map of agricultural lands in the province was created. Among the factors studied, the pH of the soil weighing 0.313 was the most important factor and soil salinity with 0.228 was the second most important factor influencing ecological potential. In general, growth-oriented agricultural development policies and improper management of farms in recent years has reduced the ecological potential of agricultural lands. The results showed that the highest and lowest ecological potential of soil in agricultural lands in the area was 6.2% and 0.07%, respectively. Development of sustainable agriculture practices, such as low tillage and no-tillage practices, reduction in the use of chemical pesticides, and use of green fertilizers to maintain and enhance the ecological potential of agricultural lands and resources, are recommended. In the policy-making process, sustainability and resource management must become a dominant notion and planning priority for policy makers and managers.

KEYWORDS: Agriculture, Ecological Potential Assessment, Geographical Information Systems, Iran, Soil

Date of submission: 16 May 2014, **Date of acceptance:** 19 Jul 2014

Citation: Naderi Mahdei K, Bahrami A. **Ecological potential assessment of soil in agricultural lands in Hamedan Province, Iran, using geographic information system.** J Adv Environ Health Res 2014; 2(4): 223-33.

Introduction

In Iran, agriculture is an important sector of the economy and plays a crucial role in achieving sustainable agricultural development. With regard to this sector, missions for self-sufficiency in food production and its contribution to export can encounter problems related to population growth and reduced rural migration. Agriculture involves the use of scientific principles and methods to identify environmental capacity and capability of each region.¹ Ecological potential assessment

(EPA) is a process that attempts to regulate human relationships with nature and develop an appropriate and harmonious relationship. EPA is an assessment of uniform and homogeneous land pieces for different types of uses. In fact, this assessment is an effective step toward designing an administrative program for sustainable development of a region. Through identification and assessment of the ecological characteristics of each region, program development can be planned in harmony with nature so that nature can ascertain the land's capabilities for development.

In recent years, external inputs have been particularly emphasized in agricultural activities; chemicals, fertilizers, pesticides, and

Corresponding Author:
Karim Naderi Mahdei
Email: knadery@yahoo.com

machinery have increased agricultural activity, and therefore, caused an overexploitation of land and natural resources. This approach, in addition to having impact on the environment, has reduced the ecological capability of agricultural lands. According to statistics provided by the Food and Agriculture Organization of the United Nations (FAO),² the lack of appropriate management and the unplanned use of agricultural inputs in Iran are far greater than other countries.

In recent decades, several models have been proposed to evaluate ecological capability globally. Most important of these have been land assessment, geomorphology, and overlay models.³ In contrast to the aforementioned models that only deal with one aspect of ecological resources (biological or physical), the combined model proposed by Makhdom can assess ecological capability. This model has 28 parameters which are classified into 7 classes.⁴ This model is more comprehensive than other models. Therefore, Makhdom's model was used in this investigation due to its abovementioned advantages. In the last few decades and especially since the debate concerning EPA, numerous studies have been conducted in this field worldwide. Verissimo et al., in their research, compared ecological capability in a catchment basin in Portugal.⁵ Using characteristics such as salinity, erosion, pH, and texture, they attempted to assess the ecological capability of agricultural land in the catchment using 3 methods of land use planning, geomorphology, and overlaying in a geographic information system (GIS) environment. After comparing the obtained results, the best method for assessing the ecological capability of lands in Portugal were offered. The results of this study illustrated that the overlay method in GIS has higher accuracy than the other 2 methods due to occurrence of fewer errors and its consideration of the percentage of each soil characteristic.⁵

Among the features selected for soil, salinity and pH have the greatest impact on ecological

potential of agricultural land. Borja and Elliott studied the ecological potential of land in European countries.⁶ They investigated factors such as texture, depth, elevation, slope, salinity, and organic matter to assess the ecological potential of agricultural land in European Union countries. The findings of the overlay method indicated that factors such as texture, salinity, and pH have the greatest impact on ecological potential of agricultural land in various parts of Europe. Among EU member states, Germany, UK, and Lithuania had the highest rates of ecological potential of agricultural land which indicated the best soil for agriculture.⁶ However, research has shown that appropriate soil management in agricultural development in European countries has had a great impact on reducing or increasing ecological potential. Countries such as Germany and Britain, with appropriate management, could increase the ecological potential of their agricultural lands.⁶ Ceia et al. assessed the ecological potential of agricultural land and soil quality in a catchment in southern Europe using factors such as tissue, salinity, erosion, pH, altitude, and fertility.⁷ This study used the 2 methods of geomorphology and overlay method in GIS to assess the ecological potential of agricultural lands.⁷

The results showed soil fertility and ecological potential had the greatest impact on agricultural ecology. However, factors such as high humidity, reduced rainfall, and excessive use of inputs, such as fertilizers and pesticides, have caused a decrease in ecological potential of agricultural lands in the catchment basin in recent years.⁷ Chainho et al. examined the effect of soil characteristics (salinity, organic matter, and pH) on the water quality in Portugal. In this study, the use of agricultural inputs (fertilizers, pesticides, and machinery), and ecological potential of the soil and its changes in agricultural land ecology were studied.⁸ The research results revealed that between 2005 and 2010, the water quality of agricultural waste was reduced by nearly 12% due to excessive use of chemical pesticides.⁸

The analytical hierarchy process (AHP) is based on paired comparisons; therefore, it can examine various issues.⁹ There are many reports on applying AHP for weighting factors. The map overlaying procedure for assessing ecological potential is one of the most important applications of GIS today.⁷ The overlaying procedure is a very comprehensive method. In Iran, there have been several studies on the ecological potential assessment for the classification of ecological zones within a catchment and or identifying fertile lands for urban development or agricultural development.¹⁰⁻¹⁵ However, there have been no studies, until today, in the field of ecological potential assessment of agricultural land using factors affecting ecological potential. In general, studies on ecological potential can be classified into 2 categories: ecological zoning,¹⁶⁻¹⁹ and diagnosing an area's potential for agricultural development.²⁰⁻²⁴ Unlike previous studies, which used one or a small number of factors, this study focuses on the method and technique of using

GIS layers. Thus, 10 factors (salinity, pH, erosion, grain size, texture, depth, elevation, and percentage of slope, direction of slope, and soil fertility) were investigated to determine the ecological potential of agricultural land in the province of Hamedan, Iran, using Makhdom's model. Moreover, the weighting of factors was performed using the AHP technique.

Materials and Methods

Hamedan Province, located in Western Iran, has a cold semi-arid climate with an annual rainfall of 340 mm. It is situated in the middle of Zagros Mountains of Iran. The study area lies between latitudes 33° 59' and 35° 48' N, and longitudes 47° 34' and 49° 36' E Greenwich meridian. The province consists of 8 cities (Figure 1). The province has an area of about 20,000 km², of which approximately 10,252 m² (about 6.52% of the province's land area) consists of plains, 5416 km² (27.8%) is covered by plateaus and hills, and about 3826 km² (19.6%) of the area comprises of mountain slopes with 40 to 100 degrees of inclination.

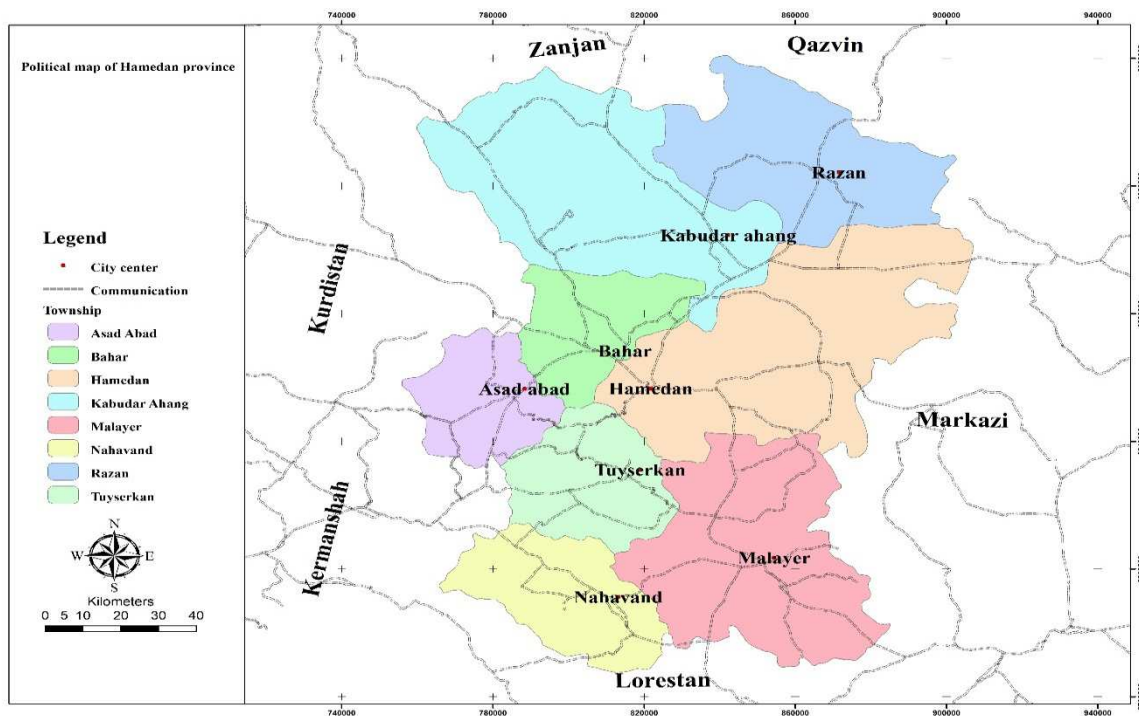


Figure 1. Location of Hamedan province in Iran

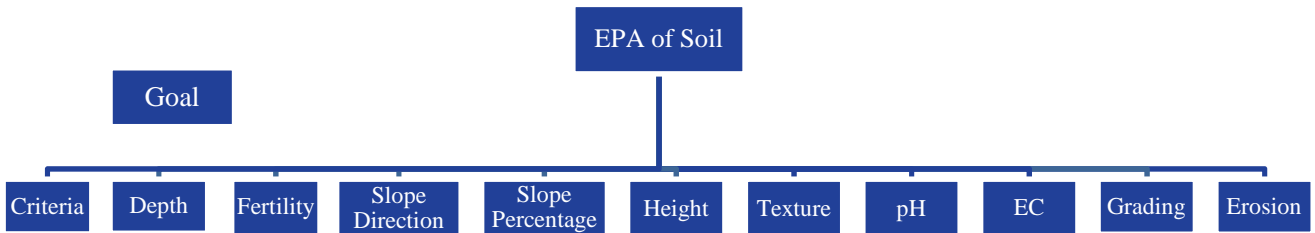


Figure 2. The structure of a hierarchical process
 EC: Electrical conductivity; EPA: Ecological potential assessment

This was a cross-sectional study in which the map of 10 factors of soil characteristics (texture, depth, erosion, aggregation, percentage of slope, direction of slope, height, soil salinity, pH, and fertility) affecting ecological potential were provided. Then, the maps were overlaid in GIS medium using ArcGIS software (Version 9.3; Esri, Redlands, CA, USA). The factors were weighed and compared using AHP method (Figure 2). For this purpose, the Delphi method was applied. The judgment of 50 specialists in the fields of agriculture, environmental science, and geography were considered and pairwise comparisons were used to specify the level of importance and priority of each of the factors with respect to each other. Expert Choice Software (Expert Choice Inc., Pittsburgh, PA, USA) was used to form a matrix of rows and columns with the same number of factors. Finally, data was assessed according to the EPA model proposed by Makhdom as follows:⁴

$$Y = ax + \sum_{n=1}^{10} [(a_1 * x_1) + (a_2 * x_2) + \dots + (a_{10} * x_{10})]$$

where a is each parameter affecting zoning, x

is effective coefficient of each parameter based on Expert Choice Software and, Y is land use levels based on soil ecological capacity depending on the type of cultivation.

Results and Discussion

The pairwise comparison was conducted for the 10 abovementioned factors using Expert Choice Software. Figure 3 presents the pairwise comparisons between those 10 factors. According to the classification presented by Makhdom’s model, soil erosion, soil salinity, acidity, fertility, soil texture, slope, height, and slope and soil grading were prepared separately (Figure 4).

Using AHP, relative weight and final weight of each factor was calculated (Table 1). Based on the results, the relative weight of factors are as follows: soil pH (4.53), soil salinity (3.30), soil aggregation (1.42), soil texture (1.23), slope percentage (1.22), soil depth (0.82), fertility (0.71), soil erosion (0.64), height above sea level (0.39) and slope direction (0.22).

	Soil texture	Soil gradin	Slope	Height	Erosion	Fertility	Slope direc	Soil depth	PH	Ec
Soil texture		3.0	5.0	7.0	5.0	1.0	7.0	1.0	7.0	7.0
Soil grading			5.0	8.0	1.0	1.0	7.0	1.0	5.0	5.0
Slope				3.0	9.0	7.0	5.0	5.0	5.0	5.0
Height					1.0	3.0	4.0	3.0	6.0	6.0
Erosion						2.0	4.0	3.0	6.0	8.0
Fertility							6.0	1.0	4.0	9.0
Slope direction								4.0	6.0	8.0
Soil depth									1.0	6.0
PH										1.0
Ec										

Figure 3. Pairwise comparisons between the 10 factors
 EC: Electrical conductivity

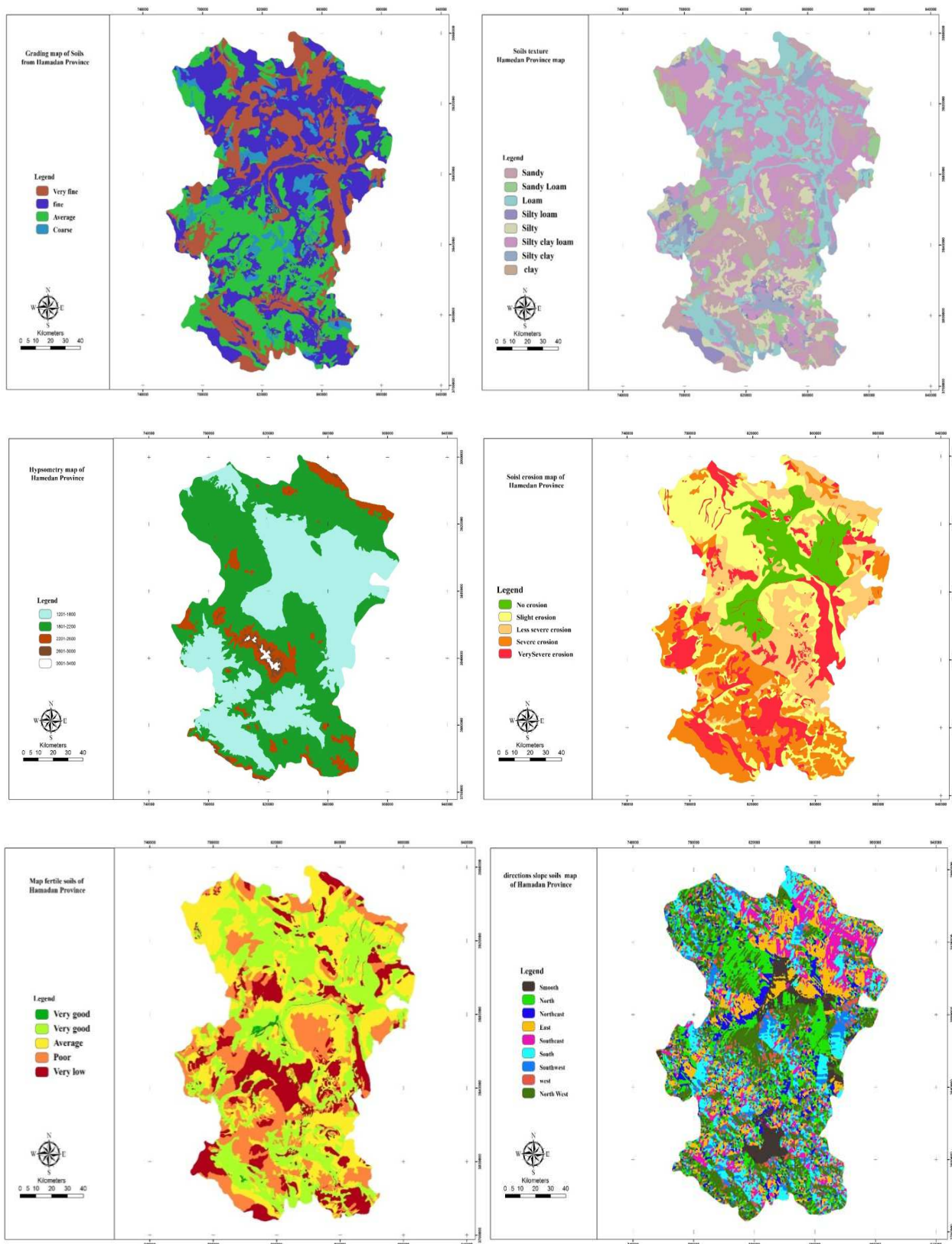


Figure 4. Maps of the possible ecological factors

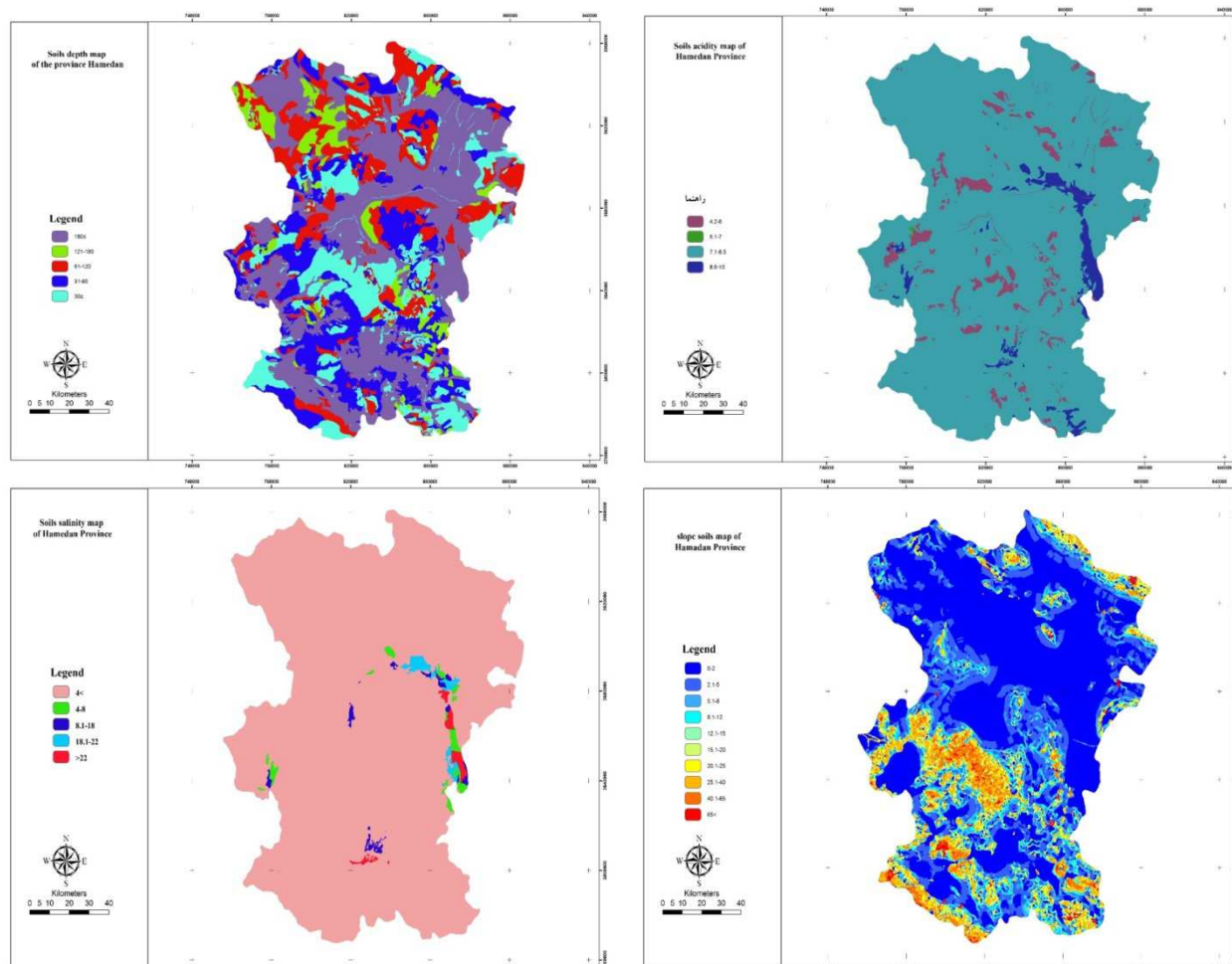


Figure 4. Maps of the possible ecological factors (Continue)

The final weights of the effective factors on ecological potential were derived from a combination of the relative weights. Based on the obtained results, among the considered factors, the pH of the soil with the final weight of 0.313 is the most effective factor and salinity is the second most effective factor impacting ecological potential of agricultural land in the province of Hamadan. The results regarding both factors are consistent with the study by Veríssimo et al.⁵ and the salinity factor result is consistent with the findings from Ceia et al.⁷ and Borja and Elliott.⁶ However, soil fertility is ranked seventh, and thus, is not consistent with the findings of Ceia et al.⁷ and Borja and Elliott.⁶ Several reasons can cause these differences. Physical differences, different policies about agricultural development, and cultural,

religious, and socio-economic differences in each area can influence an area of land and cause dissimilarities. Therefore, clearly this area of Iran cannot be compared with other parts of the world and cannot even be equated to other areas inside Iran. Depending on the region's natural and geographical, economic, and social features the ecological characteristics of agricultural lands can be affected in different ways.

Factors affecting agricultural lands and their weights were determined correctly and with acceptable accuracy (below 0.1) through a review of the literature along with the views of experts and in the form of pairwise comparisons and AHP.^{6,19,25} This review highlights the effectiveness of resources and specialized expertise in the form of AHP for the weight of the factors in such research. The zoning map of

ecological potential of lands was produced using overlaying method of layers in a GIS (Figure 5). In this method, all the layers are superimposed on one another based on the percentage of each factor and a final map of ecological zoning of agricultural land is produced. Salinity and pH factors were the most important factors. It seems that the main reason for this was the mismanagement of inputs such as fertilizers and chemical pesticides.

Table 1. Final weight of the factors studied

Factors	Relative weight	Final weight	Ranking
PH	4.53	0.33	1
EC	3.30	0.228	2
Soil grading	1.42	0.098	3
Soil texture	1.23	0.085	4
Slope	1.22	0.084	5
Soil depth	0.82	0.075	6
Fertility	0.71	0.049	7
Erosion	0.64	0.044	8
Height	0.39	0.027	9
Slope direction	0.22	0.015	10

EC: Electrical conductivity

In fact, these 2 factors can also have positive

or negative effects on other factors. The present study confirms the results of previous studies.^{6,7,14} Furthermore, the use of AHP method, combining the weight of factors, and mapping and overlaying layers to achieve the ecological potential map in agricultural lands has been confirmed.^{8,16,20,21,24} Among other notable issues in this method, accuracy, simplicity, speed, and repetitiveness, especially in ecological potential assessment of agricultural lands with high standards, are also involved in the assessment. In similar studies only a few specific factors were evaluated in terms of ecological potential of agricultural lands.^{5,18,23} The 10 most important factors in terms of impact on ecological potential of agricultural lands were selected based on the recommendations of scholars including Ceia et al.⁷ Verissimo et al.⁵, Chainho et al.,⁸ and Verissimo et al.²⁶ On the basis of aforementioned factors, the assessment model is more comprehensive than all of the possible ecological potential of agricultural lands in the province of Hamedan.^{5,7,8,26}

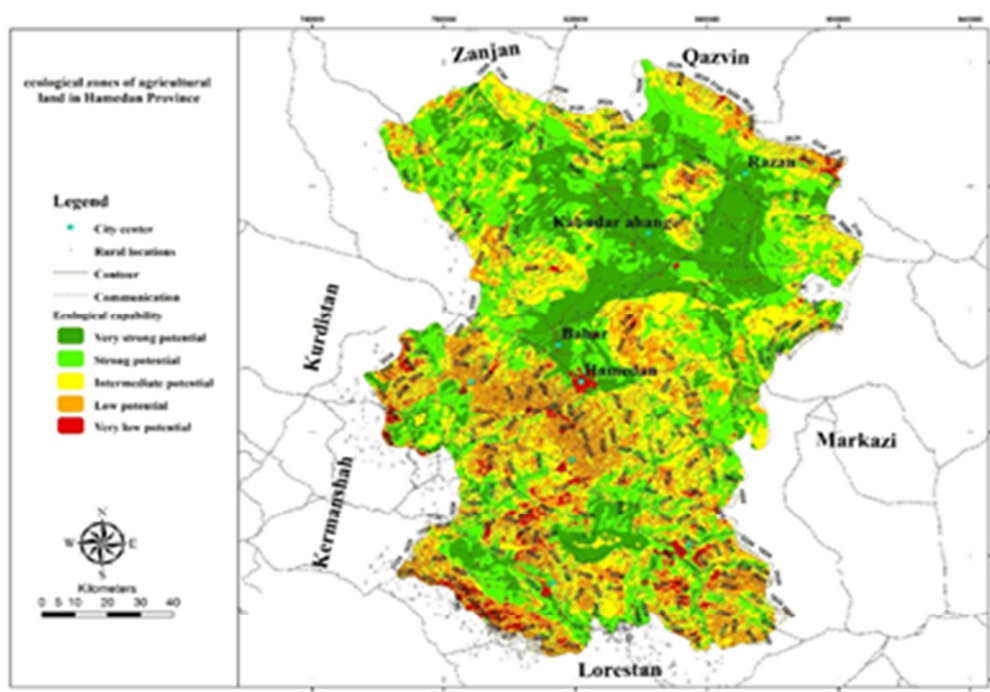


Figure 5. Ranking the ecological zones of agricultural land in the province of Hamedan

The results related to the classification of agricultural land in the province of Hamedan (Table 2) showed that the total area of 1,939,583.78 hectares of the province has immense ecological potential; 979592.33 hectares (32.51%) have very high and high capability, 549050.41 hectares (28.31%) have average capability, and 410941.04 hectares (21.19%) have low and very low ecological potential.

Table 2. Classification of areas based on ecological potential

Categories	Area (ha)	Percentage
Very high potential	393318	2.28
High potential	586274	30.23
Average potential	549050	28.31
Low potential	339381	17.50
Very low potential	71559	3.69
Total	1,939,583	100

In addition, more than 30% of agricultural land is of high ecological potential. The assessment shows the ecological status of soil in

agricultural land in the province. However, if water and climate factors are considered in the province, based on the researcher's observation in the cities of Kabudarahang and Razan, Iran, more than 20% of the wells are almost dry and the depth of groundwater is also much lower than in the past. It can be argued that the ecological potential of agricultural land in the province is much lower than that presented in the classification. According to the results of "the map terrain for all types of cultivations" (Figure 6), an area of 282747.052.2 hectares of land is suitable for the cultivation of irrigated wheat. Areas suitable for irrigated wheat cultivation and other uses have also been identified in the province (Table 3).

The results showed that less than 40% of land is suitable for irrigated crops and orchards (Table 3). However, this assessment was based on soil ecological factors. If water and climate factors are also assessed, this ratio will evidently be lower.

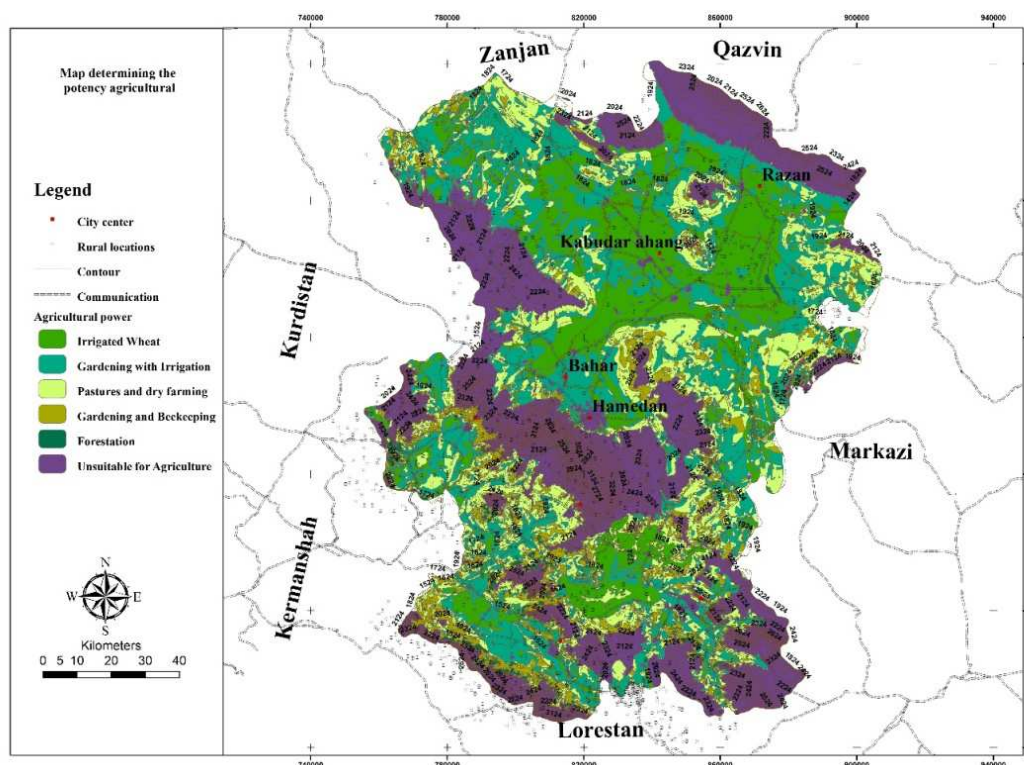


Figure 6. Map of different levels of agriculture applications

Table 3. Area of lands for various agricultural applications

Type of cultivation	Area (ha)	Percentage
Irrigated wheat	282747.052	14.58
Irrigated orchard	432876.606	22.23
Rainfed cultivation and pasture land	450034.169	23.20
Husbandry and pasture	248503.931	12.80
Forest	76599.718	3.95
Unsuitable for agriculture	448822.3011	23.14
Total	1,939,583.778	100

Conclusion

In this study, 10 factors, including soil erosion, salinity, fertility, depth, texture, slope, height, and soil grading, which affect the ecological potential of agricultural land in the province of Hamedan, were investigated. The ecological potential map of agricultural lands in the province of Hamedan was prepared according to the classification in the proposed model by Makhdom. It was found that pH, salinity, and acidity factors have the greatest impact on the ecological potential of agricultural land in the province. Mismanagement of inputs, such as fertilizers and chemical pesticides, to produce more crops and gain higher profits can account for low ecological potential. In fact, these 2 factors can also have positive or negative effects on other factors. In general, it can be said that unsuitable management of farms in recent years and wrong agricultural development policies in Iran to increase production without consideration of detrimental environmental effects has led to severe reduction of ecological potential of agricultural lands in the production of strategic crops, such as wheat, especially in the studied area.

In regards to agricultural issues, taking advantage of saline and alkaline soils is associated with a failure to absorb water and nutrients by the roots of plants and unfavorable ratio between the ion of impaired growth and yield of the plant. Since alkaline soil has very low permeability, irrigation, and drainage, these soils are particularly problematic. Furthermore, although the results show that more than 30% of agricultural lands in the province are of high ecological potential, and nearly 40% of land is

suitable for irrigated crops and orchards, the fact is that this assessment has been based on ecological potential of the soil. If water and climate factors were considered, this ratio would be much lower than the estimated amount. The reason for this issue was the exploitation of the soil and water resources for the purpose of achieving more profits in a short time. Thus, conventional management of agricultural lands has led to reduced ecological potential of the soil and water.

Therefore, in order to improve and preserve the ecological potential of agricultural land, it is recommended that agricultural development policies be directed towards producing products that use less water. It is also recommended that agricultural water use efficiency be promoted through the use of sprinklers and drip systems. In addition, it is suggested that agricultural policies be directed towards the following directions: the use of green manures, reduction of the use of chemical pesticides, the use of protective tills (low-till and no-till), and promotion of ways which have the least impact on erosion, and maintain moisture and fertile agricultural lands. Thereby, ecological potential can be protected and agricultural sustainability of agricultural land resources can be increased to an acceptable level. In this regards, a comprehensive and detailed plan on administrative and technical aspects is need to achieve sustainable development in agriculture on the basis of ecological potential of lands. In this proposed plan, an optimizing scheme for the better use of land, water, pesticides, and fertilizers, increasing performance, and safeguarding the environment through the use of sound technologies (organic-based, ecologically sound manure system, and internal input) will be necessary to maintain soil productivity and potential for the future.

For future research, the comprehensive assessment of the ecological potential of agricultural lands and the climate factor (water and weather) is recommended.

Conflict of Interests

Authors have no conflict of interests.

Acknowledgements

This paper was a part of the second author's Ph.D. thesis. The authors would like to thank the staff of the Extension and Education Department and Soil Laboratory in Bu-Ali Sina University, Hamadan, Iran.

References

1. Barzegar A. Salt affected soils (identification and exploitation). Khuzestan, Ahvaz: Shahid Chamran University Press; 2002. [In Persian].
2. Food and Agriculture Organization of the United Nations. Fao-food and agriculture. [Online]. [cited 2009]; Available from: URL: <http://www.fao.org/home/en/>
3. McHarg IL. Design with nature. Hoboken, NJ: John Wiley & Sons; 1995.
4. Reyahi Khoram M, Shariat M, Azar A, Mahjub H, Moharamnejad N. Environmental evaluation for agricultural activity by GIS; a case study. Sarhad J Agri 2007; 23(2): 339-44.
5. Veríssimo H, Lane M, Patrício J, Gamito S, Carlos Marques J. Trends in water quality and subtidal benthic communities in a temperate estuary: Is the response to restoration efforts hidden by climate variability and the Estuarine Quality Paradox? Ecological Indicators 2013; 24: 56-67.
6. Borja A, Elliott M. What does 'good ecological potential' mean, within the European Water Framework Directive? Mar Pollut Bull 2007; 54(10): 1559-64.
7. Ceia FR, Patrício J, Franco J, Pinto R, Fernández-Boo S, Losi V, et al. Assessment of estuarine macrobenthic assemblages and ecological quality status at a dredging site in a southern Europe estuary. Ocean & Coastal Management 2013; 72: 80-92.
8. Chainho P, Silva G, Lane MF, Costa J, Pereira T, Azeda C, et al. Long-term trends in intertidal and subtidal benthic communities in response to water quality improvement measures. Estuaries and Coasts 2010; 33(6): 1314-26.
9. Saaty TL. The analytic hierarchy process: planning, priority setting, resource allocation. New York, NY: McGraw-Hill, 1980. p. 437.
10. Dashti S, Monavari M, Sabzghabaei GH. Rehabilitations to received the rural sustainable development using environmental potential evaluation Zakherd watershed. Environmental Sciences 2009; 6(2): 77-86. [In Persian].
11. Parvaresh H, Dehghani M, Nohegar A. The comparison of physical per ECA ration (geomorphology), and methods for assessing the ecological capability of watershed land in the province of Hormozgan. The Journal of Land Assessment 2010; 2(2): 27-50. [In Persian].
12. Movahed A, Zadeh Dabagh N. Ecological potential evaluation of Dez river confine (Tanzimi sluice than Ghire sluice) for ecotourism. Journal of Environmental Studies 2010; 36(55): 4-6.
13. Norouzi Avargani A, Nouri SH, Kiani Selmi S. Evaluation of environmental capacities for agricultural development? (Case study: Choghakhor rural district, Borujen Township). Journal of Rural Research 2010; 1(2): 9-116. [In Persian].
14. Moradzadeh F, Babaei-Kafaki S, Mataji A. Assessment of ecological competence of surface expansion through GIS (case study: Dadabad District in Lorestan Province). Renewable Natural Resources Research 2011; 2(4): 11-23. [In Persian].
15. Gharakhlou M, Pourkhabbaz HR, Amiri MJ, Faraji HA. Ecological capability evaluation of Gazvin region for determining urban development potential points using geographic information system. Urban a Regional Studies and Research 2009; 1(2): 51-68. [In Persian].
16. Ashrafi A, Mikaniki J, Dehghani M. Agro-ecological zoning and evaluation of ecological potencies of south khorasan for jujube plantation. Journal of Geographic Space 2013; 3(7): 67-86. [In Persian].
17. Martins I, Pardal MA, Lillebo AI, Flindt MR, Marques JC. Hydrodynamics as a major factor controlling the occurrence of green macroalgal blooms in a eutrophic estuary: a case study on the influence of precipitation and river management. Estuarine, Coastal and Shelf Science 2001; 52(2): 165-77.
18. Marques JC, Neto JM, Patrício J, Pinto R, Teixeira H, Veríssimo H. Monitoring the Mondego estuary. [Online]. [cited 2007 Jan]; Available from: URL: http://scholar.google.nl/citations?view_op=view_citation&hl=nl&user=la84roQAAAAJ&citation_for_view=la84roQAAAAJ:ufrVoPGSRksC
19. Hering D, Borja A, Carstensen J, Carvalho L, Elliott M, Feld CK, et al. The European Water Framework Directive at the age of 10: A critical review of the achievements with recommendations for the future. Science of the Total Environment 2010; 408(19): 4007-19.
20. Noori H, Seidaei E, Kiani S, Soltani Z, Norouzi A. Assessment of ecologic environmental sources for determining rich farmland by GIS (central district of Kiar Sub County). Geography and Environmental Planning 2010; 21(1): 77-94. [In Persian].
21. Meire P, Ysebaert T, van Damme S, van den Bergh E, Maris T, Struyf E. The Scheldt estuary: a description of a changing ecosystem. Hydrobiologia 2005; 540(1-3): 1-11.
22. McLusky DS, Elliott M. The estuarine ecosystem:

- ecology, threats, and management. 3rd ed. Oxford, UK: Oxford University Press; 2004. p. 216.
23. Paerl HW. Assessing and managing nutrient-enhanced eutrophication in estuarine and coastal waters: Interactive effects of human and climatic perturbations. *Ecological Engineering* 2006; 26(1): 40-54.
 24. Fredriksen S, de Backer A, Boström C, Christie H. Infauna from *Zostera marina* L. meadows in Norway. Differences in vegetated and unvegetated areas. *Marine Biology Research* 2009; 6(2): 189-200.
 25. Rasouli AA, Ghasemim K, Sobhani B. The role of precipitation and elevation in determine of the favorable area for dry-farming wheat with usage of GIS study case: Ardabil province. *Geography and Development Iranian Journal* 2005; 3(5): 183-200.
 26. Veríssimo H, Bremner J, Garcia C, Patrício J, van der Linden P, Marques JC. Assessment of the subtidal macrobenthic community functioning of a temperate estuary following environmental restoration. *Ecological Indicators* 2012; 23: 312-22.



Removal of hexavalent chromium from aqueous solution using canola biomass: Isotherms and kinetics studies

Davoud Balarak¹, Yousef Mahdavi², Fardin Gharibi³, Shahram Sadeghi⁴

1 Health Promotion Research Center AND Department of Environmental Health, School of Public Health, Zahedan University of Medical Sciences, Zahedan, Iran

2 Department of Environmental Health, Student Research Committee, Mazandaran University of Medical Sciences, Sari, Iran

3 Deputy of Research, Kurdistan University of Medical Sciences, Sanandaj, Iran

4 Department of Environmental Health Engineering, Student Research Committee, Kurdistan University of Medical Sciences, Sanandaj, Iran

Original Article

Abstract

The removing of hexavalent chromium from wastewater or decreasing its chromium (VI) content up to the permitted levels is important due to its non-biodegradation, bioaccumulation, and cancer-causing and toxic effects. In the present study, biosorption of Cr (VI) from aqueous solutions using canola was investigated. The various physicochemical parameters such as pH, initial Cr (VI) ion concentration, adsorbent dose, and equilibrium contact time were optimized in batch adsorption system. The results showed that the optimum amount of each parameter was as follows: initial concentration = 10 mg/l, pH = 3, contact time = 75 minutes, and adsorbent dosage = 5 g/l. The maximum adsorption efficiency was about 99.1%. The maximum adsorption capacity was calculated and was about 10.67 mg/g of adsorbent. Moreover, the sorption data was best fitted on the Langmuir isotherm model and adsorption kinetic is adopted with the pseudo-second-order model. The results of the present study suggest that canola can be used beneficially in treating aqueous solutions containing heavy metal ions.

KEYWORDS: Adsorption, Biomass, Chromium (VI), Kinetics

Date of submission: 12 May 2014, *Date of acceptance:* 28 Jul 2014

Citation: Balarak D, Mahdavi Y, Gharibi F, Sadeghi Sh. **Removal of hexavalent chromium from aqueous solution using canola biomass: Isotherms and kinetics studies.** J Adv Environ Health Res 2014; 2(4): 234-41.

Introduction

Due to the specific characteristics of heavy metals, they are considered as major pollutants which reduce the water quality.¹⁻³ Chromium (Cr) is a heavy metal which can be found mainly in two forms, including hexavalent and trivalent.⁴⁻⁶ The discharge of wastewater by various industries, including electroplating,

leather tanning processes, chromite ore processing, wood preservation, alloy making, corrosion control, pigment and dyes, and metal finishing industries, is the main source of Cr in the environment.^{7,8} Cr is introduced as a toxic element due to its adverse effects, such as irritation of lungs and stomach, cancer in the digestive tract, low growth rates in plants, and death of animals.⁹ Therefore, the elimination of Cr from water and wastewater is an important subject. Various techniques

Corresponding Author:

Shahram Sadeghi

Email: shahram.snaa@yahoo.com

such as electrodeposition, membrane filtration, ion exchange, and biological processes have been proven to remove Cr from effluents.^{10,11} However, the disadvantages of these techniques can limit their application in Cr removal.¹² Among the aforesaid methods, adsorption is known as an efficient and reliable method.¹³ Although activated carbon is widely used for Cr removal, problems associated with activated carbon decrease the attraction of its application. Therefore, researchers are trying to find a low-cost and effective adsorbent. Recently, various natural material, such as red mud, banana peel, apple residues, orange peel, and azolla, have been used as effective adsorbents for the removal of heavy metals.¹⁴⁻¹⁶ The canola stalk is a lignocellulosic waste widely produced in Iran and around the world due to the growth of canola for the production and consumption of vegetable oils. Therefore, the canola stalk is easily available and, due to its characteristics, has been used in several studies for pollutant removal.^{17,18} The aim of the present study was the investigation of the ability of canola in Cr removal from aqueous solution and the effect of various parameters on this process, and isotherm and kinetic studies.

Materials and Methods

In this study, canola was used as low-cost natural or agricultural waste for Cr (VI) removal from aqueous solutions. The canola stalks were collected from the research farm of the School of Agriculture, University of Tabriz, Iran. The stalks were washed several times with water to remove any contaminants and dried in the oven at 105 °C for 5 hours. Subsequently, the biomass were treated with 0.1 M H₂SO₄ for 2 hours, washed with distilled water, and then, oven dried at 105 °C for 3 hours.¹⁹ After drying, the adsorbents were sieved to obtain particle size of 18 mesh prior to being used for adsorption studies.

All the chemicals used in the present study were of analytical grade and were obtained from Merck & Co., White House Station, NJ, USA. The

specific surface area of dried canola was determined through the BET-N₂ method using a BET surface area analyzer (Model ASAP 2020, Micromeritics Instrument Corporation, Norcross, GA, USA) based on nitrogen adsorption-desorption isotherms at 77 K. The surface images of dried canola before and after the adsorption process were captured by a scanning electron microscope (SEM) (XL30, Philips, Amsterdam, Netherlands). An ultraviolet-visible spectrophotometer (DR5000 spectrophotometer, Hitachi, Tokyo, Japan) was used to determine the Cr (VI) content of standard and treated solutions after adsorption experiments.

The stock Cr (VI) solution (1000 mg/l) was prepared by dissolving 3.73 g of K₂CrO₄ · 2H₂O in 1000 ml of double distilled water. The desired initial concentrations for experiments were prepared by appropriate dilution of the stock Cr (VI) solution.

The batch adsorption experiments were carried out by 100 ml of Cr (VI) solution in a series of 250 ml stopper conical flasks. The pH of solution was adjusted by the addition of 0.1 N HCl or 0.1 N NaOH solutions, as required. Then, the flasks were shaken for the desired contact time in an electrically thermostated reciprocating shaker (Model LSI-3016R, Daihan LabTech Co., Ltd, Korea) at 120-125 rpm and 30 °C. The literature review indicated that the most important variables which are effective on adsorption include pH, adsorbent dose, contact time, and pollutant concentrations. Therefore, 10-100 mg/l was selected as the initial Cr (VI) concentration. The effect of adsorbent dosage (0.1-1 g), contact time (10- 180 minutes), and pH (3-8) were studied.²⁰

The equilibrium time was estimated by sampling at regular time intervals. The samples were filtered through the Whatman no.1 paper filter (Whatman International Ltd., Maidstone, England). The UV-visible spectrophotometer was employed to determine the remaining Cr (VI) concentration in the sample solution using 1,5-diphenylcarbazide.²¹ All the experiments were carried out in triplicate.

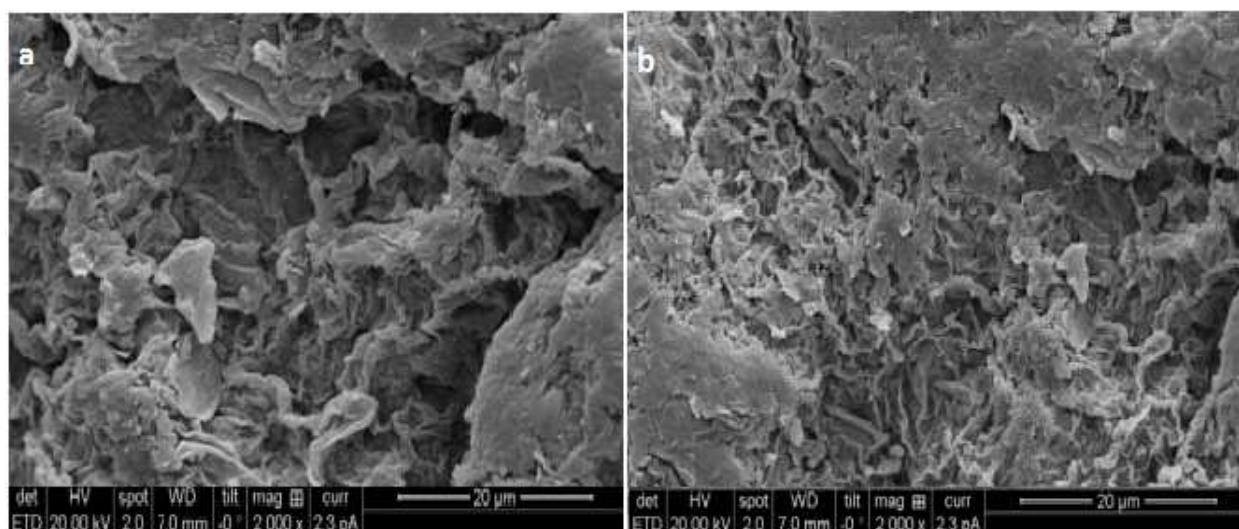


Figure 1. The Scanning electron microscopy (SEM) image of dried canola: (a) before use; (b) after use

Results and Discussion

Scanning electron microscopy (SEM) images were applied to analyze the surface structure of canola (Figure 1). Figure 1 (a) clearly shows the pore textural structure of dried canola before use. However, figure 1 (b) indicated that the clear pore textural structure is not observed on the surface of dried canola after use. This could be due to either agglomeration on the surface or the invasion of Cr into the pores of dried canola. In addition, it was found that the adsorbent has a heterogeneous surface structure with deep pores. The specific surface area of modified canola was determined and found to be 32 m²/g. Similar results were obtained for adsorption of Acid Blue 113 from aqueous solutions by canola.²²

Effect of contact time and initial Cr (VI) concentration

Among the desirable parameters, contact time is considered as a significant parameter for rapid sorption and successful practical application of biosorbents. Figure 2 shows the effect of contact time on the biosorption of Cr (VI) ions for several concentrations onto canola. The biosorption efficiency of Cr (VI) increased considerably with increasing of contact time up

to 75 minutes, and then, it remained approximately constant. Therefore, 75 minutes was selected as optimum contact time for further experiments. Initially, the biosorption took place at a rapid rate due to the adsorption of Cr (VI) molecules on the upper surface of the biosorbent. Then, it reduced due to the slower diffusion of Cr (VI) molecules into the inner structure of the biosorbent.²³ The presence of a large number of exchanging sites at the start of biosorption is another reason which could help to improve the process.²⁴ Gupta et al. assessed the effect of contact time on Cr (VI) biosorption onto green algae *spirogyra* species.²⁵ The biosorption capacity (mg/g) increased quickly at the beginning, and equilibrium was attained after 90 minutes. The Cr (VI) removal efficiency decreased by increasing of initial concentration; therefore, the adsorption rate in a concentration of 10 mg/l wever, the removal efficiency decreased in higher initial concentration of Cr (VI) due to limitation of total available adsorption sites. Similarly, the biosorption of Pb⁺² by rice husk decreased with an increase in the Pb⁺² initial concentrations. It has been suggested that the available sites on the biosorbent can be the limiting factor for Pb⁺² removal.²⁶

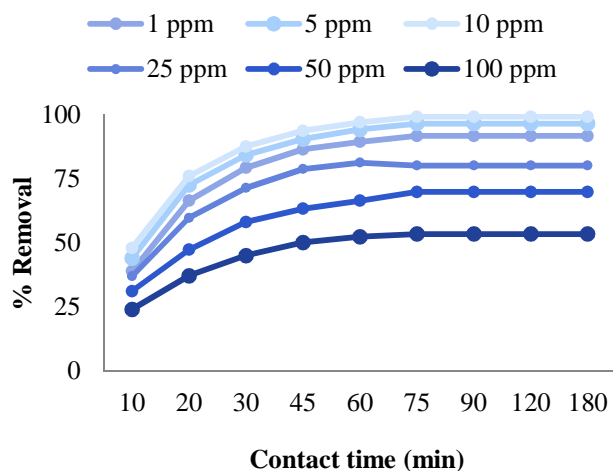
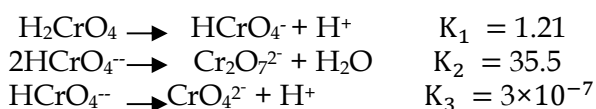


Figure 2. Effect of contact time and initial Cr (VI) concentration on removal efficiency (pH = 3, adsorbent dose = 5 g/L, temperature = 30 °C)

Effect of pH

Metal sorption depends on the solution pH. The pH of the system determines the adsorption capacity due to its influence on the surface of the canola and formation of different ions in chromium solutions. The variation of the adsorption capacity of Cr (VI) on canola with pH is shown in figure 3. The chromium ions exist in the form of HCrO_4^- at very low pH values; however, there are different forms such as $\text{Cr}_2\text{O}_7^{2-}$, HCrO_4^- , and $\text{Cr}_3\text{O}_{10}^{2-}$ at pH values of higher than 6. The predominant form is HCrO_4^- . By increasing of pH value, equilibrium shifted from HCrO_4^- to $\text{Cr}_2\text{O}_7^{2-}$ and CrO_4^{2-} .²⁷ At lower pH values, the surface of adsorbent is surrounded by hydronium ions which enhance the Cr (VI) interaction with binding sites of the biosorbent. As the pH increased, the overall surface charge on the biosorbents became negative and adsorption decreased.²¹ The following equilibrium may be written for the Cr (VI) anions present in aqueous solutions.²⁰ The equilibrium that exists between different ionic species of chromium is as follows:



Adsorption of Cr (VI) was not significant at

pH values of more than 6 due to dual complexation of the anions $\text{Cr}_2\text{O}_7^{2-}$, CrO_4^{2-} , and OH^- which can be adsorbed on the surface of the adsorbents; however, the predominant form in these pH values was OH^- .²⁸ Hence, it can be concluded that other mechanisms, such as physical adsorption, have played an important role and ion exchange mechanism might have reduced at lower pH values.²⁹

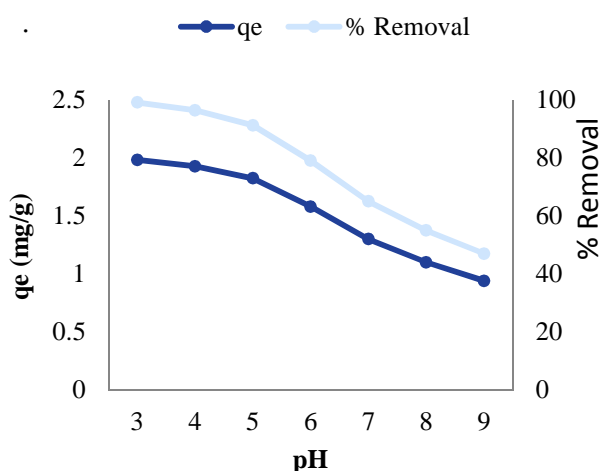


Figure 3. Effect of pH on Cr (VI) removal efficiency and adsorption capacity ($C_0 = 10$ mg/l, adsorbent dose = 5 g/l, contact time = 75 minutes, and temperature = 30 °C)

Effect of biomass dosage

The effect of biomass dosage on the biosorption of Cr (VI) ions was studied using different biomass dosages in the range of 1–10 g/l (Figure 4). The results showed that biosorption efficiency is significantly dependent on the increase of biomass dosage in the solution. The percentage of metal biosorption steeply increases with biomass loading up to 5 g/l. Moreover, it was observed that the adsorption capacity decreases by increasing of biosorbent dosage. These results can be describe by the fact that although the number of available sites for biosorption increases by increasing of the biosorbent dose, biosorption sites remain unsaturated during the biosorption reaction.^{30,31} Similarly, Kumar and Bandyopadhyay investigated the effect of biosorbent dose on the removal of Cd^{2+} by rice husk from aqueous solution.³² The results showed that an increase in the biosorbent dose from 1 to 5 g/l leads to the

increasing of the removal efficiency from 38% to 96%, and decreasing of the biosorption capacity from 7.5 to 1.24 mg/g. Similar results were reported for cadmium biosorption in an aqueous solution by *Saccharomyces cerevisiae*. Therefore, the optimum biomass dosage was determined as 4 g/l for further experiments.³³

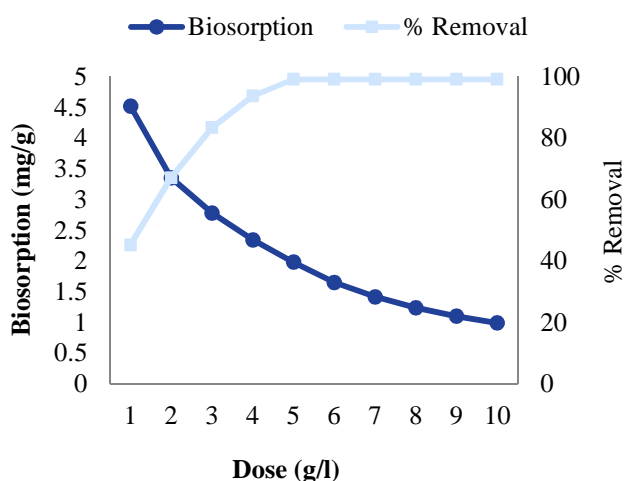


Figure 4. Effect of biomass dose on Cr (VI) biosorption on dried canola ($C_0 = 10$ mg/l, pH = 3, contact time = 75 minutes, and temperature = 30 °C)

Biosorption isotherm models

The capacity of a biomass can be described by equilibrium biosorption isotherm, which is characterized by certain constants which can express surface properties and affinity of the biomass. The biosorption isotherms were investigated using 3 equilibrium models, which are the Langmuir, Freundlich, and Temkin models. The applicability of the isotherm equations was compared by investigating the correlation coefficients, R^2 .

The Langmuir biosorption isotherm has been successfully applied for various pollutant biosorption processes and has been extensively used for the biosorption of a solute from a liquid solution. Biosorption onto specific homogeneous sites within the adsorbent is the basic assumption of the Langmuir theory. This model can be written as follows:³⁴

$$\frac{1}{q_e} = \frac{1}{q_{\max}} + \frac{1}{q_{\max} K_L} \times \frac{1}{C_e}$$

where q_e is the equilibrium Cr (VI) ion concentration on the adsorbent (mg/g), C_e the equilibrium Cr (VI) concentration in the solution (mg/l), q_m the monolayer biosorption capacity of the adsorbent (mg/g), and K_L the Langmuir biosorption constant (mg/l) related to the free energy of biosorption.

The significant feature of the Langmuir isotherm model can be defined by the dimensionless constant separation factor (R_L) which is expressed by the following equation:³⁵

$$R_L = \frac{1}{1 + K_L C_0}$$

where C_0 is the initial Cr (VI) concentration (mg/l) and K_L is the Langmuir constant (mg/l). R_L shows the nature of biosorption mechanism. Values of R_L specify the shapes of isotherms as either unfavorable ($R_L > 1$), linear ($R_L = 1$), or favorable ($0 < R_L < 1$).

The Freundlich isotherm is an empirical relationship which shows the interaction between adsorbate molecules and heterogeneous surfaces.

The linear equation is expressed as follows:³⁶

$$\ln q_e = \ln K_F + \frac{1}{n} \ln C_e$$

where q_e is the equilibrium Cr (VI) concentration on the adsorbent (mg g⁻¹), C_e the equilibrium Cr (VI) concentration in solution (mg l⁻¹), and K_F is the Freundlich constant.

The Temkin isotherm model suggests an equal distribution of binding energies over the number of the exchanging sites on the surface. The linear form of the Temkin isotherm equation is represented by the following equation:³⁵

$$q_e = B \ln A + B \ln C_e$$

where $B = RT/b$, T is the absolute temperature in K, R the universal gas constant (8.314 JK⁻¹ mol⁻¹), A the equilibrium binding constant, and the constant B is related to the heat of adsorption. Values of band A were calculated from the plot of q_e against $\ln C_e$.

The values of various isotherm constants are

described in table 1. The results show that the Cr (VI) adsorption equilibrium was best defined by the Langmuir isotherm model, which indicated that the chemisorption mechanism is involved in the adsorption of Cr (VI) on canola. In this study, the value of R_L was obtained in the range of 0-1, and this shows that the biosorption process is favorable.

Finally, the correlation coefficients (R^2) for the Freundlich and Temkin isotherm models were lower than that of the Langmuir isotherm model.

Table 1. Adsorption isotherm constants for the adsorption of Cr (VI) onto canola at two biomass dosages

Isotherm models	3 g/l	6 g/l
Langmuir		
q_m (mg/g)	2.950	4.450
K_L (mg/l)	0.071	0.014
R_L	0.190	0.340
R^2	0.998	0.999
Freundlich		
K_F (mg/g)	9.170	14.720
n	1.260	2.440
R^2	0.941	0.962
Temkin		
A (g/l)	0.350	0.570
B	15.410	26.340
R^2	0.914	0.944

q_m : The monolayer biosorption capacity; K_L : The Langmuir biosorption constant; R_L : The nature of biosorption mechanism; R^2 : correlation coefficients; K_f : The Freundlich constant

Biosorption kinetics

Kinetic studies are necessary to optimize the different operation conditions of biosorption. Various kinetic models have been suggested for explaining the order of reactions.

The kinetics of Cr (VI) onto canola was analyzed using pseudo-first-order and pseudo-second-order kinetic models. The applicability of these kinetic models was determined by measuring the coefficients of determination (R^2). The higher value of R^2 indicates the best applicability of the model for obtained data.

The pseudo-first-order kinetic model can be expressed as follows:³⁶

$$\text{Log}(q_e - q_t) = \text{log } q_e - \frac{K_1}{2.303}t$$

where q_e and q_t are the biosorption capacity

(mg/g) at equilibrium and time t , respectively, k_1 is the constant rate ($L \text{ min}^{-1}$) of pseudo-first-order kinetic model.

The values of k_1 , calculated q_e , experimental q_e , and R^2 are presented in table 2. This table showed that calculated q_e is not equal to experimental q_e , although the values of R^2 are satisfactory. Mostly, the first-order kinetic model is not fitted well for the whole data range of contact time and can be applied for the preliminary stage of the biosorption mechanism.³⁷ This suggests that the uptake of Cr (VI) probably does not follow the pseudo-first-order model. Roy et al. showed that the biosorption of heavy metals onto green algae and ground rice hulls does not follow the first-order kinetic model.³⁸

Furthermore, the pseudo-second-order kinetic model can be described as follows:³⁶

$$\frac{t}{q_t} = \frac{1}{k_2 q_e^2} + \frac{1}{q_e t}$$

where q_e is the biosorbed amount of Cr (VI) at equilibrium (mg/g) for the pseudo-second-order biosorption, q_t is the amount of biosorbed Cr (VI) at time t (mg/g), and k_2 is the pseudo-second-order kinetic constant rate (g/mg/min). The values of various pseudo-second-order constants are described in table 2. The values of calculated q_e and experimental q_e are quite close. The correlation coefficients ($R^2 = 0.999$) are also significant which indicates that the pseudo-second-order kinetic model is well fitted for kinetic data. The results showed that the pseudo-second-order kinetic model is more appropriate and effective than the pseudo-first-order kinetic model. Wong et al. suggested that the removal of Cu^{+2} and Pb^{+2} onto rice husk obeyed the pseudo-second-order kinetic model.²⁶

Conclusion

This study demonstrated the potency of canola biomass in Cr (VI) removal from aqueous solution. The results indicated that the Langmuir model provided the best correlation of the experimental data. Pseudo-second-order model was best applicable for the sorption data.

Table 2. Kinetic parameters for the adsorption of Cr (VI) onto canola at various concentrations

Concentration (mg/l)	Experimental q_e (mg/g)	Pseudo-first-order			Pseudo-second-order		
		K_1	q_e	R^2	K_2	q_e	R^2
10	1.98	0.341	6.19	0.965	0.0021	2.24	0.999
50	6.95	0.574	13.24	0.941	0.0043	7.36	0.998
100	10.67	0.922	18.45	0.972	0.0072	11.14	0.999

q_e : The equilibrium; K_1 : The constant rate; K_2 : The pseudo-second-order kinetic constant rate

The BET surface area of biosorbent was 32 m²/g. Low pH value is favorable for the biosorption of Cr (VI). The removal efficiency is enhanced with an increase in contact time and biosorbent dosage. The results indicated that canola is a promising biosorbent in the removal of Cr (VI) from aqueous solution.

Conflict of Interests

Authors have no conflict of interests.

Acknowledgements

The authors would like to express their gratitude toward the Kurdistan University of Medical Sciences for funding this research.

References

- Zhang H, Tang Y, Cai D, Liu X, Wang X, Huang Q, et al. Hexavalent chromium removal from aqueous solution by algal bloom residue derived activated carbon: equilibrium and kinetic studies. *J Hazard Mater* 2010; 181(1-3): 801-8.
- Karaoglu MH, Zor S, Ugurlu M. Biosorption of Cr (III) from solutions using vineyard pruning waste. *Chemical Engineering Journal* 2010; 159(1-3): 98-106.
- Gupta VK, Rastogi A, Nayak A. Biosorption of nickel onto treated alga (*Oedogonium hatei*): Application of isotherm and kinetic models. *J Colloid Interface Sci* 2010; 342(2): 533-9.
- Yao Q, Zhang H, Wu J, Shao L, He P. Biosorption of Cr(III) from aqueous solution by freeze-dried activated sludge: Equilibrium, kinetic and thermodynamic studies. *Frontiers of Environmental Science & Engineering in China* 2010; 4(3): 286-94.
- Sen M, Ghosh Dastidar M. Chromium removal using various biosorbents. *Iran J Environ Health Sci Eng* 2010; 7(3): 182-90.
- Rao RA, Rehman F. Adsorption studies on fruits of Gular (*Ficus glomerata*): removal of Cr(VI) from synthetic wastewater. *J Hazard Mater* 2010; 181(1-3): 405-12.
- Shen YS, Wang SL, Huang ST, Tzou YM, Huang JH. Biosorption of Cr(VI) by coconut coir: spectroscopic investigation on the reaction mechanism of Cr(VI) with lignocellulosic material. *J Hazard Mater* 2010; 179(1-3): 160-5.
- Ye J, Yin H, Mai B, Peng H, Qin H, He B, et al. Biosorption of chromium from aqueous solution and electroplating wastewater using mixture of *Candida lipolytica* and dewatered sewage sludge. *Bioresour Technol* 2010; 101(11): 3893-902.
- Wu J, Zhang H, He PJ, Yao Q, Shao LM. Cr(VI) removal from aqueous solution by dried activated sludge biomass. *J Hazard Mater* 2010; 176(1-3): 697-703.
- Liu W, Zhang J, Zhang C, Wang Y, Li Y. Adsorptive removal of Cr (VI) by Fe-modified activated carbon prepared from *Trapa natans* husk. *Chemical Engineering Journal* 2010; 162(2): 677-84.
- Barrera H, Urena-Nunez F, Bilyeu B, Barrera-Diaz C. Removal of chromium and toxic ions present in mine drainage by Ectodermis of *Opuntia*. *J Hazard Mater* 2006; 136(3): 846-53.
- Dai LP, Dong XJ, Ma HH. Molecular mechanism for cadmium-induced anthocyanin accumulation in *Azolla imbricata*. *Chemosphere* 2012; 87(4): 319-25.
- Liang S, Guo X, Feng N, Tian Q. Isotherms, kinetics and thermodynamic studies of adsorption of Cu²⁺ from aqueous solutions by Mg²⁺/K⁺ type orange peel adsorbents. *J Hazard Mater* 2010; 174(1-3): 756-62.
- Gupta VK, Gupta M, Sharma S. Process development for the removal of lead and chromium from aqueous solutions using red mud-an aluminium industry waste. *Water Res* 2001; 35(5): 1125-34.
- Anwar J, Shafique U, Waheed UZ, Salman M, Dar A, Anwar S. Removal of Pb(II) and Cd(II) from water by adsorption on peels of banana. *Bioresour Technol* 2010; 101(6): 1752-5.
- Lee SH, Jung CH, Chung H, Lee MY, Yang JW. Removal of heavy metals from aqueous solution by apple residues. *Process Biochemistry* 1998; 33(2): 205-11.
- Hamzeh Y, Azadeh E, Izadyar S, Layeghi M, Abyaz A, Asadollahi Y. Utilization of canola stalks in the decolorization of reactive dye contaminated water.

- Journal of Forest and Wood Products 2011; 63(4): 409-19.
18. Hamzeh Y, Azadeh E, Izadyar S. Removal of reactive remazol black b from contaminated water by lignocellulosic waste of canola stalks. *Journal of Color Science and Technology* 2011; 5(2): 77-85.
 19. Li Q, Zhai J, Zhang W, Wang M, Zhou J. Kinetic studies of adsorption of Pb(II), Cr(III) and Cu(II) from aqueous solution by sawdust and modified peanut husk. *J Hazard Mater* 2007; 141(1): 163-7.
 20. Miretzky P, Cirelli AF. Cr(VI) and Cr(III) removal from aqueous solution by raw and modified lignocellulosic materials: a review. *J Hazard Mater* 2010; 180(1-3): 1-19.
 21. Malkoc E, Nuhoglu Y, Abali Y. Cr(VI) adsorption by waste acorn of *Quercus ithaburensis* in fixed beds: Prediction of breakthrough curves. *Chemical Engineering Journal* 2006; 119(1): 61-8.
 22. Zazouli M, Yazdani J, Balarak D, Ebrahimi M, Mahdavi Y. Investigating the Removal Rate of Acid Blue 113 from Aqueous Solution by Canola. *J Mazandaran Univ Med Sci* 2013; 22(2): 71-8. [In Persian].
 23. Bhattacharya AK, Naiya TK, Mandal SN, Das SK. Adsorption, kinetics and equilibrium studies on removal of Cr(VI) from aqueous solutions using different low-cost adsorbents. *Chemical Engineering Journal* 2008; 137(3): 529-41.
 24. Raj C, Anirudhan TS. Chromium (VI) adsorption by sawdust carbon: Kinetics and equilibrium." *India J Chem Technol* 1997; 4, 226-228.
 25. Gupta VK, Shrivastava AK, Jain N. Biosorption of chromium(VI) from aqueous solutions by green algae *Spirogyra* species. *Water Res* 2001; 35(17): 4079-85.
 26. Wong KK, Lee CK, Low KS, Haron MJ. Removal of Cu and Pb by tartaric acid modified rice husk from aqueous solutions. *Chemosphere* 2003; 50(1): 23-8.
 27. Bansal M, Garg U, Singh D, Garg VK. Removal of Cr(VI) from aqueous solutions using pre-consumer processing agricultural waste: a case study of rice husk. *J Hazard Mater* 2009; 162(1): 312-20.
 28. Mallick S, Dash SS, Parida KM. Adsorption of hexavalent chromium on manganese nodule leached residue obtained from NH₃-SO₂ leaching. *J Colloid Interface Sci* 2006; 297(2): 419-25.
 29. Mohanty K, Jha M, Meikap BC, Biswas MN. Biosorption of Cr(VI) from aqueous solutions by *Eichhornia crassipes*. *Chemical Engineering Journal* 2006; 117(1): 71-7.
 30. Lodeiro P, Barriada JL, Herrero R, Sastre de Vicente ME. The marine macroalga *Cystoseira baccata* as biosorbent for cadmium(II) and lead(II) removal: kinetic and equilibrium studies. *Environ Pollut* 2006; 142(2): 264-73.
 31. Selatnia A, Boukazoula A, Kechid N, Bakhti MZ, Chergui A, Kerchich Y. Biosorption of lead (II) from aqueous solution by a bacterial dead *Streptomyces rimosus* biomass. *Biochemical Engineering Journal* 2004; 19(2): 127-35.
 32. Kumar U, Bandyopadhyay M. Sorption of cadmium from aqueous solution using pretreated rice husk. *Bioresour Technol* 2006; 97(1): 104-9.
 33. Ghorbani F, Younesi H, Ghasempouri SM, Zinatizadeh AA, Amini M, Daneshi A. Application of response surface methodology for optimization of cadmium biosorption in an aqueous solution by *Saccharomyces cerevisiae*. *Chemical Engineering Journal* 2008; 145(2): 267-75.
 34. Langmuir I. The adsorption of gases on plane surfaces of glass, mica and platinum. *J Am Chem Soc* 1918; 40(9): 1361-403.
 35. Zazouli M, Balarak D, Mahdavi Y. Application of Azolla for 2-chlorophenol and 4-Chlorophenol Removal from Aqueous Solutions. *Iranian Journal of Health Sciences* 2013; 1(2): 43-55.
 36. Diyanati Tilaki RA, Ghasemi M. Study Survey of Efficiency Agricultural Waste in Removal of Acid Orange 7(AO7) Dyes from Aqueous Solution: Kinetic and Equilibrium Study. *Iranian Journal of Health Sciences* 2014; 2(1): 51-61.
 37. Karthikeyan S, Balasubramanian R, Iyer CS. Evaluation of the marine algae *Ulva fasciata* and *Sargassum* sp. for the biosorption of Cu(II) from aqueous solutions. *Bioresour Technol* 2007; 98(2): 452-5.
 38. Roy D, Greenlaw PN, Shane BS. Adsorption of heavy metals by green algae and ground rice hulls. *Journal of Environmental Science and Health* 1993; 28(1): 37-50.



Assessment of health impacts attributed to PM₁₀ exposure during 2011 in Kermanshah City, Iran

Elahe Zallaghi¹, Mohammad Shirmardi², Zahra Soleimani³, Gholamreza Goudarzi⁴, Mohammad Heidari-Farsani⁵, Ghassem Al-Khamis⁶, Ali Sameri⁷

1 Applied Science Training Center, Ahvaz Municipality, Ahvaz, Iran

2 Department of Environmental Health Engineering, School of Public Health AND Student Research Committee, Ahvaz Jundishapur University of Medical Sciences, Ahvaz, Iran

3 Department of Environmental Health Engineering, School of Public Health and Allied Medicine, Semnan University of Medical Sciences, Semnan, Iran

4 Environmental Technologies Research Center (ETRC), Ahvaz Jundishapur University of Medical Sciences, Ahvaz, Iran

5 Department of Environmental Health Engineering, School of Public Health AND Students Research Committee, Ahvaz Jundishapur University of Medical Sciences, Ahvaz, Iran AND Specialist in Waste Management, Imam Khomeini Hospital, Abadan, Iran

6 Department of Environmental Health Engineering, School of Public Health, Ahvaz Jundishapur University of Medical Sciences, Ahvaz, Iran

7 Department of Parasitology and Mycology, School of Medicine, Ahvaz Jundishapur University of Medical Sciences, Arvand Branch, Abadan, Iran

Original Article

Abstract

The main aim of this study was to evaluate cardiovascular and respiratory outcomes attributed to PM₁₀ in Kermanshah, Iran. In order to gather data, an Environmental Dust Monitor instrument was used at 3 stations throughout the city at a height of at least 3 m above the ground. We obtained an input file for the model from crude data and quantified PM₁₀ using the AirQ model. Our estimation showed that 80% of cardiovascular deaths occurred on days with PM₁₀ concentrations of less than 170 µg m⁻³. The number of respiratory deaths due to PM₁₀ was estimated to be 46 people in 2011, showing a 48% reduction in such deaths compared to 2010. The number of patients with respiratory problems attributed to PM₁₀ exposure comprised 5.61% of the total number of patients admitted to hospitals due to respiratory diseases. This lower percentage of morbidity and mortality attributed to suspended particles in Kermanshah in 2011, in comparison with 2010, was due to the higher exposure days with PM₁₀ concentration of 200-250 µg m⁻³ in 2010. Every 10 µg m⁻³ increase in the concentration of suspended particles led to a 0.8% and 1.2% rise in the mortality rate due to cardiovascular and respiratory diseases, respectively. Additionally, the rates of heart and respiratory problems increased by 0.9% and 0.8%, respectively.

KEYWORDS: Assessment, Health Impacts, Mortality, Cardiovascular Diseases, Particulate Matter

Date of submission: 30 May 2014, **Date of acceptance:** 22 Jul 2014

Citation: Zallaghi E., Shirmardi M., Soleimani Z., Goudarzi Gh., Heidari-Farsani M., Al-khamis G., Sameri A. **Assessment of health impacts attributed to PM₁₀ exposure during 2011 in Kermanshah City, Iran.** J Adv Environ Health Res 2014; 2(4): 242-50.

Introduction

Corresponding Author:

Mohammad Heidari Farsani
Email: heidarimfar@gmail.com

In the standpoint of human beings and their health, health impact assessment of air quality is of paramount importance. Many studies have been conducted to illustrate mortality and morbidity resulting from air pollutants in Iran.¹⁻⁴ PM₁₀ are particulate matter with aerodynamic diameter of 10 µm or less, which can be an appropriate parameter in terms of health impact assessment. Short-term and long-term epidemiological studies have investigated the relation between suspended particles and adverse effects on health, excess mortality, and the outbreak of cardiovascular and respiratory diseases. There are clear signs indicating that the health effects of particles are mainly attributed to PM₁₀ and PM_{0.1}.⁵ Air-polluting suspended particles, regardless of chemical properties, are presented in figure 1 in terms of size.

High concentrations of suspended particulate matter (SPM) adversely affect human life in a number of ways, including the provocation of a wide range of respiratory and cardiovascular diseases, carcinogenic effects, profound impacts on defensive mechanism, and corrosion and loss of property.⁷⁻¹⁰ Important particles in air pollution studies have a size between 0.01 to 100 µm.⁸ The average concentration of PM₁₀ in the world is about 10-80 µgm⁻³. In the most polluted cities in Latin America such as Mexico City, the average concentration of PM₁₀ could reach 100 µgm⁻³ or even higher. The concentration of

suspended particles in developing countries is commonly and traditionally much higher than developed countries.⁷ In a report carried out by the World Health Organization (WHO) on urban air pollution in megacities of the world (1994), in which the air quality of 20 cities were compared, it was revealed that most of the cities engaged were among the developing countries.¹¹ According to this report, suspended particle concentrations in 17 of the total 20 studied cities were about two times higher than the WHO standards. This issue became even more intense with higher concentrations of SO₂. The annual mean range of SPM was 200-600 µgm⁻³. The maximum concentration was reported to be 1000 µgm⁻³.¹¹ The suspended particles enter the human body exclusively through the respiratory tract and immediately disrupt the function of this part of the body. High concentrations of suspended particles are detrimental to human health, especially for those suffering from chronic respiratory diseases. Previous studies have shown that increased level of suspended particles in combination with sulfur oxides is the main cause of the increased number of patients admitted to the hospitals and clinics. The most common health problems caused by suspended particles include the upper respiratory tract infections, cardiac disorders, bronchitis, asthma, pneumonia, lung inflammation, carcinogenic effects, chest discomfort, and adverse effects on defensive mechanisms.^{8,12}

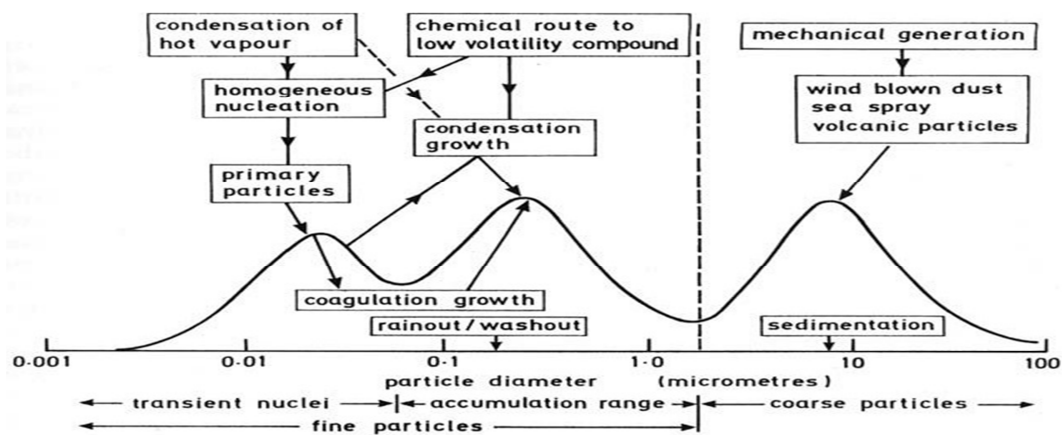


Figure 1. The trimodal size distribution, showing general relationships between the three common size ranges and the particle sources Source: Tiwary, Colls⁶

The capability of the human respiratory tract defense system against inhaled suspended particles depends highly on the size of the particles. The diameter of most suspended particles is in the range of 0.1-10 μm . The smaller particles undergo vibrational and Brownian motions, while the larger particles ($> 10\mu\text{m}$) precipitate rapidly. Due to the heightened level of dust particles in some regions of Iran in recent years, especially Kermanshah City, it is vital to evaluate the relationship between such particles and the increased number of cardiovascular and respiratory tract diseases.

Kermanshah City, with a population of approximately 843117 people, is located in the Southwest of Iran and currently considered as an industrial center of Iran as well as a source of dust events. As a result, the city is among the most polluted cities in Iran. The main objective of this study was to estimate the health effects of particulate matter (PM₁₀) on mortality due to respiratory and cardiovascular diseases in 2011 and compare the statistical results with those obtained for 2010.

Materials and Methods

Kermanshah, the capital of Kermanshah Province, is located in the Central-West Region of Iran. The geographical location of Kermanshah is 34° 19' N, 47° 7' E and it is 1322 m above sea level. According to the Damartn classification, which is based on average precipitation and average temperature, Kermanshah is placed in the category of cold and semi-arid climate with the annual average precipitation and temperature of 444.7 mm and 14.3°C, respectively. The vegetation cover is steppe with few trees in the ranges. The temperature may drop to 10°C in the winter; however, it rises to 44°C in the summer.¹³

The aim of the present study was the estimation of health endpoints attributed to PM₁₀ pollutant using epidemiological indices. The AirQ model that was introduced by the WHO in 2004 provides a valid and reliable tool

for estimating the short-term impacts of air pollutants.

The first step: sampling of PM₁₀ pollutant: For sampling of PM₁₀ particles, 3 sampling stations were selected in the city. A high-volume air samplers (model: Anderson) was used to sample and measure the concentrations of the suspended particles. Sampling, analysis, and selection of the stations were performed according to the EPA 3051A guideline.^{14,15} The temperature and pressure parameters were recorded hourly by the weather channel software (www.msn.com).

The second step: data processing and model implementation: The measured PM₁₀ concentration data was processed to provide daily average, minimum, maximum, and some statistical parameters. The processed data was entered into the AirQ model to estimate the number of cases of cardiovascular and respiratory morbidity and mortality.

Results and Discussion

Air pollution of Kermanshah attributed to PM₁₀ in 2011

The results presented in table 1 show that in all 3 studied stations, the average concentrations of PM₁₀ in the summer were higher than the winter, with the observed maximum concentration of 1810.5 $\mu\text{g}\cdot\text{m}^{-3}$ in the summer. The highest and lowest concentrations were observed in Ziba Park and Ostandari stations, respectively. According to table 1, the annual average concentration of PM₁₀ in Kermanshah in 2011 was equal to 89.54 $\mu\text{g}\cdot\text{m}^{-3}$, and was 117.91 $\mu\text{g}\cdot\text{m}^{-3}$ for the summer, which was higher than the winter. Figures 2, 3, 4, and 5 are presented according to accumulative mortality due to cardiovascular and respiratory tract diseases versus the concentration ranges of the related pollutant. Each figure includes 3 curves in which the middle curve corresponds to the central relative risk, and the upper and lower curves correspond to the relative risks of 95% and 5%, respectively.

Table 1. The required indices of the model for PM₁₀ (µg m⁻³) in 3 studied stations in Kermanshah in 2011

Parameter	Station			
	Ziba Park	Shahrdari	Ostandari	Overall mean
The annual average	90.03	89.34	89.26	89.54
The summer average	118.34	117.76	117.62	117.91
The winter average	60.60	59.80	59.78	60.06
98 th annual percentile	330.95	328.36	329.12	329.48
Annual maximum	1810.50	1809.00	1804.00	1807.83
Summer maximum	1810.50	1809.00	1804.00	1807.83
Winter maximum	283.00	283.00	278.00	281.33

Table 2. The estimation of relative risk indices, attributable proportion, and number of cases of cardiovascular disease mortality (Baseline incidence (BI) = 497) in Kermanshah in 2011

Estimation	Epidemiological indices		
	Relative risk (average)	Attributable proportion (%)	Number of cases
Lower	1.005	3.5839	151.6
Average	1.008	5.6135	237.8
Upper	1.018	11.8023	499.2

Table 3. The estimation of relative risk indices, attributable proportion, and number of cases of respiratory tract disease mortality (BI = 66) in Kermanshah in 2011

Estimation	Epidemiological indices		
	Relative risk (average)	Attributable proportion (%)	Number of cases
Lower	1.008	5.6135	31.5
Average	1.012	8.1904	46.0
Upper	1.037	21.5728	121.2

Quantification of the health effects due to PM₁₀ exposure

By using results yielded by data processing and registered data from the measurement stations for suspended particles throughout the city, and estimating the population in 2011, we obtained various indices that will be described in the following sections.

According to table 2, by considering the central relative risk, attributable proportion of cardiovascular disease mortality was 5.61% in 2011, which showed a 6.27% reduction in contrast with 2010.¹⁶

Attributable proportions, in the conditions of the estimation with the lower and upper relative risks, were 3.58 and 11.80%, respectively. By considering a baseline incidence equal to 497 per 100,000 people for cardiovascular diseases, the accumulative number of mortality due to such

diseases was 237 people, showing a reduction of 261 people in contrast with 2010.¹⁶ The maximum number of exposure to PM₁₀ and mortality due to cardiovascular diseases were observed in the concentration range of 50-60 µg m⁻³. The corresponding values estimated for mortality due to respiratory tract diseases are presented in table 3. The relative risk indices, attributable proportion, and number of cases of outpatient treatment due to both cardiovascular and respiratory tract diseases were also estimated (Tables 4 and 5).

Indices of mortality due to cardiovascular and respiratory tract diseases attributed to PM₁₀ in Kermanshah in 2011

Considering an annual average PM₁₀ concentration of 89.54 µg m⁻³ and a population of 851405 people in 2011, and estimation of mortality rate due to cardiovascular and

respiratory tract diseases attributed to PM₁₀ exposure, we obtained the health impacts based on the number of deaths in every 100,000 people by the following equation:

$$(M_t/P_t) \times 100000$$

where M_t is mortality due to cardiovascular and respiratory tract diseases attributed to PM₁₀ exposure, P_t is the total population, and the unit is mortality per 100,000 people.

For cardiovascular disease: $237/851405 = 27.83$ deaths in every 100,000 people

The results obtained from the model show that the number of cardiovascular mortality and outpatient cases attributed to PM₁₀ in the air of Kermanshah for central or average relative risk were 237 and 233, respectively, in 2011. For respiratory tract disease: $46/851405 = 5.40$ deaths in every 100,000 people

The values obtained from the model show that the number of respiratory tract diseases mortality and outpatient cases with respiratory problems attributed to PM₁₀ in the air of Kermanshah for central relative risk were 46 and 602, respectively, in 2011. Figure 2 illustrates a steady increase in the mortality rate due to cardiovascular diseases associated with a PM₁₀ concentration of 50-100 $\mu\text{g}\text{m}^{-3}$, whereas it shows a steep increase in the concentrations of higher than 350 $\mu\text{g}\text{m}^{-3}$. Indeed, figure 2 shows that 80% of the deaths due to cardiovascular diseases

occurred on days with concentrations of less than 170 $\mu\text{g}\text{m}^{-3}$. With every 10 $\mu\text{g}\text{m}^{-3}$ increment in the concentration of suspended particles, the risk of deaths due to cardiovascular diseases increased by 0.8%.

According to table 3, and based on the calculated relative risk and the results from figure 3, the accumulative number of deaths due to respiratory tract problems attributed to PM₁₀ was estimated to be 46 individuals. This rate, in comparison with 2010, shows a decrease in mortality rate of 48 individuals.¹⁶ Moreover, 80% of such deaths occurred on the days with PM₁₀ concentrations of less than 170 $\mu\text{g}\text{m}^{-3}$. The steep phase of the curve in figure 3, corresponding with $RR = 1.022$, represents the maximum mortality rate (6 people) in the range of 50-60 $\mu\text{g}\text{m}^{-3}$. As can be seen, the slope of the upper and lower curves in the figure is steep in this range. The slight slope in the concentration range of 10-20 $\mu\text{g}\text{m}^{-3}$ represents the minimum number of deaths due to respiratory tract problems. Every 10 $\mu\text{g}\text{m}^{-3}$ increase in the concentration of suspended particles led to a 1.2% increase in the risk of death due to respiratory tract problems. Figure 3 illustrates a steady increase in mortality due to respiratory tract problems associated with a PM₁₀ concentration of 50-100 $\mu\text{g}\text{m}^{-3}$, but it shows a steep increase in the concentrations of higher than 350 $\mu\text{g}\text{m}^{-3}$.

Table 4. The estimation of relative risk indices, attributable proportion, and number of cases of cardiovascular diseases attributed to PM₁₀ (outpatient treatment) (BI = 436) in Kermanshah in 2011

Estimation	Epidemiological indices		
	Relative risk (high)	Attributable proportion (%)	Number of cases
Lower	1.006	4.2701	158.4
Average	1.009	6.2712	232.7
Upper	1.013	8.8128	327.0

Table 5. The estimation of relative risk indices, attributable proportion, and number of cases of respiratory tract diseases attributed to PM₁₀ (outpatient treatment) (BI = 1260) in Kermanshah in 2011

Estimation	Epidemiological indices		
	Relative risk (high)	Attributable proportion (%)	Number of cases
Lower	1.0048	3.4455	369.4
Central	1.008	5.6135	601.9
Upper	1.0112	7.6864	824.2

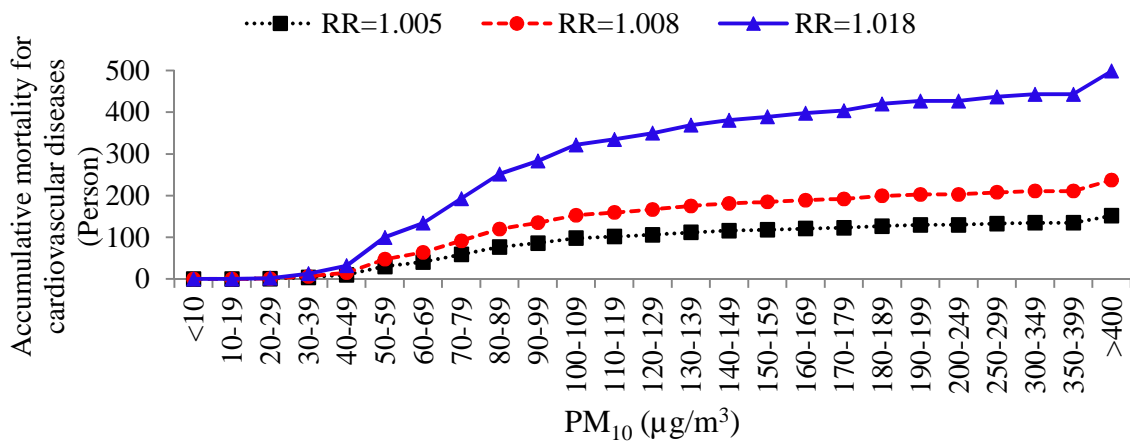


Figure 2. Accumulative mortality due to cardiovascular diseases attributed to PM₁₀ based on PM₁₀ concentration in Kermanshah in 2011

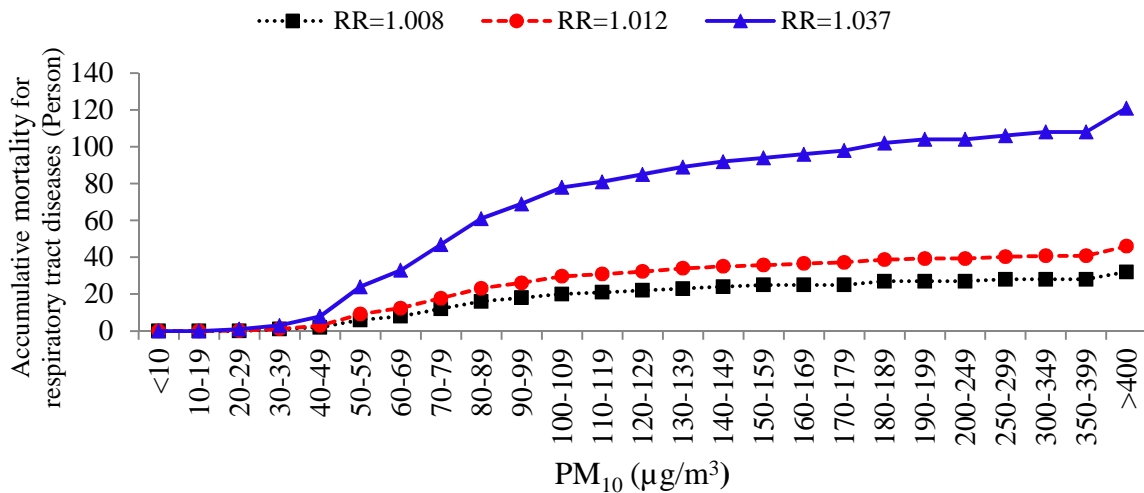


Figure 3. Accumulative mortality due to respiratory tract diseases attributed to PM₁₀ based on PM₁₀ concentration in Kermanshah in 2011

Some studies have utilized the AirQ model to estimate the health effects of particulate matter. For example, Tominz et al. used the AirQ model to estimate the health impacts of PM₁₀ in Trieste, Italy, in 2005.¹⁷ The authors reported that 1.8% of natural deaths, 2.2% of cardiovascular deaths, and 2.5% of respiratory deaths were attributable to PM₁₀ concentrations of higher than 20 µg/m³. In 2009, Goudarzi used the AirQ model to estimate the health impacts of PM₁₀ in Tehran, Iran.¹⁸ The results of the study showed that about 4% of the total number of cardiovascular and respiratory tract diseases was attributed to a

PM₁₀ concentration of higher than 20 µg/m³. In another study, Yavari et al. demonstrated that about 13% of the total number of cardiovascular and respiratory tract diseases was attributed to a PM₁₀ concentration of higher than 20 µg/m³.¹⁹ Ostro et al. analyzed the relationship between PM₁₀ and daily mortality rate between 1989 and 1991, and reported a strong association between mortality from either respiratory disease or cardiovascular disease and PM₁₀.²⁰ Based on a regression model of examining the air pollution in 10 cities of the United States, Schwartz has calculated that the relative risk for adults older

than 65 years would be 2% for each 10 $\mu\text{g}/\text{m}^3$ increase in PM₁₀.²¹

Indices of cardiovascular and respiratory tract diseases mortalities for outpatient treatment due to PM₁₀ in Kermanshah in 2011

According to the results of table 4 and figure 4, accumulative number of cardiovascular disease cases was 233, based on the estimated average relative risk (RR = 1.009) and baseline incidence rate of 436 in 10⁵ people. This showed a reduction of 251 people in comparison with 2010. Approximately, 80% of the cases occurred on the days when PM₁₀ concentration was higher than 170 $\mu\text{g}/\text{m}^3$. The accumulative numbers of such health impacts in the lower (RR = 1.006) and upper (RR = 1.013) relative risks were 158 and 327 individuals, respectively. Every 10 $\mu\text{g}/\text{m}^3$ increment in the concentration of suspended particles resulted in a 0.9% increase in the risk of cardiovascular diseases.

According to the results of table 5 and figure 5, the accumulative number of

respiratory tract disease cases due to PM₁₀ exposure, based on the estimated average relative risk (RR = 1.008) and baseline incidence of 1260 in 10⁵ people, was 602. This showed a reduction of 660 people in comparison with 2010.¹⁶ Approximately, 80% of the cases occurred on the days when PM₁₀ concentration was higher than 170 $\mu\text{g}/\text{m}^3$. Thus, the number of referrals to the hospitals due to respiratory tract diseases attributed to exposure to PM₁₀ comprised 5.61% of the total referrals. The accumulative numbers of such health impacts in the estimated lower (RR = 1.0048) and upper relative risk (RR = 1.0112) were 369 and 824 individuals, respectively. Every 10 $\mu\text{g}/\text{m}^3$ increment in the concentration of the suspended particles resulted in a 0.8% increase in the risk of respiratory tract diseases. Figures 4 and 5, respectively, illustrate steady increases in the number of outpatients due to cardiovascular and respiratory tract diseases associated with PM₁₀ concentrations of 50-100 $\mu\text{g}/\text{m}^3$, but showed steep increases in the concentrations of higher than 350 $\mu\text{g}/\text{m}^3$.

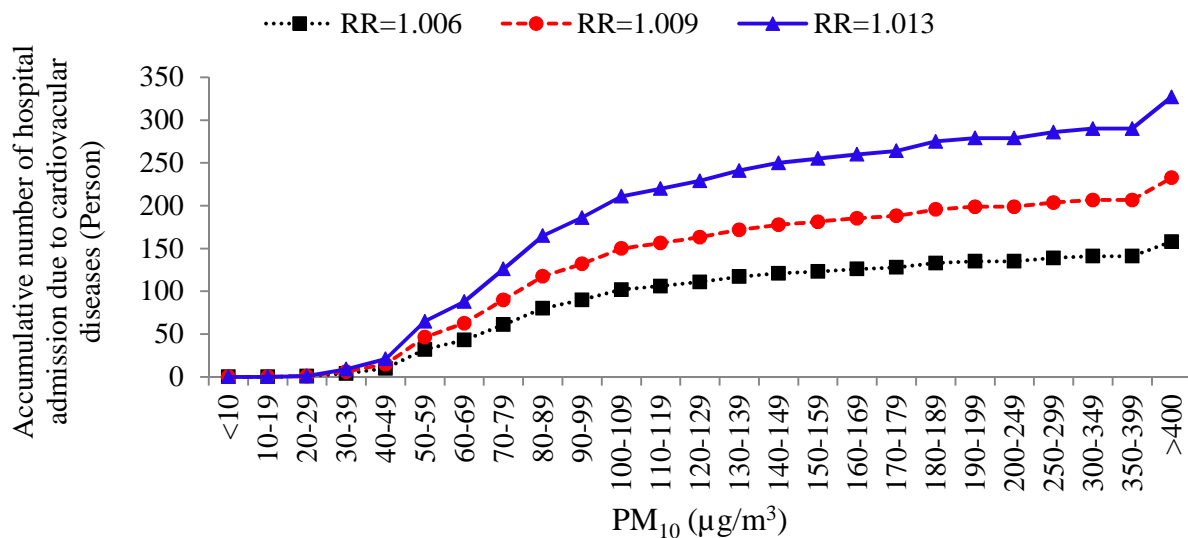


Figure 4. Accumulative number of hospital admission due to cardiovascular diseases attributed to PM₁₀ based on PM₁₀ concentration in Kermanshah in 2011

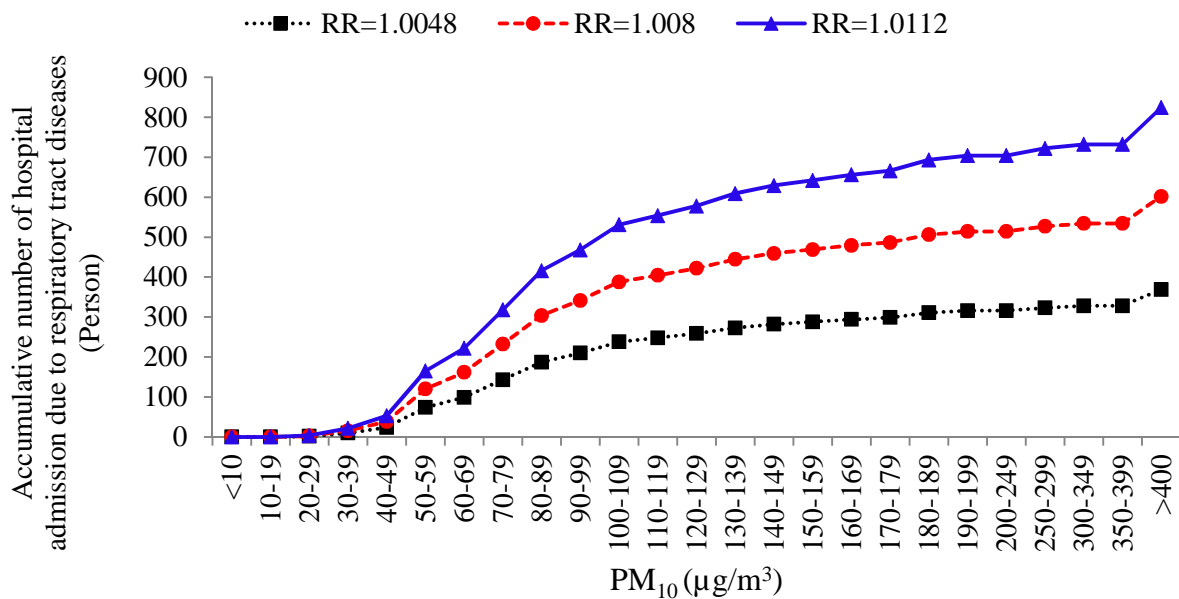


Figure 5. Accumulative number of hospital admission due to respiratory tract diseases attributed to PM₁₀ based on PM₁₀ concentration in Kermanshah in 2011

Conclusion

The average concentration of PM₁₀ during the study period was 89.54 µg m⁻³, with the maximum concentration of 1809 µg m⁻³ in the summer. The maximum and minimum concentrations were observed for Ziba Park and Ostadnari stations, respectively. The low number of morbidity and mortality cases due to suspended particles in Kermanshah in 2011, in comparison with 2010, was due to the lower average concentration of PM₁₀ or more days with lower concentration in the air. This means that individuals were exposed to a PM₁₀ concentration of 200-250 µg m⁻³ for a longer time in terms of days, compared with 2010. Moreover, the concentration of PM₁₀ did not reach lower than 30 µg m⁻³ on any day. However, the individuals were exposure to a PM₁₀ concentration of 50-60 µg m⁻³ for a longer time, compared with 2010.

Conflict of Interests

Authors have no conflict of interests.

Acknowledgements

The authors are grateful to Ahvaz Jundishapur University of Medical Sciences, and Science Research Branch of Khuzestan, Islamic Azad University for their cooperation in the study.

References

- Goudarzi Gh, Zallaghi E, Neissi A, Ahmadi Ankali K, Saki A, Babaei AA, et al. Cardiopulmonary mortalities and chronic obstructive pulmonary disease attributed to ozone air pollution. *Arch Hyg Sci* 2013; 2(2): 62-72.
- Goudarzi Gh, Mohammadi MJ, Angali K, Neisi AK, Babaei AA, Mohammadi B, et al. Estimation of health effects attributed to no2 exposure using airq model. *Arch Hyg Sci* 2012; 1(2): 59-66.
- Naddafi K, Hassanvand MS, Yunesian M, Momeniha F, Nabizadeh R, Faridi S, et al. Health impact assessment of air pollution in megacity of Tehran, Iran. *Iran J Environ Health Sci Eng* 2012; 9(1): 28.
- Zolghi A, Godarzi Gh, Gravandi S, Mohamadi M, Vosoghi Nayeri M, Visi E, et al. Estimate of cardiovascular and respiratory diseases related to particle matter pollutant in Tabriz air, northwest of Iran, 2011. *J Ilam Univ Med Sci* 2014; 22(1): 84-91. [In Persian].
- Chow JC. Measurement methods to determine compliance with ambient air quality standards for

- suspended particles. *J Air Waste Manag Assoc* 1995; 45(5): 320-82.
6. Colls J, Tiwary A. *Air Pollution: Measurement, Modelling and Mitigation*. 3rd ed. New York, NY: CRC Press; 2009.
 7. Janssen NA, Schwartz J, Zanobetti A, Suh HH. Air conditioning and source-specific particles as modifiers of the effect of PM_{10} on hospital admissions for heart and lung disease. *Environ Health Perspect* 2002; 110(1): 43-9.
 8. Fanger PO. *Thermal comfort: Analysis and applications in environmental engineering*. New York, NY: McGraw-Hill; 1970.
 9. World Health Organization. *Air Quality Guidelines: Global Update 2005: Particulate Matter, Ozone, Nitrogen Dioxide, and Sulfur Dioxide*. Geneva, Switzerland: World Health Organization; 2006.
 10. Lippmann M. *Environmental Toxicants: Human Exposures and Their Health Effects*. New Jersey, NJ: John Wiley & Sons, 2000.
 11. Mage D, Ozolins G, Peterson P, Webster A, Orthofer R, Vandeweerd V, et al. Urban air pollution in megacities of the world. *Atmospheric Environment* 1996; 30(5): 681-6.
 12. Panyacosit L. *A Review of Particulate Matter and Health: Focus on Developing Countries* [Online]. [cited 2000]; Available from: URL: http://www.iiasa.ac.at/publication/more_IR-00-005.php
 13. Kermanshah Department of Environment. *Geographical location of Kermanshah Province* [Online]. [cited 2014]; Available from: URL: <http://kermanshah.doe.ir/Portal/home/?138133>
 14. Viana M, Kuhlbusch TAJ, Querol X, Alastuey A, Harrison RM, Hopke PK, et al. Source apportionment of particulate matter in Europe: A review of methods and results. *Journal of Aerosol Science* 2008; 39(10): 827-49.
 15. Lodge JP. *Methods of Air Sampling and Analysis*. New York, NY: CRC Press; 1988.
 16. Zallaghi A. *Quantification and health effects comparison of criteria air pollutants in southwest of Iran (Ahvaz-Kermanshah-Bushehr) by using of AIR Q Model* [MSc Thesis]. Ahvaz, Iran: Islamic Azad University, Science and Research Branch; 2010. [In Persian].
 17. Tominz R, Mazzoleni B, Daris F. Estimate of potential health benefits of the reduction of air pollution with PM_{10} in Trieste, Italy. *Epidemiol Prev* 2005; 29(3-4): 149-55.
 18. Goudarzi G. *Quantifying the health effects of air pollution in Tehran and determines the third axis of the comprehensive plan to reduce air pollution in Tehran* [PhD Thesis]. Tehran, Iran: Tehran University of Medical Sciences; 2009. [In Persian].
 19. Yavari AR, Sotoudeh A, Parivar P. *Urban Environmental Quality and Landscape Structure in Arid Mountain Environment*. *International Journal of Environmental Research* 2007; 1(4): 325-40.
 20. Ostro B, Sanchez JM, Aranda C, Eskeland GS. Air pollution and mortality: results from a study of Santiago, Chile. *J Expo Anal Environ Epidemiol* 1996; 6(1): 97-114.
 21. Schwartz J. The distributed lag between air pollution and daily deaths. *Epidemiology* 2000; 11(3): 320-6.



Reduction of chromium toxicity by applying various soil amendments in artificially contaminated soil

Mahboub Saffari¹, Najafali Karimian², Abdolmajid Ronaghi², Jafar Yasrebi², Reza Ghasemi-Fasaei²

¹ Department of Soil Science, School of Agriculture, Shiraz University, Shiraz AND Institute of Science and High Technology and Environmental Sciences, Graduate University of Advanced Technology, Kerman, Iran

² Department of Soil Science, School of Agriculture, Shiraz University, Shiraz, Iran

Original Article

Abstract

Six soil amendments including municipal solid waste compost (MSWC), coal fly ash (CFA), rice husk biochar prepared at 300°C (B300) and 600°C (B600), zerovalent iron (Fe⁰), and zerovalent manganese (Mn⁰) were evaluated to determine their ability to reduce mobility of chromium (Cr) in a Cr-spiked soil. The Cr-spiked soil samples were separately incubated with selected amendments at 2 and 5% [weight by weight (W/W)] for 90 days at 25 °C. The efficacy of amendment treatments was evaluated using desorption kinetic experiment and sequential extraction procedure. Results showed that applications of various amendments had significant effects on desorption and chemical forms of Cr. Addition of amendments considerably decreased mobility factor (except for CFA_{5%}) of Cr compared to the control treatment. The addition of Fe⁰, MSWC, and B300 to soil significantly decreased Cr release, compared to other amendments. The lowest Cr desorption was achieved by Fe⁰ at 5%. Application of B600 and CFA increased soil pH and caused the oxidation of Cr(III) to Cr(VI). Based on the obtained highest values of coefficient of determination (R²) and lowest values of standard error (SE) of the estimate, the two first-order reaction model could be best fitted for describing Cr release in soil samples. In general, from the practical view, Fe⁰, MSWC, and B300 treatments are effective in Cr immobilization, while application of Fe⁰ at 5% was the best treatment for stabilization of Cr. Therefore, these treatments can be recommended for the immobilization of Cr from polluted soil.

KEYWORDS: Stabilization, Chromium, Amendments, Desorption Kinetic

Date of submission: 16 Aug 2014, **Date of acceptance:** 22 Sep 2014

Citation: Saffari M, Karimian N, Ronaghi A, Yasrebi J, Ghasemi-Fasaei R. **Reduction of chromium toxicity by applying various soil amendments in artificially contaminated soil.** J Adv Environ Health Res 2014; 2(4): 251-62.

Introduction

Soil pollution by heavy metals is a major problem in many countries. Chromium is a heavy metal, the concentration of which considerably increases in the environment due to industrial activities. Chromium exists in multiple valence states in the environment, but the most common forms are trivalent chromium [Cr(III)] and hexavalent chromium [Cr(VI)]. The mobility

of Cr in soil depends on its oxidation state.¹ The toxicity and mobility of Cr(VI) is higher than Cr(III) in soil.¹ Hence, the stabilization of Cr principally deals with the reduction of Cr(VI) to Cr(III).

Chemical stabilization techniques are used to reduce heavy metals mobility in the soil using contaminant-immobilizing amendments. The use of immobilizing amendments in polluted soils as a remediation procedure can reduce mobility and bioavailability of heavy metals by adsorption, complex formation, or (co)precipitation process. Previous researches

Corresponding Author:

Najafali Karimian

Email: Najafalikalimian@yahoo.com

have reported that Cr(VI) is reduced to Cr(III) by soil organic matter and Fe^{2+} .¹ On the other hand, Cr(III) can be oxidized to Cr(VI) by manganese oxides^{2,3} and alkaline resources (such as coal fly ash) that increase soil pH above neutral.^{4,5}

Currently, there are no common methodologies to assess chemical stabilization efficiency. Nevertheless, several methods were used to estimate the soil stabilization efficiency of various amendments in heavy metals stabilization in soils, such as sequential extraction method, leaching test, and adsorption-desorption experiments. The mobility of heavy metals is controlled by the sorption and desorption characteristics of soil.⁶ The desorption technique of heavy metals in soil can be related to their mobility and toxicity.⁷ In addition, sequential extraction procedures can be useful in monitoring the stabilization process of heavy metals in soil. A typical sequential procedure starts with a weak solvent, followed by a stronger solvent in order to sequentially solubilize various operationally defined metal fractions; exchangeable (EX), carbonate-bound (Car), reducible [Mn-oxide-bound (Mn-OX)], oxidisable [amorphous and crystalline Fe-oxide-bound (FeA-Ox and FeC-Ox)], and residual metal fractions.⁸ The Ex and Car fractions are considerably mobile, while other fractions are less mobile in soil. Several extractants were used for the evaluation of heavy metal mobility in soils and sediments using batch methods.^{9,10} Acidic solutions, dilute salt solutions, and complexing agents are usually used as extractants.^{9,11}

Application of inappropriate amendments may increase the mobility of heavy metals in

soil. In addition, very few researches have been performed on Cr stabilization due to the low reactivity of its common species in soil. Therefore, the present study was conducted to recognize appropriate amendments for Cr stabilization by chemical stabilization technique in soil. The main objectives of this study were to evaluate the influence of coal fly ash (CFA), municipal solid waste compost (MSWC), two types of rice husk biochar (B300 and B600), zerovalent iron (Fe^0), and zerovalent manganese (Mn^0) on release and chemical form of Cr in contaminated calcareous soil in order to reduce the risk of increasing of Cr in the environment.

Materials and Methods

Surface (0–30 cm) soil samples were collected (fine, mixed, mesic, Fluventic Calcixerepts) from Shiraz, Fars Province, Iran. Selected chemical and physical properties were determined using standard methods.¹² Plant available form of heavy metals was extracted using diethylene triamine pentaacetic acid (DTPA). Total content of heavy metals were determined using 4M HNO_3 and measured using an atomic absorption spectrometer (Shimadzu AA-670, Shimadzu Corp., Kyoto, KYT, Japan).¹³ In order to determine the concentration of Cr(VI), alkaline digestion was applied (0.5 mol/l NaOH + 0.28 mol/l Na_2CO_3) and the amount of Cr(VI) was measured using the colorimetric method with 1,5-diphenylcarbazide (DPC) at a wavelength of 540 nm.¹⁴ Cr(III) amount was calculated by subtracting Cr(VI) from total Cr. The selected properties of soil are presented in table 1.

Table 1. Selected chemical and physical properties of studied soil

Property	Value	Property (mg/kg)	Value
pH	7.8	Soluble Fe in DTPA	4.1
CCE (%)	39.5	Soluble Cu in DTPA	0.9
Sand (%)	27	Soluble Mn in DTPA	5.6
Clay (%)	35	Soluble Cr in DTPA	1.6
OM (%)	1.4	Soluble Cr in NaNO_3	2.8
CEC (Cmol(+)/kg)	15.8	Total Cr	109.0
EC (dS/m)	0.65	Cr(VI)	8.5

CCE: calcium carbonate equivalent; OM: organic matter; CEC: cation-exchange capacity; EC: electrical conductivity; DTPA: diethylene triamine pentaacetic acid

Various amendments were used for their abilities to decrease Cr mobility in Cr-spiked Soil; CFA, MSWC, rice husk biochar prepared at 300°C (B300) and 600 °C (B600), zerovalent iron (Fe⁰), and zerovalent manganese (Mn⁰). CFA and MSWC were collected from Zarand Coal Washing Factory and the Recycling and Municipal Solid Waste Compost Factory of Kerman, Iran, respectively. Biochar was prepared at 300 °C and 600 °C from rice husk. Husk samples (covered with aluminum foil) were

placed in a furnace for 4 hours to produce biochar. Zerovalent iron (Fe⁰, 99.5%, in the form of iron grit) and zerovalent manganese (Mn⁰, 99.5%, in the form of manganese grit) were used in the present study. The selected properties of the used amendments are presented in table 2. In addition, fourier transform infrared spectroscopy (FT-IR) (Spectrum RXI, PerkinElmer Inc., Waltham, MA, USA) was used for the recognition of the morphology and structure of the produced biochar (Figure 1).

Table 2. Selected chemical composition of amendments

Amendments	Chemical properties				
	SiO ₂ (%) [*]	Al ₂ O ₃ (%) [*]	TiO ₂ (%) [*]	Fe ₂ O ₃ (%) [*]	CaO (%) [*]
CFA	46.47	27.32	0.90	6.73	4.56
	BaO (%) [*]	SrO (%) [*]	MgO (%) [*]	K ₂ O (%) [*]	Na ₂ O (%) [*]
	0.15	0.14	2.32	3.42	0.82
	SO ₃ (%) [*]	P ₂ O ₅ (%) [*]	Mn ₃ O ₄ (%) [*]	pH	C (%) ^{**}
	4.60	4.60	0.82	9.1	67
	H (%) ^{**}	n (%) ^{**}	O (%) ^{**}	-	-
MSWC	3.80	3.92	0.96	-	-
	pH	EC (dS/m)	OM (%)	Cu (mg/kg)	Zn (mg/kg)
	7.40	19.36	38.00	19	28
	Fe (mg/kg)	Mn (mg/kg)	Pb (mg/kg)	Cd (mg/kg)	Ni (mg/kg)
25.00	11.00	13.30	0.28	1.2	
B300	pH	EC (dS/m)	C (%) ^{**}	H (%) ^{**}	n (%) ^{**}
	6.20	13.10	41.57	2.11	1.52
B600	8.70	21.20	48.99	1.55	Trace

^{*}Determined by X-ray fluorescence (XRF) analyzer; ^{**}Determined by CHN analyzer; CFA: Coal fly ash; MSWC: Municipal solid waste compost

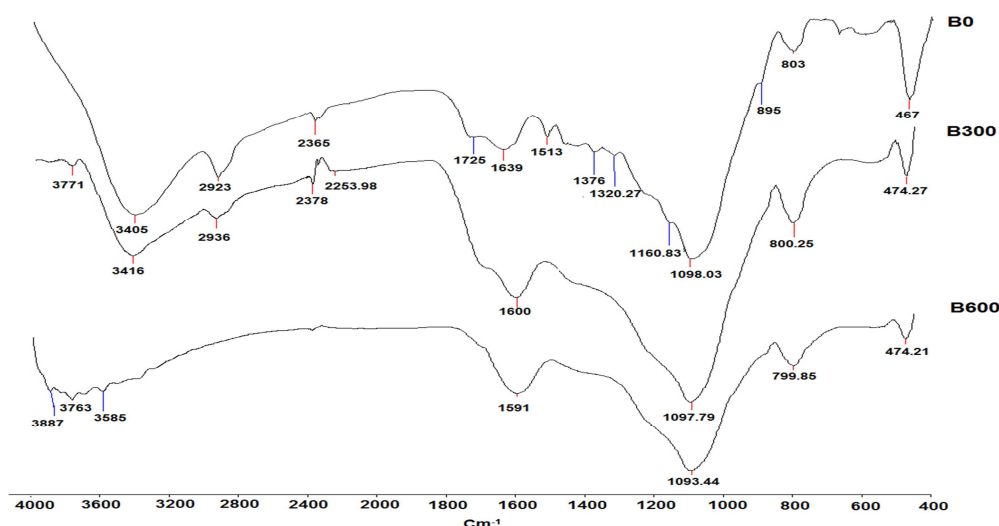


Figure 1. FTIR spectra of rice husk before (B0) and after pyrolysis (B300 and B600) [X-axis and Y-axis are wavenumber (cm⁻¹) and transmittance (%), respectively.]

Table 3. Experimental design for incubation experiment

Treatment	Amendment (applied rate) (%)	Treatment	Amendment (applied rate) (%)
S1	MSWC (2)	S7	B600 (2)
S2	MSWC (5)	S8	B600 (5)
S3	CFA (2)	S9	Fe ⁰ (2)
S4	CFA (5)	S10	Fe ⁰ (5)
S5	B300 (2)	S11	Mn ⁰ (2)
S6	B300 (5)	S12	Mn ⁰ (5)

CFA: Coal fly ash; MSWC: Municipal solid waste compost

Table 4. Summary of the sequential extraction procedure used in this study

g soil: ml solution	Extracting solution	Shaking time (h)	Chemical form of Cr	Symbol
10:40	1 m Mg(NO ₃) ₂	2	Exchangeable	EX
10:40	1 m NaOAc (pH = 5 CH ₃ COOH)	5	Carbonate-bound	Car
10:20	0.7 m NaOCl (pH = 8.5)	0.5 in boiling water	Organically-bound*	Om
5:50	0.1 m NH ₂ OH.HCl (pH = 2 HNO ₃)	0.5 in boiling water	Mn-oxide-bound	Mn-OX
5:50	0.25 m NH ₂ OH.HCl + 0.25 m HCl	0.5 at 50°C in water	Amorphous Fe-oxide-bound	FeA-Ox
5:50	0.2 m (NH ₄) ₂ C ₂ O ₄ + 0.2 m H ₂ C ₂ O ₄ + 0.1 MC ₆ H ₈ O ₆	0.5 in boiling water	Crystalline Fe-oxide-bound	FeC-Ox

* Two times extraction

For the incubation experiment, soil samples were placed in plastic and Cr(VI) was added at the rate of 500 µg/g as K₂Cr₂O₇. Selected amendments were added to each soil sample separately, at two levels [2 and 5% weight by weight (W/W)] (Table 3), and each soil sample was mixed thoroughly. The soil samples were incubated for 90 days at 25 °C. Moisture was preserved at field capacity (FC). After incubation, samples were air-dried and used for Cr desorption and fractionation study.

Soil Cr was fractionated to 7 fractions using the Singh et al.¹⁵ method. Table 4 provides an outline of the Singh et al.¹⁵ procedure. Residual forms (Res) were calculated by subtracting the sum of 6 fractions from total Cr. Cr mobility was evaluated using a mobility factor¹⁶, and calculated according to the following equation:

$$(Ex + Car / \text{sum of fractions}) \times 100$$

Desorption kinetics of Cr(VI) was studied by means of batch-type experiments; 5 g of each soil sample, in triplicate, was placed in polyethylene tubes and extracted separately with 25 ml of two extractants: 0.01 m Ethylenediaminetetraacetic acid (EDTA) at pH 7.0 and 25 ml of 0.01 m NaNO₃. Samples were shaken for periods of 0.08

to 102.25 hours (0.08, 0.25, 0.58, 1.25, 2.25, 4.25, 8.25, 16.25, 30.25, 54.25, and 102.25 hour) at 25 ± 2°C, and then, centrifuged immediately at 2500 rpm. The supernatants were filtered through filter paper and Cr concentration was determined using an atomic absorption spectrometer.

A two first-order kinetic model was used as an approximate method for describing Cr desorption. A two first-order reaction model can divide Cr into 3 fractions^{9,10}, Q₁, Q₂, and Q₃ as follows:

$$q = Q_1(1 - e^{-k_1t}) + Q_2(1 - e^{-k_2t})$$

$$Q_3 = q_{\text{total}} - Q_2 - Q_1$$

where q represents amount of Cr released at time t, Q₁ (mg/kg) is labile fraction, readily extractable, associated to the rate constant k₁, and Q₂ (mg/kg) is moderately labile fraction, less extractable, associated to the rate constant k₂, Q₃ (mg/kg) is Cr fraction, which is not extractable, and q_{total} is the total concentration of Cr in the soil.

This model was tested by the coefficient of determination (R²) and standard error (SE) of estimate.

The SE was calculated as follows:

$$SE = \left[\frac{\sum(E - E')^2}{n - 2} \right]^{0.5}$$

where E and E' are the measured and calculated amounts of Cr release in soil at time t, respectively, and n is the number of measurements. The regression of nonlinear procedure and other statistical analyses were calculated by Microsoft Excel 2007 (Microsoft Corp., Redmond, WA, USA).

Results and Discussion

Characterization of biochar amendments

According to the results of biochar analysis, elimination of unstable compounds at higher temperatures caused biochar to have higher percentages of carbon (C) but much lower hydrogen (H) and nitrogen (N) contents (Table 2). Increased pyrolysis temperature led to increased pH (from 6.2 to 8.7) and EC (from 13.1 to 21.2 dS/m). Figure 1 shows the FTIR spectra of rice husk before pyrolysis (B0), B300, and B600. The sharp peak at 3405 and 3416 cm^{-1} in B0 and B300, and the weak peaks at around 3585 cm^{-1} in B300 and B600 are due to hydroxyl group (-OH) stretching and functional group of phenols. The peaks at 2923 and 2936 cm^{-1} seen in B0 and B300 are ascribed to aliphatic C-H deforming vibration and functional group of alkanes. These functional groups disappear at temperatures higher than 600 °C. The weak band at 1725 cm^{-1} for B0, which disappears at temperatures higher than B300, is assigned to C=O stretching in the carbonyl group and neutral functional group of aldehydes. The weak band at around 1640 cm^{-1} for B0 is due to the presence of C=C stretching (functional group of alkenes). The weak band at 1539 cm^{-1} for B0 indicates the presence of N-O asymmetric stretch (nitro compounds). This band disappears at temperatures higher than 300°C indicating the volatilization of nitrogen forms. The band at around 1600 cm^{-1} for B300 and B600 indicates the presence of aromatic C=O ring stretching (likely -COOH) or aromatic C=C stretching. This band is stronger in B600 compared to B300; therefore,

pH was higher in biochar produced in high temperature than in low temperature. The weak bands at 1320 and 1376 cm^{-1} in B0 indicate the presence of the N-O asymmetric stretch (nitro compounds). This band disappears at temperatures higher than 300°C indicating the volatilization of nitrogen forms. The band at around 1090 cm^{-1} is due to aliphatic ether, alcohol C-O, or aromatic stretching in cellulose and hemicelluloses. In general, the results from FTIR analysis showed that the functional groups, such as carboxylic bonds and aromatic C = O ring stretching (likely -COOH), were higher in B600 than B300, which increased its pH.

Chemical fractions of Cr affected by amendments

Application of various amendments had considerable effects on chemical forms of Cr (Figure 2). Sequential extraction experiment showed that Cr was mostly bound to Res in soil samples. This finding is in agreement with observations by others.¹⁷⁻¹⁹ Among the chemical forms of heavy metals, EX fraction usually determines the real environmental risk. Hence, the amount of EX form could be used to assess the effect of the amendments on Cr immobilization. According to the results, the chemical form of EX was significantly decreased when soils were amended by MSWC, B300, or Fe⁰ at application rates of 2% and 5%. Organic matter and iron can convert Cr(VI) to less soluble Cr(III) through a reduction process.¹ In addition, coprecipitation with Fe hydrous oxide, which has low mobility in soil, can decrease EX fraction in treated soil by Fe⁰.²⁰ Furthermore, there was no statistically significant difference between B600 treatment and control in the EX fraction. On the other hand, CFA and Mn⁰ treatments significantly increased Ex fraction of Cr. Kim and Dixon reported that manganese oxides can increase the mobility of Cr by oxidizing Cr(III) to Cr(VI) in soil.²¹ In addition, alkaline materials, like CFA, which increase soil pH to above neutral, can oxidize Cr(III) to Cr(VI) and increased Cr mobility.^{4,5} In general, the reduction in EX form of Cr in amended soil followed the sequence of Fe⁰ > MSWC > B300 > B600 > Mn⁰ > CFA. The addition of amendments also had effects on other Cr fractions in soil samples.

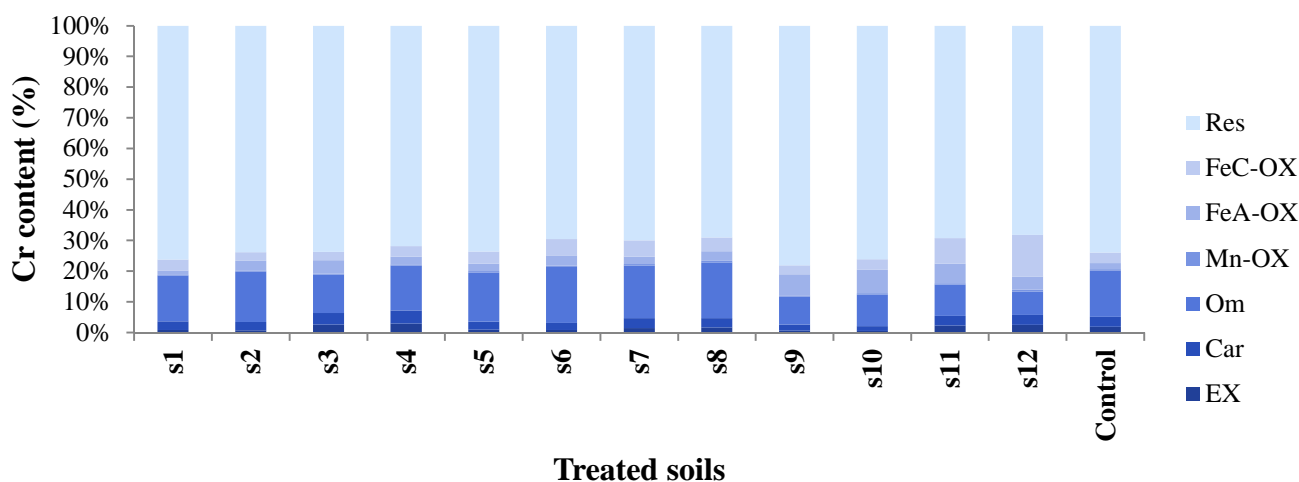


Figure 2. Percentages of various fractions of Cr in amended soil

Fe⁰, MSWC, and B300 treatments significantly decreased Car fraction. The Car fraction characterizes the most mobile and bioavailable form.²² Hence, the decreasing of Car fraction in treated soil showed that these amendments are able to increase Cr stabilization. Pantsar-Kallio et al. reported that organic materials can reduce Fe(III) to Fe(II), which in turn, reduces Cr(VI) to Cr(III).⁴ Other amendments did not have a significant effect on Car fraction. Mn⁰ treatments showed the highest percentage of Car form, especially at high rates (5%). Application of organic sources (B300, B600, and MSWC) considerably increased mean of Om fraction compared to the control soil. The Mn-OX fraction was less affected by soil amendments, while the FeC-OX and FeA-OX fractions in amended soils (especially soils treated by Mn⁰ and Fe⁰) increased (except for MSWC treatment in FeC-OX fraction) compared to the control soil. The mobility of heavy metals depends on their chemical fractions. In the control soil, the mobility factor was 5.24%. The mobility factor in S1-S12 samples was 3.72, 3.55, 6.50, 7.45, 3.71, 3.25, 4.94, 4.94, 2.63, 2.14, 5.87, and 6.61, respectively. The lowest mobility factor is associated with application of Fe⁰ especially at a high rate (5%). These results confirm the effectiveness of Fe⁰ in stabilizing of Cr in contaminated soils, as previously reported by Mench et al.²³ and Kumpiene et al.³ In general, Fe⁰

treatment was superior to other amendments in reducing Cr mobility in fractionation experiment.

Desorption kinetic of Cr affected by amendments

Figures 3 and 4 show the trends in cumulative Cr desorption in soil samples by EDTA and NaNO₃. The obtained trend from Cr desorption using both extractants showed that extractions induced a two-step release process (biphasic pattern); initial quick release at the beginning (4.25 hours) and followed by a slow reaction, until the curve appeared flat and obtained equilibrium (30.25 hours). Kirpichtchikova et al. reported that the short-term elimination of metals is dominated by the most labile fractions, while the long-term removal is determined by the replenishment of the labile pool from more recalcitrant fractions.²⁴ The biphasic pattern of the desorption of heavy metals has also been reported by others.^{9,25,26} The time of reaching equilibrium was almost similar in untreated and treated soil samples. On the one hand, it seems that in the first stage of desorption (slow release), Cr release is related to the mobile fractions (EX and Car fractions) with lower bonding energy.²⁷ On the other hand, the Cr extracted in the second stage is related to the less mobile forms.²⁸ The results showed that the total amount of Cr released by 0.01 m NaNO₃ was higher than that by 0.01 m EDTA. The Cr

released by 0.01 m NaNO_3 varied from 3.98 to 39.74 mg/kg and by 0.01 m EDTA it ranged from 4.593 to 25.29 mg/kg. The highest amount of desorbed Cr was observed in the control soil with 39.74 and 25.29 mg/Cr kg soil using 0.01 m NaNO_3 and 0.01 m EDTA, respectively. The lowest amount of desorbed Cr was observed in the $\text{Fe}^{0}_{5\%}$ treatment with 3.98 and 4.59 mg/Cr kg soil using NaNO_3 and EDTA, respectively. Application of Fe^0 at the rates of 2 and 5% considerably decreased Cr release by 89.97% and 79.11%, respectively, compared to the control soil, in the 0.01 m NaNO_3 media. Addition of Fe^0

also significantly decreased Cr release by 81.84% and 51.35% at levels of 2 and 5%, respectively, in the 0.01 m EDTA media. Kumpiene et al. used zerovalent iron for stabilization of Cr and showed that the application of Fe^0 decreased Cr concentrations in leachates (by 45%), soil pore water (by 94%), and plant shoots (by 95%).³ Application of Mn^0 decreased Cr release by 5.2 and 9% at the rates of 2 and 5%, respectively, in the 0.01 m NaNO_3 media. Cr release in Mn^0 -treated soil samples decreased by 0.45 and 6.1% at the rates of 2 and 5%, respectively, in the 0.01 m EDTA media.

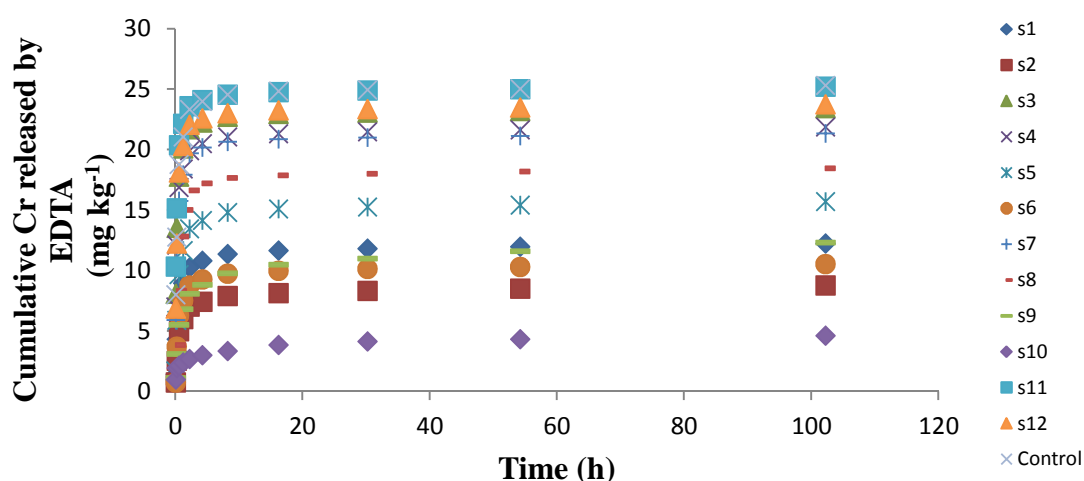


Figure 3. Variation of Cr desorption by 0.01 m EDTA in time in treated soils

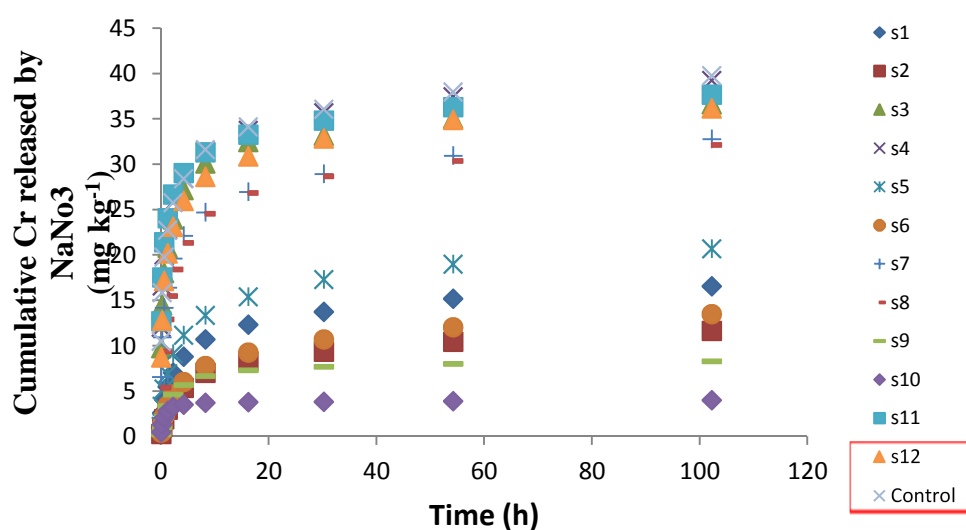


Figure 4. Variation of Cr desorption by 0.01 m NaNO_3 in time in treated soils

The results indicated that Mn^0 could not decrease Cr release efficiently, because manganese oxides can increase mobility of Cr by transformation of Cr(III) to Cr(VI) in soil.²⁰ The application of 2 and 5% MSWC led to reduction of Cr desorption by 58.35 and 70.71% in the 0.01 m $NaNO_3$ media, and 51.69 and 65.44% in the 0.01 m EDTA media, respectively. Increasing soil organic matter increased sorption sites for Cr. Addition of CFA at the rates of 2 and 5% decreased Cr release by 7.8 and 1.3% in 0.01 m $NaNO_3$ media, and 7.4 and 13.6% in 0.01 m EDTA media, respectively. Application of CFA as an alkaline material could not decrease Cr release efficiently. Increasing soil pH followed by application of CFA led to the transformation of Cr(III) to Cr(VI).^{4,5} Treatment with B600 at the rates of 2 and 5% decreased Cr release by 17.5 and 19.1% in 0.01 m $NaNO_3$ media and 15.6 and 27.1% in 0.01 m EDTA media, respectively. Desorption of Cr significantly decreased when soil samples were amended using B300 at application rates of 2 and 5%. The application of 2 and 5% B300 led to reduction of Cr desorption by 48 and 66.1% in 0.01 m $NaNO_3$ media, and 15.66 and 27.14% in 0.01 m EDTA media, respectively. The results clearly show that the application of B600 and CFA increased soil pH, and thus, increased the oxidation of Cr(III) to Cr(VI) and could not considerably decrease Cr mobility. The results also illustrated that the application of amendments at high levels (5% W/W) could provide a suitable condition for Cr adsorption. Therefore, the application of amendments at 5% (W/W) is more effective than at 2% (W/W) in reduction of Cr availability. Generally, Fe^0 , MSWC, and B300 treatments were superior to the Mn^0 , CFA, and B600 in the stabilization of Cr in desorption experiment. According to the desorption results, $NaNO_3$ extracted greater amounts of Cr from the soil samples compared to EDTA. Jalali and Sajadi Tabar reported that EDTA was not the best choice for identifying kinetic differences,⁹ but provides an upper limit of metal mobility

and can be a valuable parameter in predicting long-term transfer in soils.²⁹ Hence, using 0.01 m $NaNO_3$ media is preferred to 0.01 m EDTA media in the investigated operating conditions. The two first-order reaction model was used for metal speciation in soil and sediment samples.^{9,10,30} This model exhibited biphasic reaction; rapid extraction followed by slow extraction of metal. Hence, it was expected that this model could be described the Cr desorption. The parameters of the two first-order reaction model (Q_1 , K_1 , Q_2 , K_2 , R^2 , SE, and Q_1/Q_2) are presented in tables 5 and 6. Based on the obtained highest values of R^2 and lowest values of SE of the estimate, the two first-order reaction model could be best fitted for describing Cr release in soil samples. The results show that the values of Q_2 (less extractable) in amended soil samples (except for soil treated with B600 and Mn^0 in 0.01 m EDTA, and by CFA in 0.01 m $NaNO_3$) were lower than Q_1 (readily extractable fraction) compared to the control soil. The higher amount of Q_2 in some amended soil samples compared to the control soil confirmed the positive effect of amendment in Cr stabilization. The assumption is that the fractions of Cr determined with the two first-order reaction model is correlative with fractionation of Cr derived from the fractionation method. Hence, the simple correlation coefficient (r) was estimated for relationships among parameters of the two first-order reaction model and chemical forms of Cr (tables 7 and 8). There was a significant positive correlation between Q_1 and K_1 , EX, Mn-Ox, and FeC-Ox, between Q_2 and K_2 , Ex, Car, and K_2 , and between K_2 and Car in 0.01 m EDTA media. In addition, there was a positive significant relationship between Q_1 and Q_2 , EX, and Car, between K_1 and Car, between Q_2 and Ex, Car, and K_2 , and between K_2 and FeC-Ox in 0.01 m $NaNO_3$. Jalali and Sajadi Tabar found a significant correlation between Q_2 and acid malic with Om, inorganic precipitates fraction, and Res fractions of Nickel.⁹ Brunori et al. noticed that Q_1

could be related to Ex fraction and part of Om fraction, Q_2 could be related to the Om residual and inorganic precipitates fraction, and Q_3 could be related to residual fraction.³¹

The results of correlation coefficients between

chemical forms of Cr and parameters of the two first-order reaction model confirmed the hypothesis of Brunori et al.³¹ based on positive correlation between Q_1 and mobile fractions (EX and Car) especially in 0.01 m NaNO₃ media.

Table 5. Estimated parameters of the two first-order reaction model used to describe release kinetics of Cr with 0.01 m EDTA

Value	S1	S2	S3	S4	S5	S6	S7	S8	S9	S10	S11	S12	Control
Q_1	2.808	1.891	9.318	5.863	3.837	2.409	13.635	13.290	7.650	2.199	12.489	16.195	13.544
K_1	0.189	0.106	0.919	0.523	0.257	0.179	5.500	3.631	1.896	7.108	14.573	5.189	7.661
Q_2	9.140	6.647	13.630	15.581	11.513	7.873	7.307	4.763	4.298	2.224	12.153	7.114	11.266
K_2	2.415	1.942	8.739	5.915	2.533	2.261	0.712	0.442	0.064	0.084	1.416	0.704	0.901
R^2	0.996	0.994	0.995	0.994	0.996	0.992	0.996	0.997	0.994	0.992	0.988	0.995	0.991
SE	3.429	2.539	4.835	4.682	4.412	3.027	4.930	4.660	3.516	1.101	4.715	5.432	5.660
Q_1/Q_2	0.307	0.284	0.684	0.376	0.333	0.306	1.866	2.790	1.780	0.989	1.028	2.276	1.202

Q_1 : Readily extractable (mg/Kg); K_1 : Constant rate related to Q_1 (1/min); Q_2 : less extractable (mg/Kg); K_2 : Constant rate related to Q_2 (1/min); R^2 : coefficient of determination; SE: standard error

Table 6. Estimated parameters of the two first-order reaction model used to describe release kinetics of Cr with 0.01 m NaNO₃

Value	S1	S2	S3	S4	S5	S6	S7	S8	S9	S10	S11	S12	Control
Q_1	6.969	5.391	16.667	19.431	8.927	5.549	15.314	13.888	5.289	3.555	15.365	16.593	17.920
K_1	1.200	0.543	8.697	9.655	1.217	0.649	4.982	4.264	0.736	1.421	0.170	0.123	0.128
Q_2	9.205	6.331	17.879	17.751	11.333	7.974	15.806	16.592	2.869	3.518	20.494	17.982	19.916
K_2	0.050	0.033	0.192	0.143	0.049	0.035	0.101	0.116	0.069	0.002	9.741	5.470	7.113
R^2	0.993	0.997	0.940	0.978	0.994	0.997	0.983	0.988	0.998	0.989	0.997	0.981	0.983
SE	5.198	3.876	8.710	8.713	6.446	4.414	8.374	8.740	2.848	1.179	7.893	8.898	9.321
Q_1/Q_2	0.757	0.852	0.932	1.095	0.788	0.696	0.969	0.837	1.843	1.010	0.750	0.923	0.900

Q_1 : Readily extractable (mg/Kg); K_1 : Constant rate related to Q_1 (1/min); Q_2 : less extractable (mg/Kg); K_2 : Constant rate related to Q_2 (1/min); R^2 : coefficient of determination; SE: standard error

Table 7. Simple correlation coefficients (r) between parameters of the two first-order reaction model of Cr desorption, extracted by EDTA, with Cr fractions

	Q_1	K_1	Q_2	K_2
K_1	0.558*	-	-	-
Q_2	0.089	-0.037	-	-
K_2	-0.178	-0.409	0.743**	-
EX	0.657*	0.298	0.632*	0.465
Car	0.518	0.037	0.768**	0.578*
Om	-0.203	-0.383	0.108	0.067
Mn-Ox	0.626*	0.349	0.056	-0.312
FeA-Ox	0.032	0.474	-0.419	-0.239
FeC-Ox	0.576*	0.427	-0.045	-0.278
Res	-0.167	0.013	-0.277	-0.233

*Correlation is significant at the 0.05 level; **Correlation is significant at the 0.01 level; Q_1 : Readily extractable (mg/Kg); K_1 : Constant rate related to Q_1 (1/min); Q_2 : less extractable (mg/Kg); K_2 : Constant rate related to Q_2 (1/min); R^2 : coefficient of determination; EX: Exchangeable; Car: Carbonate-bound; Om: Organically-bound Mn-OX: Mn-oxide-bound; FeA-Ox: Amorphous Fe-oxide-bound; FeC-Ox: Crystalline Fe-oxide-bound; Res: Residual forms

Table 8. Simple correlation coefficients (r) between parameters of the two first-order reaction model of Cr desorption, extracted by NaNO₃, with Cr fractions

	Q ₁	K ₁	Q ₂	K ₂
K ₁	0.520	-	-	-
Q ₂	0.952**	0.360	-	-
K ₂	0.480	-0.397	0.604*	-
EX	0.921**	0.509	0.878**	0.494
Car	0.914**	0.617*	0.866**	0.292
Om	-0.020	0.172	0.060	-0.381
Mn-Ox	0.457	-0.158	0.519	0.433
FeA-Ox	-0.277	-0.211	-0.298	0.207
FeC-Ox	0.334	-0.311	0.407	0.576*
Res	-0.383	-0.444	-0.453	0.084

* Correlation is significant at the 0.05 level; ** Correlation is significant at the 0.01 level; Q₁: Readily extractable (mg/Kg); K₁: Constant rate related to Q₁ (1/min); Q₂: less extractable (mg/Kg); K₂: Constant rate related to Q₂ (1/min); R²: coefficient of determination; EX: Exchangeable; Car: Carbonate-bound; Om: Organically-bound Mn-OX: Mn-oxide-bound; FeA-Ox: Amorphous Fe-oxide-bound; FeC-Ox: Crystalline Fe-oxide-bound; Res: Residual forms

Conclusion

Stabilization of heavy metals is a cost effective soil remediation method, which is used to reduce the mobile contaminant fraction in soil by low-cost and widely available amendments. In the present study, 6 types of soil amendments were investigated for their abilities to reduce Cr mobility in soil; CFA, MSWC, rice husk biochar prepared at 300°C (B300) and 600°C (B600), zerovalent iron (Fe⁰) and zerovalent manganese (Mn⁰). The stabilization of Cr in Cr-spiked soil is assessed by sequential extraction and desorption kinetic methods. According to the results, addition of amendments in soil samples considerably decreased mobility factor (except for CFA_{5%}) of Cr compared to the control samples. Addition of Fe⁰, MSWC, and B300 in soil samples decreased Cr release considerably more than other amendments, compared to control treatment. The lowest Cr desorption was achieved by Fe⁰ at the rate of 5%. According to the desorption results, NaNO₃ extracted greater amounts of Cr from the soil samples compared to EDTA. Hence, the use of 0.01 m NaNO₃ media is preferred to 0.01 m EDTA media in the investigated operating conditions. The results clearly illustrate that the application of B600 and

CFA increased soil pH, and thus, increased the oxidation of Cr(III) to Cr(VI). Based on the obtained highest values of R² and lowest values of SE of the estimate, the two first-order reaction model could be best fitted for describing Cr release in soil samples. In general, from the practical view, Fe⁰, MSWC, and B300 treatments are effective in Cr immobilization, while application of Fe⁰ at the rate of 5% (W/W) was the best treatment for stabilization of Cr in polluted soil. Further research is required in order to evaluate the synergetic effects of selected amendments on Cr stabilization.

Conflict of Interests

Authors have no conflict of interests.

Acknowledgements

The authors would like to thank Shiraz University for providing research facilities and the two anonymous reviewers for their valuable suggestions.

References

1. Kumpiene J, Lagerkvist A, Maurice C. Stabilization of As, Cr, Cu, Pb and Zn in soil using amendments: A review. Waste Management 2008; 28(1): 215-25.

2. Banks MK, Schwab AP, Henderson C. Leaching and reduction of chromium in soil as affected by soil organic content and plants. *Chemosphere* 2006; 62(2): 255-64.
3. Kumpiene J, Ore S, Renella G, Mench M, Lagerkvist A, Maurice C. Assessment of zerovalent iron for stabilization of chromium, copper, and arsenic in soil. *Environmental Pollution* 2006; 144(1): 62-9.
4. Pansar-Kallio M, Reinikainen SP, Oksanen M. Interactions of soil components and their effects on speciation of chromium in soils. *Analytica Chimica Acta* 2001; 439(1): 9-17.
5. Seaman JC, Arey JS, Bertsch PM. Immobilization of nickel and other metals in contaminated sediments by hydroxyapatite addition. *J Environ Qual* 2001; 30(2): 460-9.
6. Krishnamurti GS, Huang PM, Kozak LM. Sorption and Desorption Kinetics of Cadmium from Soils: Influence of Phosphate. *Soil Science* 1999; 164(12): 888-98.
7. Violante A, Krishnamurti GS. Factors Affecting the Sorption-Desorption of Trace Elements in Soil Environments. In: Violante A, Huang PM, Gadd GM, editors. *Biophysico-Chemical Processes of Heavy Metals and Metalloids in Soil Environments*. New Jersey, NJ: John Wiley & Sons; 2007. p. 169-213.
8. Saffari M, Yasrebi J, Karimian N, Shan XQ. Effect of Calcium Carbonate Removal on the Chemical Forms of Zinc in Calcareous Soils by Three Sequential Extraction Methods. *Research Journal of Biological Sciences* 2009; 4(7): 858-65.
9. Jalali M, Sajadi Tabar S. Kinetic Extractions of Nickel and Lead from Some Contaminated Calcareous Soils. *Soil and Sediment Contamination: An International Journal* 2013; 22(1): 56-71.
10. Santos S, Costa CA, Duarte AC, Scherer HW, Schneider RJ, Esteves VI, et al. Influence of different organic amendments on the potential availability of metals from soil: a study on metal fractionation and extraction kinetics by EDTA. *Chemosphere* 2010; 78(4): 389-96.
11. Sahuquillo A, Rigol A, Rauret G. Overview of the use of leaching/extraction tests for risk assessment of trace metals in contaminated soils and sediments. *TrAC Trends in Analytical Chemistry* 2003; 22(3): 152-9.
12. Sparks DL. *Methods of Soil Analysis: Part 3, Chemical methods, Part 3*. Madison, WI: Soil Science Society of America; 1996.
13. Sposito G, Lund LJ, Chang AC. Trace Metal Chemistry in Arid-zone Field Soils Amended with Sewage Sludge: I. Fractionation of Ni, Cu, Zn, Cd, and Pb in Solid Phases I. *Soil Sci Am J* 1982; 46(2): 260-4.
14. Bartlett R, James B. Behavior of chromium in soils: III. Oxidation. *J Environ Qual* 1979; 8(1): 31-5.
15. Singh JP, Karwasra SP, Singh M. Distribution and forms of copper, iron, manganese, and zinc in calcareous soils of India. *Soil Sci* 1989; 146: 359-66.
16. Salbu B, Krekling T. Characterisation of radioactive particles in the environment. *Analyst* 1998; 123(5): 843-50.
17. Kalemekiewicz J, Soeo E. Investigations of Chemical Fraction of Cr in Soil. *Polish J of Environ Stud* 2005; 14(5): 593-8.
18. Pakula K, Kalemekiewicz D. Fractions of chromium and lead in forest Luvisols of South Podlasie Lowland. *Environ Prot Eng* 2009; 35(1): 57-64.
19. Poursan HM, Fotovat A, Haghnia G, Halajnia A, Chamsaz M. A Case Study: Chromium Concentration and its Species in a Calcareous Soil Affected by Leather Industries Effluents. *World Applied Sciences Journal* 2008; 5(4): 484-9.
20. Fendorf SE. Surface reactions of chromium in soils and waters. *Geoderma* 1995; 67: 55-71.
21. Kim JG, Dixon JB. Oxidation and fate of chromium in soils. *Soil Science and Plant Nutrition* 2002; 48(4): 483-90.
22. Yasrebi J, Karimian N, Maftoun M, Abtahi A, Sameni AM. Distribution of zinc forms in highly calcareous soils as influenced by soil physical and chemical properties and application of zinc sulfate. *Communications in Soil Science and Plant Analysis* 1994; 25(11-12): 2133-45.
23. Mench M, Bussi re S, Boisson J, Castaing E, Vangronsveld J, Ruttens A, et al. Progress in remediation and revegetation of the barren Jales gold mine spoil after in situ treatments. *Plant and Soil* 2003; 249(1): 187-202.
24. Kirpichtchikova TA, Manceau A, Spadini L, Fr d ric, Marcus MA, Jacquet T. Speciation and solubility of heavy metals in contaminated soil using X-ray microfluorescence, EXAFS spectroscopy, chemical extraction, and thermodynamic modeling. *Geochimica et Cosmochimica Acta* 2006; 70(9): 2163-90.
25. Di PL, Mecozzi R. Heavy metals mobilization from harbour sediments using EDTA and citric acid as chelating agents. *J Hazard Mater* 2007; 147(3): 768-75.
26. Sadegh L, Fekri M, Gorgin N. Effects of poultry manure and pistachio compost on the kinetics of copper desorption from two calcareous soils. *Arabian Journal of Geosciences* 2012; 5(4): 571-8.
27. Jones B, Turki A. Distribution and speciation of heavy metals in surficial sediments from the Tees Estuary, north-east England. *Marine Pollution Bulletin* 1997; 34(10): 768-79.
28. Polettini A, Pomi R, Rolle E. The effect of operating variables on chelant-assisted remediation of contaminated dredged sediment. *Chemosphere* 2007; 66(5): 866-77.

29. Labanowski J, Monna F, Bermond A, Cambier P, Fernandez C, Lamy I, et al. Kinetic extractions to assess mobilization of Zn, Pb, Cu, and Cd in a metal-contaminated soil: EDTA vs. citrate. *Environmental Pollution* 2008; 152(3): 693-701.
30. Fanguero D, Bermond A, Santos E, Carapua H, Duarte A. Kinetic approach to heavy metal mobilization assessment in sediments: choose of kinetic equations and models to achieve maximum information. *Talanta* 2005; 66(4): 844-57.
31. Brunori C, Cremisini C, D'Annibale L, Massanisso P, Pinto V. A kinetic study of trace element leachability from abandoned-mine-polluted soil treated with SS-MSW compost and red mud. Comparison with results from sequential extraction. *Anal Bioanal Chem* 2005; 381(7): 1347-54.



Estimation of target hazard quotients for metals by consumption of fish in the North Coast of the Persian Gulf, Iran

Reza Khoshnood¹, Nemat Jaafarzadeh², Zahra Khoshnood³, Mehdi Ahmadi², Pari Teymouri⁴

1 Sazab Pardazan Consulting Engineering Company, Ahvaz, Iran

2 Environmental Technology Research Center AND Department of Environmental Health Engineering, Ahvaz Jundishapur University of Medical Sciences, Ahvaz, Iran

3 Department of Experimental Sciences, Dezful Branch, Islamic Azad University, Dezful, Iran

4 Kurdistan Environmental Health Research Center AND Department of Environmental Health Engineering, Kurdistan University of Medical Sciences, Sanandaj, Iran

Original Article

Abstract

In the residential area of the North Coast of the Persian Gulf, consumption of fish is a possible source of exposure to heavy metals and other pollutants, all of which may act as potential risk factors for serious syndromes and fatal diseases. Health risks associated with Pb, Cd, and Hg were assessed based on the target hazard quotients (THQ), which can be derived from concentrations of heavy metals in fish consumed in Bandar Abbas and Bandar Lengeh, Iran. In the present study, 4 fish species (*Euryglossa orientalis*, *Psettodes erumei*, *Epinephelus coioides* and *Lethrinus nebulosus*) were randomly collected in commercial catches at local fishing ports from September 2011 to April 2012. Dorsal muscle was dissected as target sample after digestion. All samples were analyzed for their Cd and Pb contents using an inductively coupled plasma-atomic emission spectrometry (ICP-AES) and for their Hg content using an advanced mercury analyzer. The United States Environmental Protection Agency (US EPA) region III risk-based concentration table was used to estimate THQ values for both adults and children. THQ values over 1 were not observed through the consumption of fish. Total THQ values of Pb, Cd, and Hg for adults were 0.19 and 0.16 in Bandar Abbas and Bandar Lengeh, respectively. For children, they were 0.26 and 0.20 in Bandar Abbas and Bandar Lengeh, respectively, showing that the health risk associated with exposure to these 3 heavy metals was insignificant. However, according to the data concerning levels of environmental pollutants in the most consumed fish and seafood species, more specific recommendations are needed regarding human consumption (kind of species, and frequency and size of meals).

KEYWORDS: Environmental Pollutants, Fish, Heavy Metals, Iran, Risk Factors, Sea Foods

Date of submission: 25 May 2014, **Date of acceptance:** 10 Jul 2014

Citation: Khoshnood R, Jaafarzadeh N, Khoshnood Z, Ahmadi M, Teymouri P. **Estimation of target hazard quotients for metals by consumption of fish in the North Coast of the Persian Gulf, Iran.** J Adv Environ Health Res 2014; 2(4): 263-72.

Introduction

In recent years, heavy metals pollution, especially in the food chain, has attracted much attention.^{1,2} Fish and other aquatic organisms can absorb and accumulate heavy metals in their

body.³ This process depends on various parameters such as characteristics of the species under consideration, the exposure period, temperature, salinity, water pH, and seasonal changes in water characteristics. Heavy metals are released into the water by anthropogenic activities. Thus, they enter the food chain and accumulate in animal bodies such as fish. Consumption of such animals as food may have

Corresponding Author:

Reza Khoshnood

Email: rezakhoshnood@gmail.com

some adverse effects on human health.⁴

In spite of the health benefits of fish, the high levels of heavy metals accumulated in some of them contribute to the possible adverse effects, particularly in fetuses and young children. Studies on the health benefits and risks of fish consumption have focused on recreational, subsistence, and commercial fish.⁵

The Beijing Declaration, held by the World Health Organization (WHO) in 2007, expresses the rights of all individuals to a safe and adequate diet.⁶ The declaration emphasizes the importance of a safe diet and provides guidelines for food control.⁷

Fish is an important source of proteins, minerals, vitamins, and polyunsaturated fatty acids (PUFAs), especially omega-3 PUFAs. Fish consumption has been reported to reduce the risk of coronary heart disease, decrease mild hypertension, and prevent certain cardiac arrhythmias.⁷ On the other hand, seafood consumption might be an important way of human exposure to chemical contaminants.⁵

Several methods have been proposed for estimation of the potential risks to human health caused by toxic metals. Among them, the target hazard quotients (THQ), proposed by the US Environmental Protection Agency (USEPA), has been recognized as a reasonable index for the evaluation of heavy metals intake by consumption of contaminated food.⁸ The THQ is a ratio of the consumed dose of a toxic metal via an oral reference dose (RfD) proposed by the USEPA. A THQ value above 1 means that contaminated foods intake has likely some noticeable harmful effects on the exposed population. The higher the THQ value is, the higher the probability of the hazard risk on the human body will be. Based on THQ values, studies have been performed on the potential risk assessment of dietary intake of heavy metals via the consumption of seafood.^{8,9}

Urban and suburban areas of Bandar Abbas and Bandar Lengeh, Iran, have been polluted by some sources of heavy metals. Nevertheless,

information on the health risks of these elements is quite limited. The main objective of this study was to use the THQ concept to estimate the health risks of Pb, Cd, and Hg via consumption of fish on the general public in these two cities.

Materials and Methods

Hormozgan Province is located in Southern Iran (Figure 1). It is the first largest commercial port and harbor in Iran. Rapid development of agriculture and industries, and lack of legislation and regulations has led to the discharge of heavy metals, such as Cu, Zn, Pb, Cd, Hg, and Cr into the environment in large quantities through atmospheric deposition, solid waste disposal, sludge application, and wastewater irrigation.

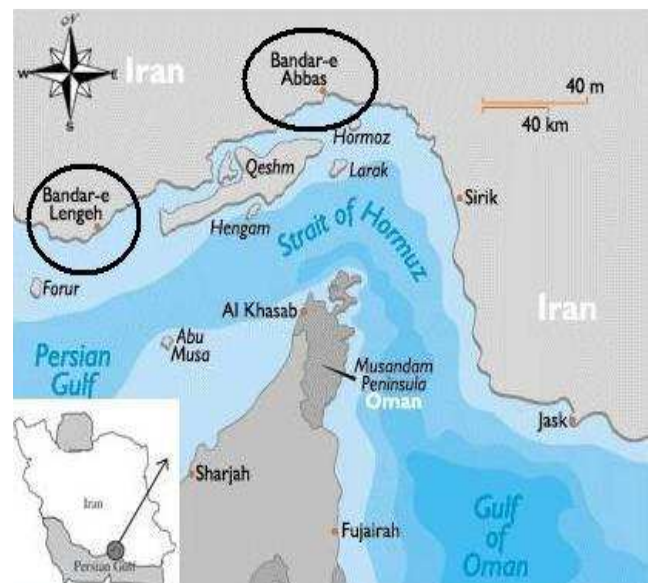


Figure 1. Sampling location map

Two large residential areas, which are known as the two largest fishing ports in this province were selected as the study areas. Wastewater irrigation and sludge application are the prevailing processes that have resulted in heavy metal contamination in these areas. In the present study, 4 economically important fish species with a high consumption rate in the local population were selected. They included 2 species of flat fish, Oriental sole (*Euryglossa*

orientalis) and Deep flounder (*Psettodes erumei*), 1 specie from the Serranidae family (Hamoor), Orange spotted grouper (*Epinephelus coioides*), and one specie from the Lethrinidae family (Shehri), Spangled emperor (*Lethrinus nebulosus*) (Table 1). The selected fish species belong to different families and have different trophic/ecological characteristics, i.e., they include demersal top carnivores (e.g. Hamoor) and benthic feeders (e.g. Flat fishes).

Fish species were randomly collected from commercial catches landed at local fishing ports from September 2011 to April 2012, and the biometrics of sampled fish were determined.

After the collection, fish samples were immediately stored on ice in an isolated box¹⁰, and transferred to reference laboratory belonging to the Hormozgan Environmental Deputy. The samples were thoroughly washed under tap water to eliminate dust and dirt. After that, a part of the dorsal muscle (edible tissue) from each of the samples was dissected as the target sample and prepared for processing. All samples were dried at 60°C for 48 hours in the laboratory oven.^{7,11}

Glassware was soaked in HNO₃ (10% v/v) and cleaned with ultrapure water. Subsequently,

0.2-0.4 g of prepared sample was digested in Teflon beaker using ultrapure nitric acid (65% v/v, 5 ml). The digesting process was completed using a microwave, operated for about 30 minutes at 200 °C. Prepared samples were transferred to the test tube and brought up to volume (50 ml).¹²

All samples were analyzed 3 times for Cd and Pb using an inductively coupled plasma-atomic emission spectrometry (ICP-AES) (Varian Model-liberty series II, Palo Alto, USA) and for Hg using an advanced mercury analyzer (LECO AMA 254, LECO Corp., St. Joseph, MI, USA).

In order to assess the analytical capability of the proposed methodology, accuracy of heavy metals analysis was tested with fish protein for trace metals (DORM 2), and dogfish liver for trace metals (DOLT 2). Results confirmed that observed and reference values were not statistically different ($P < 0.05$) (Table 2).

Average body weight of people and mean dietary fish consumption rate were derived from national and local organizations such as the Institute of Standard and Industrial Research of Iran (ISIRI), Iranian Department of Environment, and Iranian Fishery Organization reports.

Table 1. Overview of sampled species

Scientific name	Common Name	Station	Length (cm)	Weight (g)	No. of samples
E. orientalis	Oriental sole	BA	38.3 ± 4.01	605.0 ± 140.09	10
		BL	28.1 ± 6.49	513.0 ± 252.51	10
P. erumei	Deep flounder	BA	48.1 ± 5.36	1672.0 ± 289.52	10
		BL	31.0 ± 6.37	1309.0 ± 320.25	10
E. coioides	Orange spotted grouper	BA	48.0 ± 9.50	2278.9 ± 360.95	10
		BL	54.3 ± 6.58	2437.9 ± 350.26	10
L. nebulosus	Spangled emperor	BA	26.17 ± 4.3	312.5 ± 70.25	10
		BL	23.18 ± 4.89	533.9 ± 39.25	10

BA: Bandar Abbas; BL: Bandar Lengeh

Table 2. Comparison of the obtained and reference concentrations (µg/g dry weight)

CRM		Pb	Cd	Hg
DORM-2	Certified	0.065 ± 0.007	0.043 ± 0.008	0.789 ± 0.074
	Obtained	0.063 ± 0.008	0.045 ± 0.009	0.079 ± 0.270
DOLT-2	Certified	0.220 ± 0.020	20.800 ± 0.500	4.640 ± 0.260
	Obtained	0.230 ± 0.030	20.700 ± 0.400	4.60 ± 0.220

CRM: Canadian Reference Materials; DORMM-2: Fish protein for trace metals; DOLT-2: Dogfish liver for trace metals

The methodology for estimation of THQ was provided in the USEPA region III risk-based concentration table.¹³ For carcinogenic effects, risk is expressed as excess probability of contracting cancer over a lifetime. For non-carcinogenic effects, risk is expressed as a THQ, the ratio between the exposure and the reference dose.

A THQ of less than 1 shows that the exposed population, probably, has not experienced any evident adverse effects. The dose calculations were carried out using the standard assumption from an integrated USEPA risk analysis considering an average adult body weight of 55.9 kg, and child body weight of 32.7 kg. Evidently, children are more sensitive to pollutants. There will be a certain amount of discrepancy in health risks between age groups and the locality of the inhabitants. In this respect, the THQ was determined based on the USEPA methods described by the following equation:

$$THQ = \frac{E_F \times E_D \times E_{IR} \times C}{R_{FD} \times W_{AB} \times T_A} \times 10^{-3} \quad (\text{Eq. 1})$$

where E_F is the exposure frequency (365 days/year), E_D is the exposure duration (72 years) equivalent to the average lifetime in Iran, F_{IR} is the food ingestion rate (g/person/day), C is the metal concentration in food (Ag/g), R_{FD} is the oral reference dose (mg/kg/day), W_{AB} is the average body weight

(55.9 kg for adults and 32.7 kg for children), and T_A is the average exposure time for non-carcinogens (365 days/years of exposure, assuming 70 years in this study). It was further assumed that cooking has no effect on the toxicity of heavy metals in seafood.¹⁴ For the inhabitants of the two studied areas, the daily fish consumption was 22.14 g/person/day for adults and 15.16 g/person/day for children.

Results and Discussion

Concentrations of Pb, Cd, and Hg in fish in the two studied areas are shown in table 3. *E. coioides*, *L. nebulosus*, and *P. erumei* had the highest concentrations of Pb, Cd, and Hg, respectively, in Bandar Abbas. *E. coioides* had the highest concentration of both Pb and Cd, and *P. erumei* accumulated the highest concentration of Hg in Bandar Lengeh (Table 3).

The average concentrations of the 3 metals were higher in Bandar Abbas than Bandar Lengeh. This result is mainly due to unmanaged shipping activities, river runoff, untreated sewage discharge by coastal settlements, and toxic and industrial wastes discharge into the sea adjacent to Bandar Abbas.

The concentrations of metals in fish from this region during this study were compared with those reported previously (Table 4).

Table 3. Average concentrations of heavy metals in fish species ($\mu\text{g/g}$ dry weight)

Station\metals	Species	Pb		Cd		Hg	
		Range	Mean	Range	Mean	Range	Mean
Bandar Abbas	<i>E. orientalis</i>	0.18-0.25	0.20	0.09-0.51	0.17	0.14-0.27	0.21
	<i>P. erumei</i>	0.16-0.34	0.31	0.22-0.61	0.23	0.10- 0.55	0.28
	<i>E. coioides</i>	0.07-0.76	0.54	0.17-0.21	0.20	0.12-0.23	0.19
	<i>L. nebulosus</i>	0.14-0.37	0.32	0.12-0.30	0.27	0.07-0.26	0.17
Bandar Lengeh	<i>E. orientalis</i>	0.16-0.23	0.21	0.14-0.20	0.16	0.15-0.24	0.21
	<i>P. erumei</i>	0.01-0.09	0.04	0.01-0.14	0.09	0.14-0.31	0.26
	<i>E. coioides</i>	0.11-0.36	0.29	0.14-0.35	0.31	0.09-0.17	0.11
	<i>L. nebulosus</i>	0.16-0.27	0.21	0.23-0.33	0.27	0.11-0.21	0.14

Table 4. Heavy metal concentrations ($\mu\text{g.g}^{-1}$ dry weight) in fish in other water areas

Species or population	Location	Hg	Pb	Cd	Reference
<i>E. encrasicolus</i>	Sicily, Mediterranean Sea	0.03 ± 0.03	< 0.001	0.18 ± 0.17	
<i>S. pilchardus</i>	Sicily, Mediterranean Sea	0.08 ± 0.03	< 0.001	0.08 ± 0.09	4
<i>M. barbatus</i>	Sicily, Mediterranean Sea	0.08 ± 0.26	0.84 ± 0.069	< 0.06	
<i>Ostrea plicatula</i>	Xiamen, China	0.008	0.211	0.334	
<i>R. philippinarum</i>	Xiamen, China	0.008	0.151	0.133	8
<i>S. constricta</i>	Xiamen, China	0.007	0.215	0.054	
<i>Tegillarca granosa</i>	Xiamen, China	0.008	0.210	0.369	
<i>T. mutibilis</i>	Bandar Abbas, Iran	-	-	8.69 ± 6.23	15
<i>Psettodes erumei</i>	Hormozgan Province, Iran	-	-	0.25 ± 0.12	16
<i>Euryglossa orientalis</i>	Hormozgan Province, Iran	-	-	0.12 ± 0.05	
<i>Corpus corpino</i>	Caspian Sea, Iran	-	138.75 ± 26.2	72.87 ± 22.2	
<i>Mugila auratus</i>	Caspian Sea, Iran	-	75.11 ± 37.4	27.96 ± 12.1	17
<i>Rutilus frisikutum</i>	Caspian Sea, Iran	-	121.36 ± 53.2	38.84 ± 18.9	
Anchovy fish	Jingsu River, Taihu Lake	-	$1.5 \times 10^{-2} \pm 1.3 \times 10^{-1}$	$7.0 \times 10^{-4} \pm 3.6 \times 10^{-3}$	18
<i>Istiophorus platypterus</i>	Gulf of California	1.48×0.93 (0.23–3.62)	$3.6 \times 10^{-1} \pm 2.9 \times 10^{-1}$ (1.6×10^{-1} –1.5)	$5.5 \times 10^{-1} \pm 3.7 \times 10^{-1}$ (2.6×10^{-1} –1.55)	19
<i>Tetrapturus audax</i>	Gulf of California	1.72 ± 0.61 (0.81–3.12)	$3.5 \times 10^{-1} \pm 8.0 \times 10^{-2}$ (1.8×10^{-1} – 4.9×10^{-1})	$3.7 \times 10^{-1} \pm 4.0 \times 10^{-1}$ (1.2×10^{-1} –1.38)	
European Anchovy	Adriatic Sea	$7.0 \times 10^{-2} \pm 9.0 \times 10^{-2}$ 2.0×10^{-2} – 2.1×10^{-1}	$1.0 \times 10^{-1} \pm 1.0 \times 10^{-2}$ (9.0×10^{-2} – 1.0×10^{-1})	$1.0 \times 10^{-2} \pm 1.0 \times 10^{-2}$ (1.0×10^{-2} – 2.0×10^{-2})	
Four spotted megrim	Adriatic Sea	$3.5 \times 10^{-1} \pm 1.9 \times 10^{-1}$ (1.4×10^{-1} – 6.9×10^{-1})	$2.0 \times 10^{-2} \pm 1.0 \times 10^{-2}$ (ND– 2.0×10^{-2})	$4.0 \times 10^{-2} \pm 1.0 \times 10^{-2}$ 3.0×10^{-2} – 7.0×10^{-2}	9
Starry ray	Adriatic Sea	$3.9 \times 10^{-1} \pm 3.6 \times 10^{-1}$ (7.0×10^{-2} – 8.9×10^{-1})	$2.0 \times 10^{-2} \pm 2.0 \times 10^{-2}$ (ND– 6.0×10^{-2})	$1.0 \times 10^{-2} \pm 3.0 \times 10^{-2}$ (2.0×10^{-2} – 1.0×10^{-2})	
Rosefish	Adriatic Sea	1.25 ± 0.85 (2.4×10^{-1} –2.98)	$1.3 \times 10^{-1} \pm 9.0 \times 10^{-2}$ (3.0×10^{-2} – 3.3×10^{-1})	$3.0 \times 10^{-2} \pm 1.0 \times 10^{-2}$ (1.0×10^{-2} – 8.0×10^{-2})	
<i>Cyprinus carpio</i>	Meiliang Bay, Taihu Lake	-	$1.8 \times 10^{-1} \pm 3.0 \times 10^{-2}$	$2.1 \times 10^{-2} \pm 8.0 \times 10^{-3}$	
<i>Carassius auratus</i>	Meiliang Bay, Taihu Lake	-	$2.9 \times 10^{-1} \pm 1.0 \times 10^{-2}$	$1.3 \times 10^{-2} \pm 8.0 \times 10^{-3}$	20
<i>Hypophthalmichthys molitrix</i>	Meiliang Bay, Taihu Lake	-	$1.8 \times 10^{-1} \pm 4.6 \times 10^{-2}$	$3.0 \times 10^{-3} \pm 1.0 \times 10^{-3}$	
<i>Aristichthys nobilis</i>	Meiliang Bay, Taihu Lake	-	$1.8 \times 10^{-1} \pm 3.1 \times 10^{-2}$	$4.0 \times 10^{-3} \pm 1.0 \times 10^{-3}$	
<i>Gymnocypris namensis</i>	Nam Co Lake, Tibet Plateau	-	4.7×10^{-2}	2.5×10^{-2}	21

Table 4. Heavy metal concentrations ($\mu\text{g}\cdot\text{g}^{-1}$ dry weight) in fish in other water areas (Continue)

Species or population	Location	Hg	Pb	Cd	Reference
Gymnocypris waddellii	Yamdro Lake, Tibet Plateau	-	7.9×10^{-2}	2.4×10^{-2}	
Ptychobarbus dipogon	Lhasa River, Tibet Plateau	-	2.4×10^{-2}	2.4×10^{-2}	
Lagocephalus lagocephalus	Ghana, Atlantic coast	$6.6 \times 10^{-2} \pm 2.3 \times 10^{-2}$	-	-	22
Pseudotolithus senegalensis	Ghana, Atlantic coast	$3.1 \times 10^{-2} \pm 2.5 \times 10^{-2}$	-	-	
Brahydentera aurita	Ghana, Atlantic coast	$12.2 \times 10^{-2} \pm 3.0 \times 10^{-2}$	-	-	
Fish	Dong Li District, Tianjin	2.0×10^{-2} (1.0×10^{-3} - 4.3×10^{-2})	1.0×10^{-2} (2.0×10^{-3} - 2.0×10^{-2})	2.0×10^{-3} (4.0×10^{-4} - 5.0×10^{-3})	23
Fish	Xi Qing District, Tianjin	2.0×10^{-2} (4.0×10^{-3} - 4.0×10^{-2})	6.0×10^{-2} (1.0×10^{-3} - 2.8×10^{-1})	6.0×10^{-3} (2.0×10^{-4} - 3.0×10^{-2})	
Fish	Jin Nan District, Tianjin	4.0×10^{-2} (5.0×10^{-3} - 1.0×10^{-1})	7.0×10^{-2} (3.0×10^{-3} - 2.8×10^{-1})	8.0×10^{-3} (4.0×10^{-4} - 3.0×10^{-2})	
Fish	Bei Chen District, Tianjin	7.0×10^{-1} (6.6×10^{-2} - 7.0×10^{-1})	5.0×10^{-3} (3.0×10^{-3} - 6.0×10^{-3})	2.0×10^{-3} (1.0×10^{-3} - 3.0×10^{-3})	
Bluefish	New Jersey, USA	$2.6 \times 10^{-1} \pm 2.0 \times 10^{-2}$	$6.0 \times 10^{-2} \pm 1.0 \times 10^{-2}$	$6.0 \times 10^{-3} \pm 2.0 \times 10^{-3}$	24
Chilean sea bass	New Jersey, USA	$3.8 \times 10^{-1} \pm 6.0 \times 10^{-2}$	$1.1 \times 10^{-1} \pm 1.0 \times 10^{-2}$	$4.0 \times 10^{-3} \pm 1.0 \times 10^{-3}$	
Croaker	New Jersey, USA	$1.4 \times 10^{-1} \pm 2.0 \times 10^{-2}$	$9.0 \times 10^{-2} \pm 1.0 \times 10^{-2}$	$1.0 \times 10^{-3} \pm 4.0 \times 10^{-4}$	
Flounder	New Jersey, USA	$5.0 \times 10^{-2} \pm 1.0 \times 10^{-3}$	$6.0 \times 10^{-2} \pm 1.0 \times 10^{-2}$	$1.0 \times 10^{-2} \pm 2.0 \times 10^{-3}$	
Enedrias nebulosus	Masan Bay, Korea	-	5.0×10^{-2}	1.0×10^{-2}	
Pleuronichthys cornutus	Masan Bay, Korea	-	1.1×10^{-1}	ND	25
Conger myriaster	Masan Bay, Korea	-	4.0×10^{-2}	ND	
Acanthogobius flavimanus	Masan Bay, Korea	-	7.0×10^{-2}	3.0×10^{-2}	
Hexagrammos otakii	Masan Bay, Korea	-	4.0×10^{-2}	1.0×10^{-1}	
Sebastes marmoratus	Masan Bay, Korea	-	1.5×10^{-1}	1.0×10^{-1}	
Lethrinus lentjan	United Arab Emirates	-	-	$1.1 \times 10^{-1} \pm 2.0 \times 10^{-2}$	26
Makaria mazara	Taipei, Taiwan	10.3 (1.71-22.9)	1.43 (1.11×10^{-1} - 6.8×10^{-1})	1.2×10^{-1} (1.5×10^{-2} - 3.1×10^{-2})	27
Thunnus albacores	Taipei, Taiwan	9.75 (8.8-10.4)	2.1×10^{-1} (1.7×10^{-1} - 3.1×10^{-1})	7.0×10^{-2} (1.5×10^{-2} - 3.1×10^{-2})	
Trichiurus lepturus	Taipei, Taiwan	1.28 (0.14-6.85)	1.3×10^{-1} (5.0×10^{-3} - 4.2×10^{-1})	1.3×10^{-1} (3.0×10^{-2} - 3.2×10^{-1})	
Chanos chanos	Taipei, Taiwan	2.54 (0.24-4.60)	1.2×10^{-1} (5.0×10^{-3} -1.9)	3.5×10^{-2} (5.0×10^{-3} - 2.7×10^{-1})	

Table 4. Heavy metal concentrations ($\mu\text{g}\cdot\text{g}^{-1}$ dry weight) in fish in other water areas (Continue)

Species or population	Location	Hg	Pb	Cd	Reference
Cyprinus carpio	Taipei, Taiwan	2.19 (0.69–5.40)	9.5×10^{-2} (1.0×10^{-1} – 2.5×10^{-1})	1.0×10^{-1} (ND– 1.0×10^{-1})	
Euryglossa orientalis	Persian Gulf, Iran	2.1×10^{-1}	2×10^{-1}	1.6×10^{-1}	This study
Psettodes erumei	Persian Gulf, Iran	2.7×10^{-1}	1.7×10^{-1}	1.6×10^{-1}	This study
Epinephelus coioides	Persian Gulf, Iran	1.5×10^{-1}	4.1×10^{-1}	2.5×10^{-1}	This study
Lethrinus nebulosus	Persian Gulf, Iran	1.5×10^{-1}	2.6×10^{-1}	2.7×10^{-1}	This study

Table 5. Concentrations of Pb, Cd, and Hg in 4 types of fish samples ($\mu\text{g}/\text{g}$ dry weight)

Areas	Metals					
	Pb		Cd		Hg	
	Mean	Range	Mean	Range	Mean	Range
Bandar Abbas	0.34	(0.07-0.76)	0.21	(0.09-0.61)	0.21	(0.07-0.42)
Bandar Lengeh	0.18	(0.01-0.36)	0.20	(0.01-0.35)	0.18	(0.09-0.31)

Mean values of Cd, in our investigation, except for *L. nebulosus*, were lower than those reported for *Lethrinus lentjan* in the United Arab Emirates.²⁶

Our results for Cd were lower than those reported in Xiamen in China,⁸ in Sicily in the Mediterranean Sea,⁴ and the Gulf of California.¹⁹

On the other hand, our results were higher than those reported from Adriatic sea,⁹ Jingsu River,¹⁸ Meiliang Bay,²⁰ Nam Co Lake,¹⁸ Dong Li District, and Xi Qing District, Jin Nan District, and Bei Chen District,²⁰ New Jersey,²⁴ and Taipei.²⁷ The concentration of Cd observed in our studied fish was similar to that in *Hexagrammos otakii* and *Sebastes marmoratus* fish from Masan Bay.²⁵

The concentrations of Pb in the current study were lower than those reported in fish muscle in Sicily in the Mediterranean Sea,⁴ 240 shellfish (including oyster, short-necked clam, razor clam, and mud clam) collected from 6 administrative regions in Xiamen of China,⁸ and in *Istiphorus platypterus* and *Terrapurus audax* in the Gulf of California.¹⁹

The comparison of our results with other results in table 5 showed that the concentration of

Pb in the Persian Gulf was higher than that in the Jinsu River,¹⁸ Adriatic Sea,⁹ Lake Nam Co,²¹ and Dong Li District, Xi Qing District, Jin Nan District, and Bei Chen District,²³ New Jersey,²⁴ and Masan Bay.²⁵ The concentration of Pb was similar to that in fish from Taipei city in Taiwan.²⁷

Lower concentrations of mercury were found in our study in comparison t that in Taipei,²⁷ New Jersey,²⁸ Bei Chen District,²³ and the Adriatic Sea.⁹ Hg concentration in fish tissues in our study were higher compared with that in fish muscle in Sicily,⁴ shellfish in Xiamen,⁸ Flounder fish in New Jersey,²⁴ fish species in Dong Li, Xi Qing, and Jin Nan Districts,²³ and *Lagocephalus lagocephalus* and *Pseudotolithus senegalensis* in Ghana,²² Atlantic Coast, and in European Anchovy in the Adriatic Sea.⁹ Similar concentrations of Hg were observed in Rose Fish in the Adriatic Sea⁹ and *Braehydentera aurita* in Ghana.²³

Health risks posed by exposure to Pb, Cd, and Hg to the local inhabitants in the two coastal regions of the Persian Gulf, Iran, through the consumption of contaminated fish were investigated based on estimated THQs. The results showed that THQ values were lower than 1 for both adults and children by consuming fish alone (Table 5).

Table 6. THQs and EWI for individual metals caused by the consumption of fish

	Areas	Pb		Cd		Hg	
		THQ	EWI	THQ	EWI	THQ	EWI
Adults	Bandar Abbas	0.01	0.55	0.04	0.17	0.14	0.90
	Bandar Lengeh	0.01	0.55	0.03	0.13	0.12	0.38
Children	Bandar Abbas	0.02	0.18	0.06	0.25	0.18	0.74
	Bandar Lengeh	0.01	0.55	0.04	0.17	0.15	0.52

RfDs are based on 1×10^{-3} $\mu\text{g/g/day}$ for Cd, 4×10^{-3} $\mu\text{g/g/day}$ for Pb, and 5×10^{-4} $\mu\text{g/g/day}$ for Hg.¹⁵ The THQ of the studied metals through the consumption of fish for residents (adults and children) from the two districts were derived and listed in table 6. The results show that there are no THQ values higher than 1 through the consumption of fish, suggesting that the health risks associated with heavy metals exposure are insignificant.

An important aspect in assessing the risk to human health from potentially harmful chemicals in food is the knowledge that the dietary intake of such substances must remain within determined safety margins. For Hg, Cd, and Pb, the WHO has established a safe intake level, known as provisional tolerable weekly intake (PTWI). The PTWI for Cd, Pb, and Hg is 5, 7, and 25 $\mu\text{g/kg}$ body weight, respectively.²⁹

In our case, the estimated weekly intakes (EWI) of Cd, Pb, and Hg through the consumption of fish (Pb: 0.18-0.55 $\mu\text{g/kg}$ body weight, Cd: 0.13-0.25 $\mu\text{g/kg}$ body weight, Hg: 0.38-0.90 $\mu\text{g/kg}$ body weight) were lower than the established weekly intake limits (Table 6).

To further elucidate the specific risk contribution in each district, detailed information on food consumption structure and the metals concentrations in these areas will hopefully be obtained by future efforts with the associated institutions.

Conclusion

In the present study, the concentrations of heavy metals (Hg, Pb, and Cd) were determined in fish from the Persian Gulf. The considerable variation in levels of these contaminants among

different species highlights the important role of ecological and physiological factors in concentrating pollutants. The THQ values below 1 of Cd, Hg, and Pb showed no risk for the consumers' health. Nevertheless, analysis of mercury data suggests that dietary consumption of certain fish species can vary this neurotoxin intake substantially, thus, determining great differences in health risks. Consequently, intake might be of concern, especially in the cases where the exposure is closer to the tolerable weekly intake. As a final conclusion, we suggest providing more specific recommendations regarding human consumption (species, frequency, and size of meals) according to the data concerning levels of environmental pollutants in the most consumed fish and seafood species.

Conflict of Interests

Authors have no conflict of interests.

Acknowledgements

We would like to express our sincere gratitude to Dr. Hossein Pasha, who kindly assisted us in data analysis. We are also grateful to M. Ehsanpour and Mehdi Ghobeiti Hassab for their valuable help in fish sampling and laboratory analysis.

References

1. Harmanescu M, Alda LM, Bordean DM, Gogoasa I, Gergen I. Heavy metals health risk assessment for population via consumption of vegetables grown in old mining area; a case study: Banat County, Romania. *Chem Cent J* 2011; 5: 64.
2. Yahyavi M, Afkhani M, Khoshnood R. Determination of Heavy Metals (Cd, Pb, Hg and Fe) in Two Commercial Shrimps in Northern of Hormoz Strait.

- Annals of Biological Research 2012; 3(3): 1593.
- Ginsberg GL, Toal BF. Quantitative approach for incorporating methylmercury risks and omega-3 fatty acid benefits in developing species-specific fish consumption advice. *Environ Health Perspect* 2009; 117(2): 267-75.
 - Copat C, Bella F, Castaing M, Fallico R, Sciacca S, Ferrante M. Heavy metals concentrations in fish from Sicily (Mediterranean Sea) and evaluation of possible health risks to consumers. *Bull Environ Contam Toxicol* 2012; 88(1): 78-83.
 - Babatunde AM, Waidi Oyebanjo A, Adeolu AA. Bioaccumulation of Heavy Metals in Fish (*Hydrocynus forskahlii* (*Hydrocynus forskahlii*, *Hyperopisus bebe occidentalis* and *Clarias gariepinus*) Organs in Downstream Ogun Coastal Water, Nigeria. *Trans J Sci Technol* 2012; 2(5): 119-33.
 - World health organization. Beijing declaration on food safety [Online]. [cited 2007]; Available from: URL: http://www.who.int/foodsafety/fs_management/meetings/Beijing_decl.pdf.
 - Khoshnood Z, Khoshnood R, Mokhlesi A, Ehsanpour M, Afkhami M, Khazzali A. Determination of Cd, Pb, Hg, Cu, Fe, Mn, Al, As, Ni and Zn in important commercial fish species in northern of Persian Gulf. *Journal of Cell and Animal Biology* 2015; 6(1): 1-9.
 - Li J, Huang Z, Hu Y, Yang H. Potential risk assessment of heavy metals by consuming shellfish collected from Xiamen, China. *Environ Sci Pollut Res Int* 2013; 20(5): 2937-47.
 - Storelli MM. Potential human health risks from metals (Hg, Cd, and Pb) and polychlorinated biphenyls (PCBs) via seafood consumption: estimation of target hazard quotients (THQs) and toxic equivalents (TEQs). *Food Chem Toxicol* 2008; 46(8): 2782-8.
 - Vieira C, Morais S, Ramos S, Delerue-Matos C, Oliveira MB. Mercury, cadmium, lead and arsenic levels in three pelagic fish species from the Atlantic Ocean: intra- and inter-specific variability and human health risks for consumption. *Food Chem Toxicol* 2011; 49(4): 923-32.
 - Pyle GG, Rajotte JW, Couture P. Effects of industrial metals on wild fish populations along a metal contamination gradient. *Ecotoxicol Environ Saf* 2005; 61(3): 287-312.
 - Regional Organization for the Protection of the Marine Environment. Manual of oceanographic observations and pollutant analyses methods (MOOPAM). 3rd ed. Jabriya, Kuwait: Regional Organization for the Protection of the Marine Environment; 1999.
 - United States Environmental Protection Agency. Risk based concentration table. Washington, DC: USEPA; 2000.
 - Zhuang P, McBride MB, Xia H, Li N, Li Z. Health risk from heavy metals via consumption of food crops in the vicinity of Dabaoshan mine, South China. *Sci Total Environ* 2009; 407(5): 1551-61.
 - Astani M, Vosoughi AR, Salimi L, Ebrahimi M. Comparative study of heavy metal (Cd, Fe, Mn, and Ni) concentrations in soft tissue of gastropod *Thais mutabilis* and sediments from intertidal zone of Bandar Abbas. *Advances in Environmental Biology* 2012; 6(1): 319-2.
 - Jaafarzadeh Haghghi N, Khoshnood R, Khoshnood Z. Cadmium determination in two flat fishes from two fishery regions in north of the Persian Gulf. *Iranian Journal of Fisheries Sciences* 2011; 10(3): 537-40.
 - Tabari S, Saravi SS, Bandany GA, Dehghan A, Shokrzadeh M. Heavy metals (Zn, Pb, Cd and Cr) in fish, water and sediments sampled from Southern Caspian Sea, Iran. *Toxicol Ind Health* 2010; 26(10): 649-56.
 - Liu F, Ge J, Hu X, Fei T, Li Y, Jiang Y, et al. Risk to humans of consuming metals in anchovy (*Coilia sp.*) from the Yangtze River Delta. *Environ Geochem Health* 2009; 31(6): 727-40.
 - Soto-Jimenez MF, Amezcua F, Gonzalez-Ledesma R. Nonessential metals in striped marlin and Indo-Pacific sailfish in the southeast Gulf of California, Mexico: concentration and assessment of human health risk. *Arch Environ Contam Toxicol* 2010; 58(3): 810-8.
 - Chi QQ, Zhu GW, Alan L. Bioaccumulation of heavy metals in fishes from Taihu Lake, China. *J Environ Sci (China)* 2007; 19(12): 1500-4.
 - Yang R, Yao T, Xu B, Jiang G, Xin X. Accumulation features of organochlorine pesticides and heavy metals in fish from high mountain lakes and Lhasa River in the Tibetan Plateau. *Environ Int* 2007; 33(2): 151-6.
 - Voegborlo RB, Akagi H. Determination of mercury in fish by cold vapour atomic absorption spectrometry using an automatic mercury analyzer. *Food Chemistry* 2007; 100(2): 853-8.
 - Wang X, Sato T, Xing B, Tao S. Health risks of heavy metals to the general public in Tianjin, China via consumption of vegetables and fish. *Sci Total Environ* 2005; 350(1-3): 28-37.
 - Burger J, Gochfeld M. Heavy metals in commercial fish in New Jersey. *Environ Res* 2005; 99(3): 403-12.
 - Kwon YT, Lee CW. Ecological risk assessment of sediment in wastewater discharging area by means of metal speciation. *Microchemical Journal* 2001; 70(3): 255-64.
 - Al-Yousuf MH, El S, Al-Ghais SM. Trace metals in liver, skin and muscle of *Lethrinus lentjan* fish species in relation to body length and sex. *Sci Total Environ* 2000; 256(2-3): 87-94.
 - Han B, Jeng WL, Chen RY, Fang GT, Hung TC, Tseng RJ. Estimation of target hazard quotients and potential health risks for metals by consumption of seafood in Taiwan. *Arch Environ Contam Toxicol* 1998; 35(4):

- 711-20.
28. Burger J. Fishing, fish consumption, and knowledge about advisories in college students and others in central New Jersey. *Environ Res* 2005; 98(2): 268-75.
29. WHO/FAO. Toxicological recommendations and information on specifications. Proceedings of the 61st Meeting JOINT FAO/WHO expert committee on food; 2003 Jun 10-19; Rome, Italy.